UNLOCKING THE ROLE OF CHAPERONES ON LIPASE FROM *Photobacterium marinum* J15

By

FATIN LIYANA BINTI ALIAS

Thesis Submitted to the School of Graduate Studies, Universiti Putra Malaysia, in Fulfilment of the Requirements for the Degree of Master of Sciences

June 2024

FBSB 2024 3

Abstract of thesis presented to the Senate of Universiti Putra Malaysia in fulfilment of the requirement for the degree of Master of Sciences

UNLOCKING THE ROLE OF CHAPERONES ON LIPASE FROM *Photobacterium marinum* J15

By

FATIN LIYANA BINTI ALIAS

June 2024

Chairman : Adam Leow Thean Chor, PhD
Faculty : Biotechnology and Biomolecular Science

Lipase, a Family I lipolytic enzyme, catalyzes fatty acid synthesis and hydrolysis. It is classified into six subfamilies due to its conserved pentapeptide motif, Gly-Xaa-Ser-Xaa-Gly, and exhibits broad substrate specificity and regiospecificity, making it valuable for various applications. *Photobacterium* strain J15, a gram-negative bacterium isolated from Johor seawater, Malaysia, displays lipolytic activity. The gene encoding lipase (LipJ15) and its chaperone (Lif15) was codon-optimized, yielding proteins of 42.57 kDa and 33.24 kDa, respectively. Interestingly, LipJ15 shares only 56.14% amino acid sequence identity with *Pseudomonas aeruginosa* lactonizing lipase, suggesting unique structural features. Cloning and expression of LipJ15 were conducted using the recombinant pET-32b(+)::LipJ15+pBB550 system in *E. coli* Origami (DE3). The pBB550 vector carried chaperone genes (dnaK, dnaJ, GroESL). Expression at 0.3 mM IPTG and 20°C resulted in abundant soluble protein, as confirmed by SDS-PAGE. However, lipase activity was low at 0.3 mM IPTG (3.55 U), with the highest

activity at 0.6 mM IPTG (7.37 U). Structural analysis of LipJ15 revealed an α/β-hydrolase fold comprising 38.1% helices, 13.9% strands, and a catalytic triad (Ser92, Asp239, His261) within the conserved GXSXG motif. The structure also included a disulfide bridge and a Ca^{2+} binding site. Evaluation using the Ramachandran plot, Verify3D, and ERRAT confirmed the model's quality, with 89.8% of residues in favored regions. Protein-ligand docking analysis demonstrated LipJ15's high specificity toward short-chain substrates. Its structure could significantly contribute to structural biology by serving as a template for solving unsolvable protein structures with low sequence identity through molecular replacement, enhancing our understanding of related enzymes.

Keywords: chaperone, disulphide bridge, expression, lipase
SDG: GOAL 9: Industry, Innovation and Infrastructure

Abstrak tesis yang dikemukakan kepada Senat Universiti Putra Malaysia sebagai memenuhi keperluan untuk ijazah Master Sains

MERUNGKAI PERANAN CHAPERONES TERHADAP LIPASE DARIPADA *Photobacterium marinum* J15

Oleh

FATIN LIYANA BINTI ALIAS

Jun 2024

Pengerusi : Adam Leow Thean Chor, PhD
Fakulti : Bioteknologi dan Bimolekular Sains

Lipase, enzim lipolitik daripada Kumpulan I, memangkinkan sintesis dan hidrolisis asid lemak. Enzim ini dikelaskan kepada enam sub-kumpulan disebabkan oleh motif pentapeptida Gly-Xaa-Ser-Xaa-Gly yang terpelihara. Ia mempunyai spesifikasi substrat dan regiospesifik yang luas, menjadikannya berguna untuk pelbagai aplikasi. Strain *Photobacterium* J15, bakteria gram-negatif yang di dapati daripada air laut Johor, Malaysia, menunjukkan aktiviti lipolitik. Gen yang mengkodkan lipase (LipJ15) dan chaperone-nya (Lif15) telah dioptimumkan kodon, menghasilkan protein bersaiz 42.57 kDa dan 33.24 kDa. Menariknya, LipJ15 hanya berkongsi 56.14% identiti urutan asid amino dengan lipase laktonisasi *Pseudomonas aeruginosa*, menunjukkan ciri struktur yang unik.Pengklonan dan ekspresi LipJ15 dijalankan menggunakan sistem rekombinan pET-32b(+)::LipJ15+pBB550 dalam *E. coli* Origami (DE3). Vektor pBB550 membawa gen chaperone (dnaK, dnaJ, GroESL). Ekspresi pada 0.3 mM IPTG dan suhu 20°C menghasilkan protein larut yang banyak seperti yang

disahkan melalui analisis SDS-PAGE. Namun, aktiviti lipase pada 0.3 mM IPTG adalah rendah (3.55 U), sementara aktiviti tertinggi diperoleh pada 0.6 mM IPTG (7.37 U).Analisis struktur LipJ15 menunjukkan susunan α/β-hidrolase dengan 38.1% heliks, 13.9% strand, dan triad katalitik (Ser92, Asp239, His261) dalam motif GXSXG. Struktur ini juga mengandungi ikatan disulfida dan tapak pengikatan Ca^{2+}. Penilaian menggunakan plot Ramachandran, Verify3D, dan ERRAT mengesahkan kualiti model, dengan 89.8% residu berada dalam kawasan yang paling digemari.Analisis doking protein-ligan menunjukkan spesifisiti tinggi LipJ15 terhadap substrat rantaian pendek. Strukturnya berpotensi menyumbang secara signifikan dalam biologi struktur dengan berfungsi sebagai templat untuk menyelesaikan struktur protein yang sukar diselesaikan kerana identiti urutan rendah, sekali gus meningkatkan pemahaman tentang enzim berkaitan.

Kata Kunci: chaperone, ekspresi, ikatan disulfide, lipase
SDG: MATLAMAT 9: Industri, Inovasi dan Infrastruktur

ACKNOWLEDGEMENTS

All praises to Allah for His blessings, giving me a beautiful life and good health throughout the years of finishing my study. Special appreciation to my supervisor, Associate Professor Dr. Adam Leow Thean Chor for giving me the opportunity to work on this project, for the invaluable guidance, encouragement and constant support while completing this study.I also would like to thank my supervisory committee, Associate Professor Dr. Normi Mohd Yahaya and Professor Dr. Mohd Shukuri Mohamad Ali and the other principal investigators in EMTech research group for their encouragement, insightful comments and helpful discussions. My sincere thanks also dedicated to my lab partner Nima Ghahremani Nezhad for his help, suggestion and cooperation in data collection. Special thanks to all the members of Synthetic Biology lab especially my closest collegues, Aishah, Shaw Xian, Kanchana and Sunusi for their supports, knowledge and friendship. Last but not least, I am eternally grateful to my beloved parents, Alias Haron and Raha Abdul Rahman and my siblings, Angah and Adik for their prayers, encouragement and utmost support. To my dearest husband Mohd Shahirman for always be there for me as my biggest supporter throughout the bumpy road and to my darling daughter, Maryam Sofea, the bright smile you give me makes all my tiredness melts away. To those who indirectly contributed in this research, your kindness means a lot to me. Thank you.

This thesis was submitted to the Senate of Universiti Putra Malaysia and has been accepted as fulfilment of the requirement for the degree of master science (*Enzyme Biotechnology*). The members of the Supervisory Committee were as follows:

Adam Leow Thean Chor, PhD
Associate Professor
Faculty of Biotechnology and Biomolecular Science
Universiti Putra Malaysia
(Chairman)

Normi binti Mohd Yahaya, PhD
Associate Professor
Faculty of Biotechnology and Biomolecular Science
Universiti Putra Malaysia
(Member)

Mohd Shukuri bin Mohamad Ali, PhD
Professor
Faculty of Biotechnology and Biomolecular Science
Universiti Putra Malaysia
(Member)

Cahyo Budiman, PhD
Associated Professor
Biotechnology Research Institute
Universiti Malaysia Sabah
(Member)

ZALILAH MOHD SHARIFF,PhD
Professor and Dean
School of Graduate Studies
Universiti Putra Malaysia

Date: 24 February 2025

TABLE OF CONTENTS

LIST OF TABLES

LIST OF FIGURES

LIST OF ABBREVIATIONS

α	Alpha
Å	Angstrom
β	Beta
°C	Degree Celsius
%	Percentage
A600nm	Absorbance at wavelength 600 nanometer
µL	Microliter
µm	Micrometer
APS	Ammonium persulfate
bp	Base pair
$CaCl_2$	Calcium chloride
g	Gram
h	Hour
IPTG	Isopropyl β-D-1-thiogalactopyranoside
kb	Kilobase
kDA	kilodaltons
M	Molar
mg/ml	Miligram per mililiter
min	Minute
ml	Mililiter
mm	Milimeter
nm	Nanometer
OD	Optical density
SDS	Sodium dedocyl sulphate
TEMED	N, N, N, N- Tetramethyllenediamide
U	Unit
U/ml	Unit per mililiter
U/mg	Unit per milligram
µl	Microliter
v/v	Volume per volume
w/v	Weight per volume

CHAPTER 1

INTRODUCTION

Lipases are enzymes that are highly desired within biotechnological processes (Andualema and Gessesse 2012). In the global market, they rank as the fourth most significant category of enzymes, following carbohydrases, phytases and proteases (Pulido et al. 2020). Lipases are hydrolytic enzymes that catalyse ester bond cleavage and formation. These enzymes can be obtained from a range of sources, such as animals, plants, and microorganisms. Because of their broad substrate specificity and regiospecificity, these enzymes are very useful in a wide range of applications, particularly in food and beverage, fine chemicals, and pharmaceuticals (Cowan et al., 2020).

The genome sequence of *Photobacterium* sp.J15, isolated from seawater in Johor, was sequenced and annotated to gain insights into the bacterium's properties, including its industrially relevant metabolic pathways (Roslan et al. 2016).The genome encodes several interesting enzymes including potential anticancer asparaginase, GDSL esterase and a few lipases. Interestingly, lipase J15 (942 bp) is encoded at upstream of lipase J15 chaperone (867 bp) under the regulation of the same promoter.

PSI-Blast against Protein Data Bank (PDB) revealed that it shares low protein sequence identities (41 – 56 %) to lipases from *Pseudomonas* spp., *Proteus* spp. and *Burkhoderia* spp. However, LipA from *Burkholderia cepacia*

exhibits high activity and tolerance to short-chain alcohols, but it requires a chaperone for correct folding. Surprisingly, *Proteus mirabilis* lipase does not rely on chaperone for folding despite shares 38% identity to *Burkhoderia cepacia* lipase (Korman et al. 2013). Heterologous expression using *E. coli* has been selected strategy for the production of lipase with regards to its easy growth and low production costs (Wu et al. 2012; Pulido et al. 2020).

However, expression in this microbe frequently leads in aggregated protein synthesis as well to the active enzyme (Rosano and Ceccarelli 2014). One of the main barriers to functional expression of recombinant proteins is their insoluble heterologous expression as inclusion bodies (inactive form) (Bhatwa et al. 2021). Many approaches, such as changes at the molecular or post-expression levels, have therefore been developed to overcome this barrier (Alias et al. 2023). Modifications at the molecular level include selecting a suitable promoter, vector, and tags. Post-expression modifications include the refolding of produced protein from inclusion bodies (IBs), which can be accomplished by chemical and physical approaches.

For long-term functional expression, molecular modifications will be simpler than refolding strategies, which often require a lot of time and chemicals to produce the functional enzyme. One of the most intriguing molecular modification options is the co-expression of molecular chaperones and the gene of interest, which will create soluble protein by facilitating proper folding to the native protein form. DnaK, DnaJ, GroES, and GroEL are popular molecular chaperones utilised in *E.coli* expression systems to express

bioactive proteins with appropriate native folding to prevent the production of IBs (De Marco et al. 2019).

Therefore, it is worth to investigate whether the folding of lipase J15 dependent on the chaperone that would improve the proper folding of lipase J15 derived from locally isolated J15 which can be utilised in industrial application. The aim of this study is to investigate the folding of *Photobacterium marinum* lipase J15 (LipJ15) in *E.coli*, The specific objectives are:

i. To clone the LipJ15 lipase gene, both independently and co-expressed with its native chaperone, Lif15.
ii. To express the LipJ15 lipase functionally in the presence and absen ce of various foreign chaperones.
iii. To characterize the LipJ15 lipase through *in silico* analysis.

CHAPTER 2

LITERATURE REVIEW

2.1 Biocatalysis

Enzymes are widely known as highly effective and efficient biocatalysts for a wide range of processes due to their high selectivity and activity. The first wave of biocatalysts appeared more than a century ago, when scientists discovered that entire living cells could perform valuable chemical transformations such as the synthesis of an L-ephedrine precursor (Basso and Serban 2019). The second wave of biocatalysis, which took place in the final quarter of the 20th century, saw advancements in enzyme, substrate, and media screening, along with the emergence of early protein engineering technologies, which expanded the substrate range of enzymes to include unnatural molecules.

The so-called "directed evolution" (Bornscheuer et al. 2012) method of biocatalysis, which uses advanced molecular biology and high-throughput screening for rapid and extensive modification of biocatalysts, was the start of the third wave of biocatalysis in the late 1990s. The fourth wave of biocatalysis is driven by protein engineering efforts are providing biocatalytic access to novel and frequently unnatural reactions (Bornscheuer 2018). Enzymes are now being used to synthesize an increasing number of compounds, thanks to major discoveries that been made over the years in enzyme development and protein engineering, as well to the green chemistry advantages characterizing biocatalytic processes.

Additionally, enzymes can minimize the number of reaction steps and the volume of hazardous solvents needed, making the process more cost-effective and environmentally sustainable (Cowan and Fernandez-Lafuente 2011). Due to these reasons, enzymes have emerged as highly significant catalysts with great potential in a wide range of practical applications in sectors ranging from food to medicines (Wohlgemuth 2010).

2.2 Classification of lipases

This section discusses the classification lipases based on specificity while the following section is focused to sources of lipases. Lipases are quite popular in research and they catalyse a wide variety of reactions (Sarmah et al. 2018). The classification of lipases, as described in the following sections, provides a clearer understanding of their availability, functionality, and broad applicability. Specificity is a key factor in representing the industrial uses of lipases, which can be divided into three major categories.: (i) substrate-specific, (ii) regioselective and (iii) enantioselective.

As demonstrated by the utilization of lipases in the production of high purity diacylglycerols (Borza et al. 2015) and substrate-specific lipases for biodiesel (Patel et al. 2022) can be efficiently used in reactions where they selectively target a particular substrate within a mixture of crude raw materials, facilitating the production of the desired product. Alcohol and fatty acids are two common substrates that substrate-specific lipases can act with (Chandra

et al. 2020). According to a recent study, enzyme stability and substrate specificity are crucial for using lipases in a variety of industrially significant processes(da Silva et al. 2023).

Unlike other side reactions, regioselective lipases typically guide the reaction in a favorable direction. Such a lipase characteristic is extremely important in the chemical and pharmaceutical industries, particularly in the production of isomeric molecules that function optimally only under specified conditions. There are three classifications of regioselective lipases such as non-specific lipases, 1,3 specific lipases, fatty acid specific lipases and enantioselective lipases. For non-specific lipases is favourable and capable of working efficiently on various substrates.

Generally, triacylglycerols will hydrolyse into free fatty acids and glycerol with mono and diacylglycerols as the intermediates. Less thermodegradation as a result of ambient operating conditions is shown to be a benefit of the procedure (Valério et al. 2022). For 1,3-specific lipases catalyze the hydrolysis of triacylglycerols at the C1 and C3 positions, resulting in the formation of fatty acids, 2-monoacylglycerols, and 1,3- or 2,3-diacylglycerols. Acyl migration forms resulting to the formation of 1,3-diacylglycerol and 1- or 3- monoacylglycerols due to the instability of final two compounds (Mao et al. 2023). When compare with monoacylglycerols from triacylglycerols, the formation of diacylglycerols is much faster (Subroto 2020). There are recent studies regarding this 1,3 specific lipases (Li et al. 2021; He et al. 2023).

Esters that have long chain fatty acids with double bonds on C-9 were hydrolyzed by fatty acid specific lipases. In previous studies, to identify the microbial strains for producing lipases specific towards saturated medium- and long-chain fatty acids, screening was performed (Abed et al. 2020). From prochiral precursors, enantioselective lipases preferentially hydrolyze one of the isomers of a racemate compared to the other. Enantiomers can be separated in a racemic mixture by these lipases (Degórska et al. 2022). Enantiospecific lipases catalyze various processes, including the hydrolysis of menthol benzoate for cosmetic and food products (Verma et al. 2021), the transesterification of secondary alcohols for pharmaceutical products (Borza et al. 2015), and the hydrolysis of glycidic acid methyl ester for medical products (Su et al. 2014).

The lipolytic enzymes comprise carboxyl-esterases (EC 3.1.1.1) and true lipases (EC 3.1.1.3) (Kovacic et al., 2019). Both enzymes can catalyze the hydrolysis and synthesis of long-chain triglycerides, producing fatty acids, diacylglycerol, monoacylglycerol, and glycerol (Moraleda-Muñoz and Shimkets 2007; Chandra et al. 2020). Aside from hydrolytic activity, they exhibit inter-esterification, esterification, aminolysis, and alcoholysis activity, all of which contribute to a wide range of industries (Karadzic et al. 2006; Rajendran et al. 2009).

Bacterial lipolytic enzymes were systematically classified by Arpigny and Jaeger (1999) into eight families (I-VIII) based on differences in their amino acid sequences and biochemical properties. Family I lipases, categorized as

true lipases, are further divided into six sub-families (Kovacic et al., 2019). True lipases (hydrolyse >10 carbon chain) are mostly a members of family I lipases which are obtained from either Gram-negative or Gram-positive bacteria.

There are six other subfamilies of family I lipases. True lipases derived from *Pseudomonas* sp. and other Gram-negative bacteria, with a size of 30-32 KDa, are classified in subfamilies I.1, I.2, and I.3 (Kovacic et al., 2019). The N-terminal secretion signal peptide and Ca^{2+} binding site are found in the lipases from subfamilies I.1 and I.2.

Table 2.1: Shows the comparison of esterases and lipases

Differences	
Esterases	**Lipases**
catalyse short acyl substrate (<10 carbon atoms)	catalyse long acyl substrate (>10 carbon atoms)
Similarities	
active site: a nucleophilic serine, an aspartic acid/glutamic acid, a histidine	
Conserved pentapeptide sequence Gly/Ala-X-Ser-X-Gly	
Common α/β hydrolase fold	

However, subfamily I.3 contains signal peptides at C-terminal end. The conserved pentapeptide Gly-Xaa-Ser-Xaa-Gly is present in all the three of the above subfamilies of lipases. While the subfamilies I.4 and I.5 also has similar conserved pentapeptides which comprise alanine residues replacing the first glycine in the conserved pentapeptide Ala-Xaa-Ser-Xaa-Gly. The

secreted lipases of the genera *Bacillus* and *Geobacillus* are from these subfamilies. The mesophilic *Bacillus* sp. contains the smallest (20 KDa), Ca^{2+} independent lipase, which belongs to subfamily I.4. While subfamily I.5 lipases are typically found in thermophilic *Geobacillus* species and are both alkaliphilic and thermophilic. Moreover, this family contains zinc-binding sites and is 45 KDa in size (Jaeger and Eggert 2002). Most of the *Staphylococcus* genera are grouped under subfamily I.6 lipases, which comprise an N-terminal signal peptide with a molecular weight of about 75 KDa.

The GDSL family and membrane esterase are other names for the family II lipase enzyme. Instead of the conventional pentapeptide Gly-Xaa-Ser-Xaa-Gly, the conserved motifs of this enzyme include Gly-Asp-Ser-(Leu) or GDS (L) peptides containing the active-site serine (Su et al., 2020). Family III includes extracellular lipases from psychrophilic bacteria. For instance lipases produced by several *Streptomyces* species and *Moraxella* species. It reveals a 20% similarity to human platelet activating factor acetylhydrolase (PAF-AH) intracellular and plasma monomeric isoforms (Kovacic et al., 2019).

Family IV lipase, which closely resembles mammalian hormone sensitive lipases (HSL), is also known as the HSL (hormone-sensitive lipase) family. Family V enzymes include lipases, which are found from mesophilic, thermophilic, and psycrophilic bacteria. These enzymes amino acid sequences share 20–25% of their similarities with those of other non-lipolytic enzymes with the α/β-hydrolase fold (Kovacic et al., 2019). Family VI lipases

typically carboxyesterases and have a size range of 23–26 KDa and even a 40% similarity in sequence to eukaryotic lysophospholipases. Family VII lipases are the largest esterases, ranging in size from 50 to 65 KDa, with sequences that are similar to those of eukaryotes' acetylcholine esterase. These lipases hydrolyze short chains of fatty acid-containing lipid. Family VIII consists of three enzymes that are related to -lactamases class C within the two enzyme residues have the conserved motif Gly-Xaa-Ser-Ala-Gly (Kovacic et al., 2019).

After nearly two decades, many novel bacterial lipases have been discovered. Most of these lipases, however, could not be classified using Arpigny and Jaeger 1999 classification system. Due to the lack of an in-depth comparison being done on the published data, this issue has over time resulted in an inconsistent classification system of lipase families for novel lipases (Rozi et al. 2022).

This classification system has recently been expanded to incorporate new lipases across 19 families and eight sub-families of true lipases. However, many lipolytic enzymes remain unclassified (Verma et al. 2020). Thanks to recent discoveries, the 35 families and 11 genuine lipase sub-families of this classification system were finally updated (Hitch and Clavel 2019). By using this new system, any potentially novel bacterial lipases might be categorised into the families that have been characterised, preventing the issue of inconsistent descriptions in the literature.

2.3 Source of Lipases

The source of lipases can be found plants, animals and microbial organisms. Microbes are considered the most promising sources of lipases due to their vast industrial potential, ease of culture management, availability, and scalability (Yao et al. 2021). In plant, lipases can be found from many parts of a plant such as seeds, fruits, latex, and leaves. Mostly, the plant lipases can be found in seed, for instance castor bean, African bean, elm, sunflower, coconut, almond, wheat grain, rice, oat and barley. This is because seed high concentration of triacylglycerols, thus act as a source of energy for plant growth. During germination, lipase activity in plant seeds increases as it converts triacylglycerols into soluble sugars (Zhou et al. 2019). Plant lipases seem to be particularly appealing because of their low cost, limited applicability, simple acceptance, and direct use as biocatalysts. However, very few plant lipases have been studied because of their shortage, instability, and loss of activity when applied to conventional methods of purification (Chandra et al. 2020).

In animal cells, they synthesize lipases that enable the digestion of fats and lipids However, due to complication factors including culture handling and product separation, animal lipases are more frequently utilised in clinical diagnosis than in commercial production. These lipases are far less studied than the lipases from bacteria and plants. Some of the animal tissue-derived lipases employed in various researches. Pancreatic lipase, one of the various animal lipases, has been widely used as a research tool in the fields of lipid

chemistry and biochemistry because it efficiently catalyses the hydrolysis of primary alcohol esters (Sarmah et al. 2018). It should be highlighted that lipases can also come from insect tissues and are primarily involved in the growth of the insect's larval stage (Santana et al. 2017; Zhang et al. 2023) or in the development of the insects gut (MsangoSoko et al. 2022).

Microbial lipases can be classified into fungal, yeast, and bacterial lipases. Microbial lipases are more appealing for industrial applications due to their adaptability and their simplicity of production(Choudhury and Bhunia 2015; Sarmah et al. 2018; Toldrá-Reig et al. 2020; Sena et al. 2021; da Silva et al. 2023). Microbial lipase's remarkable specificity makes it a powerful tool for biotechnological applications, which are discussed further. Most microbial lipases are derived from bacterial and fungal species and are extracellular in nature. In addition to physicochemical parameters such as temperature, pH, and dissolved oxygen, medium composition has a significant impact on their production (Andualema and Gessesse 2012; Chandra et al. 2020).

Fungal lipases are the most extensively used lipases among all microbial species because of their unique characteristics, such as temperature and pH stability, substrate specificity, convenience in extraction, and efficient activity in organic solvents (Kumar et al. 2023).Depending on the carbon and nitrogen composition of the medium, these lipases can be both extracellular and intracellular. Several studies are reported on fungal lipases in recent past (Singh and Mukhopadhyay 2012; Alabdalall et al. 2021; Cesário et al. 2021). Considering their unique traits and convenience for cultivation, yeast lipases

are a very important source of lipases for a variety of industries, including the pharmaceutical, chemical, and biodiesel industries.

Bacterial lipases can be membrane-bound, extracellular, or intracellular. Although most lipases are glycoproteins, certain extracellular bacterial lipases are lipoproteins. According to reports, bacterial lipases are abundant, commonly substrate nonspecific, and thermo-stable (Sarmah et al. 2018). According to recently studies, the majority of bacterial lipases are discovered to be thermally stable and potential biocatalysts for industrial application (Lan et al. 2016; Valério et al. 2022). The bacterial lipases that have shown promising application in biodiesel production (Korman and Bowie 2012; Thangaraj et al. 2019; Karakaş and Arslanoğlu 2020; Sena et al. 2021).

2.4 Structural Features and Catalytic Mechanisms of Lipases

Despite size variations and low primary sequence identity, the structural folding patterns of the lipases are quite similar. This structure which is known as a α/β hydrolase fold, is similar by a variety of different hydrolases, including proteases, epoxide, hydrolases, dehalogenases, peroxidases, and esterases (White et al. 2018). As illustrated in Figure 2.1, the canonical α/β hydrolase fold is characterized by a central β-pleated sheet composed of eight parallel β-strands, except for the β2-strand, which runs antiparallel to the others. Helices link the β-3 to β-8 strands, which are packed on either side of the central β-sheet (Anobom et al. 2014). The active site of α/β hydrolases contains a highly conserved catalytic triad, composed of a

nucleophilic residue (serine, cysteine, or aspartic acid), a catalytic acidic residue (aspartic acid or glutamic acid), and a histidine that functions as a general base catalytic residue. In contrast to other proteins carrying the catalytic triad, these are always found in this order in the amino-acid sequence. The nucleophilic residue in lipases is generally a serine, found in the so-called "nucleophilic elbow," which is characterised by the highly conserved pentapeptide GXSXG (Figure 2.1). The catalytic acidic residue is located after the β6 or β7 strands of the central β-sheet and forms a hydrogen bond with the catalytic histidine, which is situated in a loop following the β-8 strand of the α/β hydrolase fold (Figure 2.1). The lipase active site contains a large, hydrophobic binding site for the scissile fatty acid (FA), which accommodates the acyl chain of the ester bond to be hydrolyzed. Substrate anchoring at the pentapeptide site residues is often stabilized by additional binding pockets that interact with the other acyl chains of the substrate (Rabbani et al., 2023).

The oxyanion hole, or "pocket," found in lipases, is another crucial component. It contributes in stabilising the negatively charged intermediate synthesized during ester-bond hydrolysis. The oxyanion hole consists of two residues: one that always follows the nucleophilic residue, and the other, which has a flexible orientation. The C-terminal neighbour X of a conserved glycine residue that contacts the nucleophilic elbow is the positionally variable residue of the oxyanion hole in the GX class of lipases. In the GGGX class, compared to the GX type, the oxyanion hole residue is shifted one position toward the C-terminus. It consists of a glycine residue followed by a

conserved hydrophobic residue, X. The positionally variable oxyanion hole residue in the Y class is a tyrosine (Albayati et al. 2020).

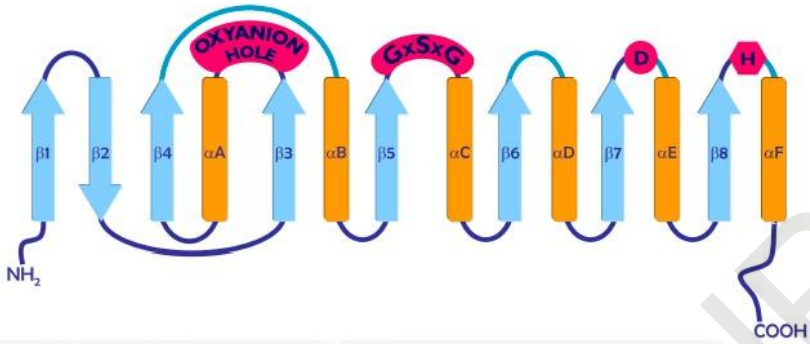

Figure 2.1: Shows the canonical fold of α/β hydrolases, with strands represented by arrows and helices by cylinders. The locations of the histidine (H) and aspartate (D) residues, along with the GXSXG motif and the oxyanion hole, are highlighted (Source: Borrelli and Trono, 2015)

The "lid," a mobile domain with one, two, or three helices or a loop region that is a common feature of most lipases. The lid covers the active site when there is no lipid-water interface, but when there is an interface, the conformation of the enzyme is changed, detaching the lid and allowing the substrate and solvent access to the catalytic site (Khan et al. 2017). Lipases from *Bacillus pumilus*, *Bacillus licheniformis* and *Bacillus subtilis*, as well as a lipase from guinea-pig pancreas, lack the lid domain, resulting in low molecular weights and no interfacial activation (Ma et al. 2015; Nakamura et al. 2018). In addition, the lipase from *Pseudomonas* sp. MIS38, which belongs to Family I.3, has two lids: lid1 (commonly known as bacterial lipase lid) and lid2 (which is unique to this *Pseudomonas* sp. MIS38 lipase and other Family I.3 lipases) (Angkawidjaja et al. 2007).

Lipases utilise common serine hydrolase mechanism for catalysis. The initial

steps in substrate hydrolysis involve lipid binding and a catalytic serine attacking the carbonyl carbon of the susceptible ester bond (Figure 2.2a). This leads to the formation of a tetrahedral intermediate, where four atoms are bonded to the carbonyl carbon in a tetrahedral arrangement, and a negative charge develops on the carbonyl oxygen atom (Figure 2.2b).

The negatively charged carbonyl oxygen and the main-chain -NH groups of two amino acid residues in the oxyanion hole form hydrogen bonds, which help stabilize the intermediate. One of the two hydrogen bonds in the lipases of the Y class is produced with the hydroxyl group of a tyrosine side chain. The catalytic histidine, to which a proton from the serine hydroxyl group is transferred, enhances the serine residue's nucleophilicity.

The catalytic acidic residue helps to promote this transfer by orienting the histidine's imidazole ring so that the charge created on it can be neutralised. Subsequently, a proton is donated to the oxygen atom of the susceptible ester bond, causing it to break and releasing the alcohol product, while the acyl chain is esterified to the nucleophilic serine (Figure 2.2c). The following process is called deacylation, in which a water molecule hydrolyzes the covalent bond, releasing the acyl product and allows the enzyme to regenerate (Figure 2.2d) (Ehlert et al. 2019).

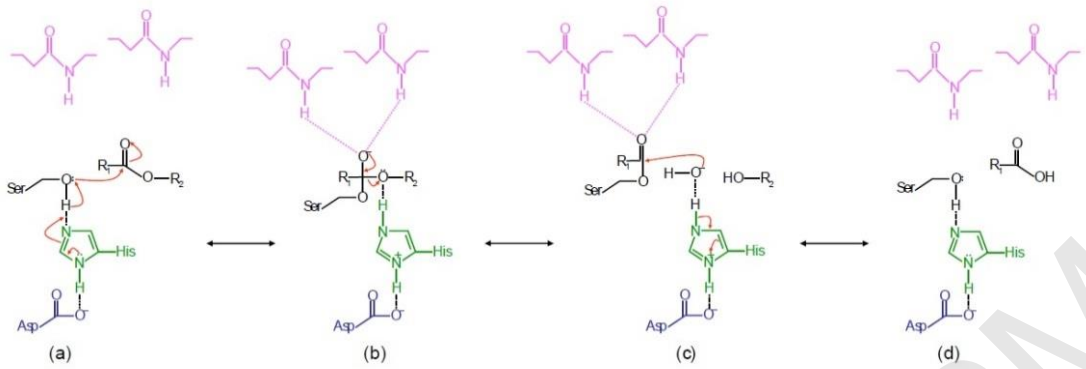

Figure 2.2: Mechanism of ester bond hydrolysis catalyzed by lipases. Aspartate and histidine are represented in blue and green, respectively; serine, substrate, and water are shown in black; and the oxyanion hole residues are depicted in magenta. (a) Nucleophilic attack by the serine hydroxyl on the carbonyl carbon of the susceptible ester bond; (b) formation of the tetrahedral intermediate; (c) acyl-enzyme intermediate, release of the alcohol, and nucleophilic attack by water; (d) free enzyme and release of the acyl product. (Source: Borrelli and Trono, 2015)

2.5 Application of lipases

The importance of microbial lipases is discussed in this section in context of their industrial applications. Lipases have the potential to significantly contribute to the development of the bioprocess industries due to their varied uses in catalysing a wide range of reactions involved mostly in raw material bioprocessing or organic chemical synthesis.

2.5.1 Biodiesel

Recently, various oils or fats have been transesterified with alcohol to produce biodiesel, which is a promising alternative fuel. The research of developing biofuel or biodiesel technology from sustainable resources has been encouraged due to the rise in environmental pollution issues lsuch as

climate changes, greenhouse emissions, and rising fossil fuel prices (Chandra et al. 2020; Cipolatti et al. 2020). Thus, the use of lipolytic enzymes not only addresses the massive volume of lipid waste materials in a sustainable and environmentally beneficial manner but also raises concerns about energy security and potential fossil fuel replacements(Chandra et al. 2020).

Enzymatic transesterification offers numerous benefits over chemical transesterification, including easy purified byproduct recovery, less waste production, and reduced energy use (Arumugam and Ponnusami 2017; Valério et al. 2022). Many researches on lipase-catalyzed biodiesel synthesis employing various edible and non-edible oils have been reported in the literature. While there is an abundance of raw materials for biodiesel production, the focus has primarily been on non-edible oils to minimize conflicts with the food production sector (Sarmah et al. 2018).

Several lipases, including one from *Burkholderia cepacia*, have been found to catalyse the transesterification of castor oil, non-edible oil, for biodiesel production (Kumar et al. 2019), More in-depth studies are focused to illustrating the improvements in the production of biodiesel through enzymatic transesterification, covering the crucial operational factors that affect lipase activity and stability as well as technological solutions for industrial application of enzymatic process (Toldrá-Reig et al. 2020)], significance of process parameter optimization, enzyme modification, the choice of feedstock and alcohol, and the reduction of biodiesel production costs

(Cavalcante et al. 2021; Kalita et al. 2022).The *Streptomyces* sp. was demonstrated as a useful lipase-producing microbe for biodiesel manufacture and discovered to be appropriate (Silano et al. 2019). As a significant step toward reducing environmental pollution and reusing waste oil, the cost of producing biodiesel is significantly lower when using waste and non-edible vegetable oil (Monika et al. 2023). The higher thermostability and short-chain alcohol tolerance of lipase make it an ideal choice for use in the production of biodiesel. Immobilized *Candida antarctica* lipase catalysed the methanolysis of soybean oil to produce biodiesel (Lv et al. 2019).

It was found that *Fusarium heterosporum* lipases produced in *A. oryzae* were beneficial for reducing the phospholipid concentration in oils utilised for the synthesis of biodiesel (Quayson et al. 2020). Li et al. demonstrated that oils containing phospholipids could be converted into biodiesel, accelerating the process by threefold. They also showed that this approach could enhance the efficiency of biodiesel production from waste oils generated in various industries (Li et al. 2015). For instance, *Geotrichum* sp. lipase was utilized to produce biodiesel from waste cooking oil, whereas *P. fluorescens* lipase was used in the way of waste sunflower oil (Costa et al. 2020; Ferrero et al. 2020). The type of lipase utilised in production is mostly determined by the raw material.

Nowadays, cold-active/adapted lipases have been discovered to be more energy efficient than other lipases for the production of biodiesel, and the synthesis of biodiesel by other lipases has been applied at higher

temperature. The most of cold-active/adapted lipases classified and characterized are bacteria, with just a few fungal isolates reported, such *Aspergillus nidulans* (Kumar 2020), *Geotrichum* sp. (Cai et al. 2009; Tshisevhe et al. 2021) and *Penicillium expansum* (Lončarić et al. 2021). The most dynamic biocatalyst is immobilised lipase from *Pseudomonas fluorescens* (Rios et al. 2019; Sun et al. 2023; Xiong et al. 2023), followed by *Pseudomonas cepacia* immobilised lipase (Silva Dias et al. 2019). A marine fungus called *Aspergillus awamori* BTMFW032 that was isolated from saltwater was found to produce biodiesel and harvest extracellular lipase (Basheer et al. 2011).

2.5.2 Detergent

Following the commercial success of proteases as detergent additives, the enzyme industry invested heavily in introducing lipases as a second group of detergent enzymes. Furthermore, the compatibility of lipase was evaluated by comparing it to different commercially available detergents and bleaching chemicals used to remove fat (Choudhury and Bhunia 2015). The usage of enzymes can be found in all detergent formulas that are now popular in underdeveloped countries. Laundry detergent is becoming increasingly popular due to its ability to impart softness, antistaticity, and water dispersibility.

There are numerous laundry detergent brands on the market, each claiming distinct advantages (Chandra et al. 2020). As a result, a huge number of *Pseudomonas* species have been investigated in order to develop appealing

and effective lipase applications in many industries (Hwang et al. 2014; Borrelli and Trono 2015; Yuan et al. 2020; Sahoo et al. 2021)

Enzymes have played a key role in the evolution and development of industrial detergents, which have become a primary application area for enzymes. Detergents are utilized in a wide range of applications, including dishwashing, laundry, household cleaning, as well as industrial and institutional cleaning (Gürkök 2019). Detergent enzymes are used to remove protein, starch, oil, and fat stains and to boost the efficacy of detergents (Al-Ghanayem & Joseph, 2020).

Enzymes in laundry detergents help reduce weight, eliminate damaged cotton fibers, and enhance whiteness, color, and fabric care. Hydrolase enzymes are widely used in detergent products, with amylase and protease being the most commonly employed. To improve stain removal and fabric care, a combination of enzymes, including proteases, amylases, pectinases, cellulases, and lipases, is sometimes used (Li et al. 2012). Amylases and lipases, respectively, are excellent at removing starchy food deposits and stains caused by fatty products (Singh et al. 2016).The use of enzymes in detergent products is favourable since these products include fewer bleaching chemicals and phosphates, which benefits public and environmental health (Singh et al. 2016).

Lipases are employed in detergent formulations, along with proteases and amylases, to improve detergent performance. Lipase adsorbs on the fabric surface, forming a stable fabric-lipase complex that catalyses the breakdown

of chemical bonds when water is added (Hasan et al. 2006). Lipases are increasingly being used in the detergent industry, and lipases that are thermophilic, alkalophilic, soluble in water, low-substrate specific, and tolerant to detergent proteases and other surfactants have been found to be compatible for use in both washing powders and liquid detergents (Chauhan et al. 2013). *Staphylococcus arlettae*, *Burkholderia cepacia*, *P. fluoresces*, and *Candida* species are some of the most common lipase sources used in the detergent industry (Ahmed et al. 2010; Phuah et al. 2015; Dulęba et al. 2019).

2.5.3 Food industry

Enzyme use in the food industry is categorized into various sectors, such as baking, dairy, juice production, and brewing. Microbial enzymes are particularly prevalent in baking, which is the largest application area in the food industry, where they help improve dough stability, enhance crumb softness and structure, and extend shelf life. The growing use of microbial enzymes in cheese production has significantly contributed to the rise of enzymes in the dairy sector, making it the second-largest application area, following the beverage industry (Singh et al. 2016). Baking enzymes are employed to enhance flour quality, dough stability, texture, volume, and color, while also helping to preserve crumb softness, maintain a consistent crumb structure, and improve bread freshness (Singh et al. 2016).

Enzymes are viewed as natural answers in today's baking market to meet escalating quality demands. Bread production is among the most common

food processing activities globally. The application of enzymes in bread making highlights their crucial role in ensuring quality control and enhancing production efficiency. Lipases are used to enhance the flavor profile of baked goods by esterifying short-chain fatty acids and to extend the shelf life of bakery products (Li et al. 2012). Dairy enzymes, a key segment of the food enzyme industry, play a vital role in enhancing organoleptic properties (such as aroma, flavor, and color) and improving the production of milk-based products.

The application of various enzymes, including proteases, lipases, esterases, lactase, aminopeptidase, lysozyme, lactoperoxidase, transglutaminase, and catalase, is well-established in the dairy industry, ranging from coagulants to bio-protective enzymes (Singh et al., 2016). Dairy enzymes are used to make cheese, yoghurt, and other milk products (Mir Khan and Selamoglu 2020). Lipases are currently used in flavour enhancement, speedier cheese making, the development of customised milk products, and the lipolysis of milk fat (Juan et al. 2015; Zhang et al. 2016).

2.5.4 Leather and textiles

The leather industry, being more traditional, faces significant health and environmental risks due to the waste and pollutants generated at various stages of production (Biškauskaitė et al., 2021). Biodegradable enzymes offer an effective solution for improving leather quality while reducing waste (Biškauskaitė et al., 2021). The first use of enzymes in leather production

was for the dehairing process, which requires large amounts of enzymes such as proteases, lipases, and amylases (Teja et al., 2022; Kanagaraj et al., 2023).

Additionally, lipases are utilized in the degreasing process to remove lipids (Yao et al., 2019). Leather processing is typically divided into three stages: pre-tanning, which involves cleaning the hides or skins; tanning, which stabilizes them; and post-tanning, which enhances their aesthetic qualities (Maina et al., 2019; Hasan et al., 2022). Among these stages, lipases play a key role in removing subcutaneous fat, dehairing, and stuffing leather, as their ability to break down lipids is essential. Lipases are employed during soaking, bating, and degreasing, processes that can be carried out using enzymes instead of costly and toxic solvents (Ma et al., 2014; Sarmah et al., 2018). Instead of using the harmful chemicals, *Yarrowia lipolytica* was used in the degreasing process for sheep skin (Moujehed et al. 2022). Lipases are typically employed in conjunction with other hydrolytic enzymes like as proteases to improve leather treatment.

The textile industry is a significant source of environmental pollution, primarily due to the large amounts of waste generated from fabric desizing, bleaching chemicals, and dyes (Scholz, 2019; Azanaw et al., 2022). Enzymes are increasingly used in this industry to promote the development of eco-friendly fiber processing methods and to enhance the quality of the final products (Choi et al., 2015). The two main types of enzymes used in cotton pretreatment and finishing processes are hydrolases and oxidoreductases.

Hydrolases include amylase, cellulase, cutinase, protease, pectinase, and lipase/esterase, which are involved in fabric biopolishing, bioscouring, anti-felting of wool, cotton softening, denim finishing, desizing, wool finishing, and the modification of synthetic fibers (Singh et al. 2016).

Lipases are commonly employed in the textile industry to degrease textile raw materials and improve performance(Uddin 2019). The physical and chemical alterations of the treated wool fibre, as well as the commercialization of lipase, have been studied (Chandra et al. 2020). The fatty acids discovered on the surface of wool fibre were removed after being treated with anhydrous alkaline lipase, which also improved the wool's quality (Taleb et al. 2022). The dewaxing effect of silk fibers using lipase, as well as the combined dewaxing and degumming of silk fibers with both lipase and protease, has been evaluated. The study assessed the impact of proper enzyme usage and dosages on fiber quality, including the rate of weight loss (Shen 2019), dyeing, wettability, microstructure, gloss, and other properties compared to without the use of lipases (Kalantzi et al. 2013). Furthermore, the desizing process of cotton fabric, amylase, and lipase can reduce waste water pollution by decomposing starch into water-soluble molecules (Chandra et al. 2020).

2.6 Heterologous expression and challenges

One of the strategies to increase the expression of lipase in prokaryotic system is utilization of engineered promoters. For example, the extracellular

and intracellular expression of T1.2RQ lipase in *Bacillus subtilis* WB800 resulted in a 1.53- and 13-fold increase in specific activities, respectively, when the Pgrac01 promoter was replaced with Pgrac100 (Elemosho et al., 2021). In *E. coli* carrying the pET vectors under the T7 promoter, lipase expression showed promising results (Eddehech et al., 2021). While expression levels and lipase types are variable factors to consider, another key determinant of lipase activity and kinetics is substrate specificity, which leads to different activities depending on the substrates used. The specific activities of expressed lipases in bacterial hosts can vary significantly and depend on several factors, including the host, vector, promoter, and substrate (Kaur et al., 2016; Eddehech et al., 2021; Elemosho et al., 2021; Zhao et al., 2022).

The expression of soluble lipases in *Escherichia coli* or other host systems remains a challenging task in biotechnology and enzyme engineering due to issues related to protein folding, misfolding, and aggregation. Lipases, like many other enzymes, often require chaperones—proteins that assist in the correct folding and stability of other proteins. The use of chaperones can significantly improve the soluble expression of lipases, but it introduces both strategies and challenges. Below is a detailed exploration of these strategies and challenges, including insights from recent research.The strategies to enhance the soluble lipase expression is by co-expression of molecular chaperones. By co-expressing molecular chaperones alongside the lipase gene is a well-established strategy. Chaperones assist in the proper folding of the target protein, preventing aggregation and promoting solubility.

Common chaperones include GroEL/ES, DnaK/DnaJ/GrpE and trigger factor. Recent studies have demonstrated that co-expressing these chaperones can reduce protein aggregation and enhance the production of soluble lipase. For example, a study on the expression of *Candida antarctica* lipase B (CALB) in *E. coli* showed that co-expression with the GroEL/ES system increased the yield of soluble CALB, making it more active in vitro (Koyanagi et al., 2021). Additionally, optimizing expression conditions, such as temperature and induction time, in combination with chaperones, can improve the overall yield and solubility of lipases. A study by Qu et al. (2021) on Pseudomonas lipase expression showed that adjusting the induction conditions such as temperature shift along with the use of DnaK/DnaJ resulted in significantly increased yields of soluble lipase.

However, there are challenges in the use of chaperones for soluble lipase expression. One major challenge when co-expressing chaperones with lipase is that it can overload the host's protein-folding machinery, leading to cellular stress (Prabhu et al., 2018). This can limit the overall protein yield and even lead to a decrease in the expression of the target protein. Excessive chaperone expression may compete for cellular resources, potentially reducing the availability of other factors required for optimal expression (Mathangasinghe et al.,2021).

2.7 Role of chaperone

Many small proteins refold in the absence of other components or an energy

source after being removed from a denaturant in vitro. This means that the amino-acid sequence which encoded in the DNA provides all the information required to specify a protein's three-dimensional structure (Hartl et al. 2011). However, studies over the last few decades have conclusively shown that many proteins in the cellular environment require molecular chaperones in order to fold properly and in a biologically relevant timeframe (Viegas et al. 2020; Raschmanová et al. 2021; Ravitchandirane et al. 2022). Early on in the evolution of densely populated organisms, molecular chaperones were fundamentally needed to prevent protein aggregation during folding and preserve proteins in soluble yet conformationally dynamic states. Furthermore, it follows that the chaperone system acts as an essential buffer, enabling the evolution of new protein functions and phenotypic features, as mutations frequently impair a protein's capacity to adopt a stable fold (Wyganowski et al. 2013).

Chaperones do not resemble typical macromolecular structures with a clearly defined substrate. The principal molecular chaperones (TABLE 1) have limited specificity but are needed for protein folding, a complex and highly selective process (Hartl et al. 2011). They perform various roles in proteome maintenance, including assisting in de novo protein folding, refolding stress-denatured proteins, facilitating oligomeric assembly, aiding protein trafficking, and supporting proteolytic degradation. Chaperones involved in de novo folding and refolding, such as HSP70s, HSP90s, and chaperonins (HSP60s), are complex molecular machines that promote folding through ATP- and cofactor-regulated binding and release cycles. These chaperones typically

recognize hydrophobic amino acid side chains exposed by non-native proteins and may work in conjunction with ATP-independent chaperones, such as small HSPs, which act as "holdases" to prevent aggregation (Webster et al. 2019; Hu et al. 2022).

Table 2.2: ATP-dependent chaperones, examples of their cofactors and functions.

Chaperones*	Cofactors	Functions
Chaperonins		
HSP60 (also known as CPN60), GroEL (*Escherichia coli*), CCT (mammals), thermosome (archaea)	HSP10 (also known as CPN10), GroES, prefoldin	Protein folding, prevention of aggregation
HSP70 system		
DnaK (*E. coli*), Ssa, Ssb (*Saccharomyces cerevisiae*), BiP (also known as GRP78) (mammals; ER)	HSP40, DnaJ, Sis1, Hdj1, NEFs, GrpE, HSP110	Unfolding, disaggregation, stabilization of extended chains, translocation across organelle membranes, folding, regulation of the heat-shock response, targeting substrates for degradation
HSP90 system		

Table 2.2: Continued

HptG (*E. coli*), GRP94 (ER)	HOP, p50, AHA1, p23, FKPB52, UNC45	Binding, stabilization and maturation of steroid receptors and protein kinases, delivery to proteases, buffer for genetic variation, regulation of substrate selection and fate, myosin assembly
HSP100		
ClpA, ClpB, ClpX, HslU (bacteria; mitochondria and chloroplasts), p97, RPT1–RPT6 (eukaryotic)	HSP70 system, ClpP, ClpS	Unfolding, proteolysis, thermotolerance, resolubilization of aggregates, remodelling

AHA1, activator of HSP90 ATPase 1; BiP, binding immunoglobulin protein; CCT, chaperonin-containing TCP1 complex; ER, endoplasmic reticulum; FKBP52, 52 kDa FK506-binding protein; GRP78, 78 kDa glucose-regulated protein; HSP, heat shock protein; HOP, HSC70–HSP90-organizing protein; NEFs, nucleotide exchange factors. *****The species and/or localization is specified in brackets.
(Source: Saibil, 2013)

2.8 Lipase specific foldase

Lif (lipase-specific foldase) proteins are classified as foldases and play a crucial role in lipase folding, leading to the production of active lipase (Rios et al., 2018; Verma et al., 2020). There are three strategies for producing active lipase using lipase-specific foldases. First, the lip and lif genes can be

expressed in different vectors and hosts, with the foldase and enzyme being co-incubated. Second, the lip and lif genes are expressed in separate vectors but within the same expression host. Finally, both the lip and lif genes can be expressed on a single plasmid, utilizing one or two promoters to generate functional lipase (Pulido et al. 2020). *Pseudomonas aeruginosa* Lif consists of five domains: the transmembrane -helical domain (TMD), the unstructured variable linker domain (VLD), the extended helical domain (EHD), and two mini-domains (MD1 and MD2). The catalytic folding domain (CFD), which includes MD1, EHD, and MD2, is essential for LipA activation. (Viegas et al. 2020).

Furthermore, the importance of co-expression of lipase (lipBT) and foldase (lifBT) derived from *Burkholderia territorii* GP3 was emphasised in order to produce fully activated lipase by expressing them in *E. coli* BL21 (DE3) pLysS. (Putra et al. 2019). It is important to note that strong hydrophobic interactions between the lip and lif residues may result in the formation of the lip-lif complex upon co-expression of the lip and lif genes; yet, lipase activity is not affected by the complex (Alnoch et al. 2018).

2.9 Protein disulphide isomerase

Protein disulfide isomerase (PDI) is a catalytic enzyme with three catalytic activities: redox-dependent chaperone, thiol-disulfide oxireductase, and disulfide isomerase (Khan and Mutus 2014). Protein disulfide isomerase (PDI) functions as a multifunctional redox chaperone in various cellular

locales, one of which is to improve protein folding and decrease aggregation by catalysing the production and breakage of thiol-disulfide bonds of Cys amino acids (Parakh and Atkin 2015; Contesini et al. 2020). For example, co-expression of MAS1 with PDI enhanced MAS1 lipase expression by 1.7 fold above single MAS1 expression in *Pichia pastoris* (Lan et al. 2016; Alias et al. 2023).

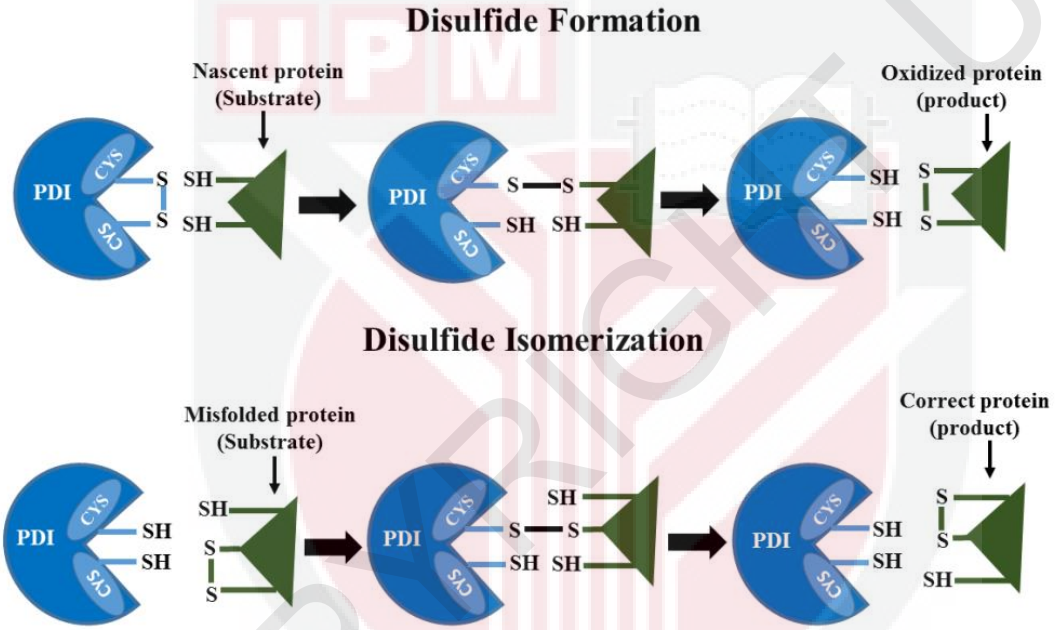

Figure 2.3: The multifunctional role of the PDI. A Shows the catalytic mechanism of PDI in the production of disulfide bonds in the protein (substrate). B shows how the PDI catalyses the conversion of a misfolded protein into the proper folded protein (substrate).
(Source: Alias et al., 2023)

PDI has two major functions which are the isomerization and reduction. The isomerization means it catalyzes the rearrangement of incorrectly formed disulfide bonds into the correct ones. While reduction means it can reduce disulfide bonds, which is important in certain cellular processes like protein quality control or in the ER stress response.In addition to its well-established

role in protein folding, PDI is implicated in other cellular processes, including cell signaling, apoptosis, and immune responses (Xu et al., 2021). It may also interact with other proteins to help maintain cellular homeostasis, especially under stress conditions.

Recent studies have extended the understanding of PDI beyond its classical role in protein folding, uncovering its involvement in several physiological and pathological processes, such as neurodegenerative diseases and inflammation. A recent study explored the role of PDI in neurodegenerative diseases like Alzheimer's and Parkinson’s (Yan et al., 2021). It suggested that PDI is involved in the folding of amyloid precursor proteins, and dysfunction of PDI might contribute to the misfolding and aggregation of these proteins (Fu et a;., 2020). Inhibiting or modulating PDI activity may offer therapeutic avenues for these conditions.

Inflammation is linked to various diseases, and recent work has demonstrated that PDI is involved in regulating immune cell function, especially in T-cell activation and response. A 2023 paper found that PDI plays a role in controlling the activation of inflammatory pathways, highlighting its potential as a target for controlling immune-related diseases (Shu et al., 2023).

CHAPTER 3

METHODOLOGY

3.1 Strain, vectors and reagents

The pET-32b(+) was used as the cloning and expression vector throughout the study. The cloning and the expression hosts, *Escherichia coli* TOP10 and *E. coli* Origami B (DE3) were obtained from the lab culture collection, respectively. The pBB550 was obtained from Institute of Biosciences (IBS,UPM). The pBB550 is a vector contains the insert molecular chaperone such as dnaK, dnaJ, GroESL. All restriction enzymes and T4 DNA ligase used in this study were purchased from NEB (Ipswich, MA, USA) and Thermo Fisher Scientific (Waltham, Massachusetts, United States), respectively.

3.2 Codon optimization and Gene Synthesis of LipJ15 and LifJ15

Photobacterium sp. J15 lipase (LipJ15) and lipase chaperone (LifJ15) gene sequences were obtained from GeneBank (accession number LSNH01000002.1), and the coding sequences of lipase and lipase chaperone were codon-optimized and synthesized by Integrated DNA Technologies as pUCIDT::PMLJ15 . Specific nucleotides of the LipJ15 and LifJ15 genes were changed according to codon preference to optimize protein expression in *E. coli.*

3.3 Cloning of synthetic PMLJ15 gene

The plasmid designated pUCIDT::PMLJ15 was first transformed into competent *E. coli* TOP10 cells by the heat shock procedure. The pUCIDT:: PMLJ15 plasmids were extracted following a plasmid mini prep from an overnight culture of a single colony of successfully transformed cells. Then, the pUCIDT::PMLJ15 plasmids were digested with *Msc*I and *Bpu*1102I (*BIp*I) at 37°C for 1 h. The digested PMLJ15 were analyzed on 1% agarose gel, and the desired band was excised from the gel and purified using DNA gel purification kit. The purified PMLJ15 was then ligated into similarly digested pET-32b(+) vector using T4 DNA ligase at 4°C for 18 h. The ligation ratio was 3:1 (insert:vector). The recombinant plasmid was then transformed into *E. coli* Top10. The ligated product (now designated pET-32b(+)::PMLJ15) were analyzed on 1% agarose gel and further confirmed by Colony PCR and Sanger sequencing (Apical Scientific Sdn. Bhd.).Then the verified recombinant plasmid was transformed into expression host, *E.coli* Origami B (DE3).

The ligated product was confirmed by colony PCR amplification using the following designed primers with *Msc*I and *Bpu*1102I for restriction sites (RE) incorporated on the forward and reverse primers respectively:

Forward primer for PMLJ15:
5'-GTT CTG GCC ATA TGC ACC-3'
Reverse primer for PMLJ15:
5'-TAT TGC TCA GCG GTG GCA-3'
The underlined sequences are the respective restriction endonuclease (RE)

sites. After incubation at 95 °C for 1 min, 35 repeated cycles of thermal denaturation at 95 °C for 1 min, annealing at 47 °C for 60 s, and extension/termination at 72 °C for 5 min were performed. The PCR products were analysed on 1% agarose gel.

3.4 Co-expression LipJ15 with pBB550

The heat shock procedure was done twice. The 50ul of competent cell was thaw on ice for five minutes. Then, about 1ug of pET-32b(+)::LipJ15 (approximately 2.5 ul) was added in the competent cell. The mixtures were let in the ice for 30 minutes. After 30 minutes of incubation, the mixture was put in the 42^{o}C of water bath for 45 seconds. Then immediately was put in the ice for five minutes. At the room temperature, 500ul of sterile LB medium was added in the mixture and was incubated for 1 hour at 37^{o}C. After 1 hour incubation, the mixture was pour into the LB agar then let it overnight at 37^{o}C.The preparation of competent cell of *E.coli* TOP10/pET-32b(+)::LipJ15 was prepared. After competent cell preparation was done, the second heat shock procedure was done by transformed the pBB550 in the *E.coli* TOP10/pET-32b(+)::LipJ15. Thus, there will be two plasmids in the *E.coli* TOP10 which are LipJ15 and pBB550.

3.5 Optimization Expression of recombinant lipase in *E.coli*

The positive transformant was cultured overnight initially into 10 ml LB medium supplemented with 100ug/ml of ampicillin. Next day, 2% overnight

grown culture was inoculated into 50ml LB (1.25 gram of LB powder with 50ml distilled water) containing 100ug/ml of ampicillin and incubated at 37°C with shaking at 200rpm. A total range of 0.0mM to 0.6mM of IPTG was added to cultures with A600 of 0.5-0.7 and the cells were grown at 20°C for 16 h. The culture were harvested by centrifugation and resuspended cells in 50 mM Tris–HCl buffer, pH 8.0. The resuspended culture was subjected to sonication (Q55 Sonicator from QSonica,USA) with 4 × 30 s with 30s pause followed by centrifugation (10,000 ×*g*, 10 min) to obtain the supernatant. The crude protein was subjected to molecular protein determination by SDS-PAGE and lipase assay.

3.6 SDS-PAGE analysis

The molecular weight of PMLJ15 was estimated by using standard protocol described by (Laemmli 1970) .All the protein samples were mixed with 2X SDS sample buffer (1M Tris HCl , pH 6.8, 10% SDS, 0.5% bromophenol blue, 0.5% β-mercaptoethanol).The samples were boiled for 5 min prior to loading into the gel. The polyacrylamide gel was prepared and casted by using the following recipes:

Table 3.1: Recipes for polyacrylamide gel preparation

4 ml of stacking gel (4%)	10 ml of resolving gel (12%)
0.5 ml of bisacrylamide (40%)	3.0 ml of bisacrylamide (40%)
0.5 ml of Tris-HCl (1.0 M, pH 6.8)	2.5 ml of Tris-HCl (1.5 M, pH 8.8)

40 µl of SDS (10%),	100µl of SDS (10%),
2.92 ml of distilled water	4.3 ml of distilled water
5.0 µl of TEMED	8.0 µl of TEMED
40 µl of APS (10%)]	100 µl of APS (10%)].

The casted gel was assembled into the gel tank, which was filled with 1X running buffer [25 mM Tris-HCl, 200 mM glycine and 0.1% (w/v) SDS]. The gel was loaded with 10 µl aliquots of the prepared samples. The molecular mass of the protein was estimated using a protein standard marker (Unstained protein marker from Thermo scientific USA). The electrophoresis was conducted at 120 V for 90 min. The gel was then stained using Coomassie Brilliant Blue R 250 staining solution for 30 min. Excess stain was removed by soaking the gel for 2 h in destaining solution [50% distilled water, 40% methanol, 10% acetic acid (v/v)].

3.7 Detection of lipase activity by zymogram

Native polyacrylamide gel electrophoresis (Native PAGE) was performed using discontinuous gel system of Davis (1964). Gels were cast with 4% stacking gel and 8% resolving gel. The electrophoresis was conducted at 120 V for 90 min. The gel was then stained with 20% isopropanol for 20 min. Then, the gel was destain with distilled water for three times before soaking the gel with distilled water for 20 min. The gels were overlaid on tributyrin agar plate that was supplement with antibiotics and incubated at 37°C.

Depending on the amount of lipase, the activity was observed within 5–15 min to see a clear background.

3.8 Quantitative determination of lipase activity

3.8.1 Preparation of ρ-nitrophenol standard curve

A 300 µg/ml PNP (stock solution - 10X) of p-nitrophenol was prepared by diluting 0.03 g of ρ-nitrophenol in 100 ml distilled water. From this stock solution, 10 ml was pipette out into a clean 100 ml standard volumetric flask and make up to the mark using distilled water. This solution contains 30 µg/ml PNP (working standard solution). The standard assay mixture with total volume of 3.0 ml contained 2.0 ml of 0.1N NaOH and ρ-nitrophenol calibration curve at prepared concentration range of 0 - 30 µg and volume range 0 - 1 ml (refer Appendix C). The yellow color intensity was then measured using spectrophotometer at wavelength of 410 nm. The graph of absorbance vs concentration was then plotted. The graph is presented in the Appendix D.

3.8.2 Lipase assay

The lipase assay was carried out using ρ-nitrophenol butyrate (ρNPB) as the substrate. The assay mixture of 20 µl of 8 mM ρ-NP butyrate in acetonitrile, 220µl of 50 mM Tris-HCl buffer (pH 8.0) and 10 µl of enzyme. The mixture was incubated at 30 °C for 10 min with 250 rpm shaking. The hydrolytic

activity was measured at 415 nm using a microplate reader. One enzyme unit (U) was defined as the release of 1 µmol of p-NP per min under the standard assay conditions (Nolasco-Soria et al. 2024).

3.9 ELISA assay to identify the quantification of expressed his-tagged protein

His-Tag Elisa Detection Kit was used to determine the His-tag concentrations of recombinant PMLJ15 (Goodell et al. 2008). His-tagged PMLJ15 (50 µl), were added to the well of His-Tag plate. 50 µl of Anti-His monoclonal antibody was added to wells, followed by 260 µl of washing solution. The microplates were patted on paper to remove the residual liquid in the well. Afterwards, 100 µl of antibody tracer was added to wells and incubated for 30 min at room temperature, followed by the 260 µl washing solution. After that, the plate was patted, and the stop solution was added. Finally, the absorbance was read at OD 450 nm. The concentration of his-tagged protein was determined by extrapolating its OD value to the standard curve.

3.10 Homology modelling and structure evaluation

Homology modeling of J15 lipase was carried out using AlphaFold2 (https://alphafold.ebi.ac.uk/) to predict the protein structure of the LipJ15. The Lip15 model was evaluated by using PROCHECK (Laskowski et al. 1993), Verify 3D (Laskowski et al. 1993) and ERRAT (Colovos and Yeates 1993). The modelling were performed for lipase alone because the chaperone do

not involve in the biocatalysis reaction. The chaperones only act as helper to help the proper folding of the LipJ15 to be functional. A computational method called homology modelling, also known as comparative modelling, predicts a protein's three-dimensional structure by comparing its sequence to that of one or more known proteins. The AlphaFold2 transformed this procedure by offering incredibly precise protein structure predictions, even for proteins without known homologs.

3.11 Structural Analysis

3.11.1 Primary structure analysis

Evolutionary tree of LipJ15 was constructed by using MEGA 11 software (Tamura et al. 2021) at which 20 proteins with highest sequence identities to PMLJ15 were obtained via BLAST (Basic Local Alignment Search Tool) (Johnson et al. 2008).

3.11.2 Secondary structure analysis

The secondary structure analysis of LipJ15 was conducted by using PDBsum (Laskowski 2001), a web-based database of summaries and analyses of PDB structures. PDB file of LipJ15 was uploaded into the database and the secondary structures were analysed which include β-sheets, β-hairpins, helices, β-turns and γ-turns.

3.11.3 Overall structure analysis

The overall structure analysis of LipJ15 encompasses the analysis of B-factor and chemical interactions. The structure of LipJ15 was visualised using YASARA (http://www.yasara.org). The B-factor of all atoms in LipJ15 structure was plotted.The chemical interactions which include intramolecular and intermolecular interactions were analysed by using YASARA. The analysed interactions include hydrophobic interactions, hydrogen bonds, ionic interactions and π-π interactions.

3.11.4 Protein-Ligand Docking

Molecular docking is the process of predicting the preferred orientation and binding affinity of two molecules (typically a ligand and a receptor, such as a protein) when they interact to form a stable complex. Protein-ligand docking was conducted by using AutoDock via YASARA software. The ligand (substrates) used were ρNP-octanoate (C8) and ρNP-palmitate (C18) at which the SDF files were downloaded from PubChem repository (https://pubchem.ncbi.nlm.nih.gov/).

The LipJ15 was prepared by removing water molecules, adding missing hydrogen atoms, and checking for any structural issues. This preparation can be done in YASARA, where by load the protein structure (from PDB or AlphaFold2 predictions) and use tools for energy minimization, hydrogens addition, and protonation state adjustments. Similarly, the ligand (C8 and

C18) also has been prepared. This includes optimizing the structure, adding hydrogen atoms, and ensuring it has a proper 3D conformation.Grid maps were generated by AutoDock to represent the potential energy of the ligand (C8 and C18) when interacting with different parts of the LipJ15.

YASARA facilitates the creation of grid maps by defining the docking region on the LipJ15. Once the grid maps are generated, the actual docking process begins. YASARA interfaces with AutoDock to perform the docking simulation. After docking was completed, YASARA provided several visualization and analysis tools to examine the docking results. The binding modes of the ligand are displayed, and the best docking pose was selected based on the lowest energy score.

3.12 Structural comparison of LipJ15 with its close homologs

A DALI search (Holm and Rosenström 2010) was performed to identify enzymes which highest structural homology to LipJ15. PDB file of LipJ15 structure was uploaded into the server and the results were presented by Z score, rmsd, identity and number of aligned residues. The closest homolog of LipJ15 was then further analysed structurally.

CHAPTER 4

RESULT AND DISCUSSION

4.1 LipJ15 Structural Analysis

4.1.1 Primary Structure Analysis

Lipases have a molecular weight of 19-60 kDa and are known to be monomeric proteins (Chandra et al. 2020a). LipJ15 is a 31.5 kDa in size comprises of 295 amino acid residues. The amino acid composition is shown in Table 3. The total number of negatively charged residues (Asp and Glu) and positively charged residues (Arg, His and Lys) at neutral pH are 31 and 25, respectively resulting to the theoretical isoelectric point (pI) of 4.87.

```
        10         20         30         40         50         60
MGTSTDGINQ QGYTETKYPI VLVHGLFGFD TLAGMDYFYG IPQALTKSGA KVYVAQISAT

        70         80         90        100        110        120
NSTEVRGEQL LAQVEEVLAV TGAEKVNLIG HSHGGPTTRY VASVAPELVA SVTSIGGVNK

       130        140        150        160        170        180
GSYIADLTRN TIPEGSIPEG IGVKLAEGLT TLINLLSGGS HLPQDPLASL DALTTVGLME

       190        200        210        220        230        240
FNKKYPEGVP STYCGEGEFL ADNGVYYYSW TGTSNFTNLL DPTDGAMVIL GLAFDEPNDG

       250        260        270        280        290
LVGKCSTHLG KVIRDDYKMN HLDEINGMLG VTHLFETAPT TVYRQHANRL QQQGL
```

Figure 4.1: Amino acid sequence of Lip15. LipJ15 have 31.5 kDa in size comprises of 295 amino acid residues.

Analysis of amino acid composition shows that LipJ15 composed of mostly hydrophobic amino acids (51.01%) which are located in the core of the

protein. Among hydrophobic amino acids, Gly and Leu are the most abundant with 11.97% and 10.62%, respectively. Glycine is one of the best turn forming residues (Zhang et al. 2021) while Leucine act as helix stabilizer (Hadži et al. 2022). Besides, there are two cysteine residues in the LipJ15 sequence.

Table 4.1 : Amino acid composition of LipJ15

Amino Acid	Number of amino acid	Percentage (%)
Alanine (A)	20	6.85
Arginine (R)	6	2.05
Asparigine (N)	14	4.79
Aspartic Acid (D)	14	4.79
Cystine (C)	2	0.68
Glutamine (Q)	11	3.77
Glutamic Acid (E)	17	5.82
Glycine (G)	35	11.97
Histidine (H)	8	2.74
Isoleucine (I)	14	4.79
Leucine (L)	31	10.62
Lysine (K)	11	3.77
Methionine (M)	5	1.71
Phenylalanine (F)	8	2.74
Proline (P)	13	4.45
Serine (S)	17	5.82
Threonine (T)	28	9.59
Tryptophan (W)	1	0.34
Tyrosine (Y)	14	4.79
Valine (V)	23	7.88

The primary sequence of LipJ15 has been deposited in NCBI (National Center for Biotechnology Information) under the Accession no. WP_064608141.1 (Roslan et al., 2016). Analysis of the primary sequence of LipJ15 using BLASTp suggested that this enzyme shares the highest sequence identity of 71.77% with triacylglycerol lipase from *Vibrio cholerae* (accession no. P15493.2) against Swiss-Prot and 56.14% with lactonizing lipase from *Pseudomonas Aeruginosa* crystal structure (Accession no. 1EX9_A) against PDB database. The evolutionary tree of LipJ15 is shown in Figure 4.2. A total of 20 proteins were selected from the Blastp results with the highest identity to LipJ15.

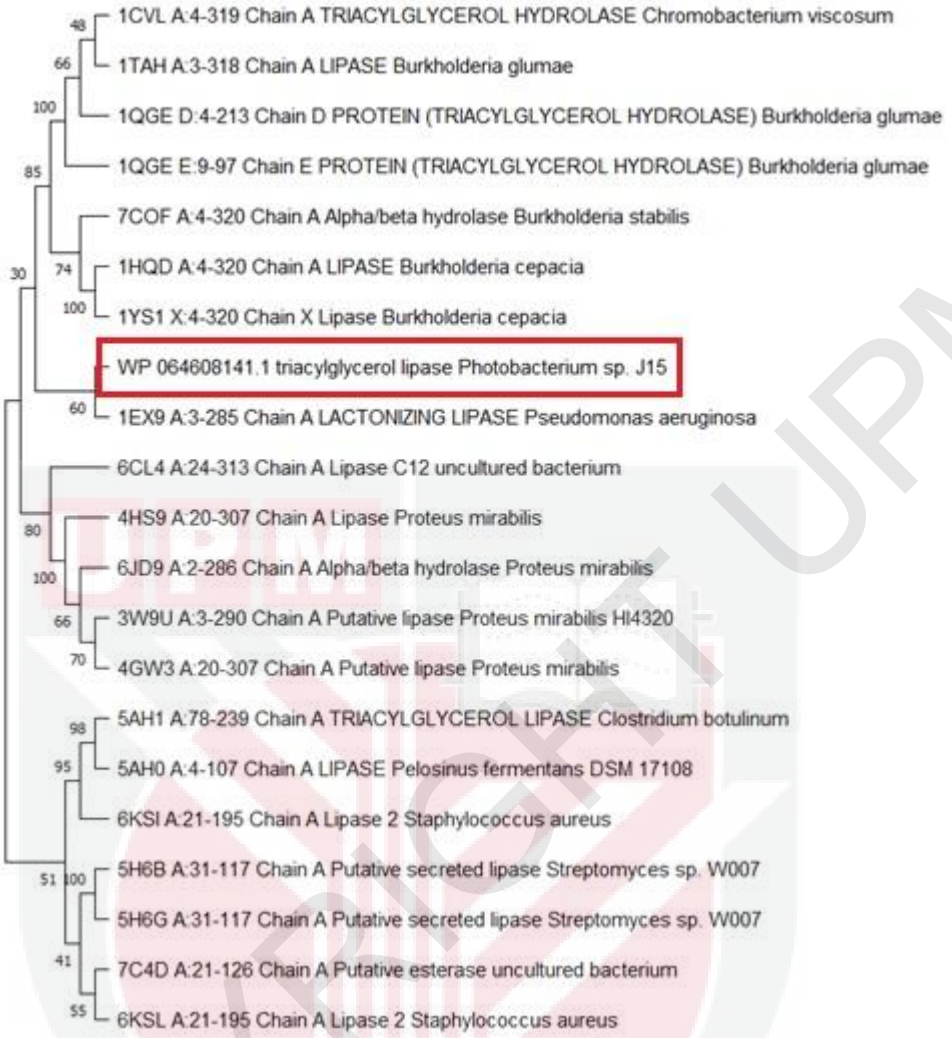

Figure 4.2: Evolutionary tree of LipJ15. Analysis involved 20 amino acid sequences. The evolutionary history was inferred by using the Maximum Likelihood method based on the Poisson correction model. The bootstrap consensus tree inferred from 100 replicates is taken to represent the evolutionary history of the taxa analysed. Evolutionary analyses were conducted in MEGA11.

A phylogenetic tree, often known as an evolutionary tree, is a diagram that illustrates the evolutionary relationships of several species, organisms, or genes. MEGA 11 was used for the evolutionary analyses (Tamura et al. 2021).The evolutionary tree shown in Figure 4.2 was generated by using maximum likelihood method and presented as bootstrap consensus tree with the boostrap values in percentage are shown next to the branches. From the evolutionary tree, it shows that Lip15 is closely related to lactonizing lipase

from *Pseudomonas aeruginosa*. Thus, the lipase subfamilies of LipJ15 is belongs to Family I.1.

4.1.2 Secondary Structure Analysis

The secondary structure analysis of LipJ15 was conducted by using PDBsum (Laskowski 2001), a web-based database of summaries and analyses of PDB structures. PDB file of LipJ15 was uploaded into the database and the secondary structures were analysed.The structure of LipJ15 comprises of two β-sheets from nine β-strands, two β-hairpins, 11 helices, 31 β-turns, and four γ-turns as shown in Figure 4.3. The two β-sheets (assigned as β-A and β-B) comprises of one mixed β-sheet and one antiparallel β-sheets. The mixed β-sheet (β-A) is cross over by hydrogen bonded, connecting a set of seven β-strands (Ile19-Val22, Val51-Val53, Val85-His90, Val108-Ile114, Leu199-Ala200, Val204-Gly211 and Lys250-Tyr256). The antiparallel β-sheets (β-B), involved two β-strands each (Thr30-Leu31 and Met34- Asp35), both β-sheets are stabilised by hydrogen bonds.

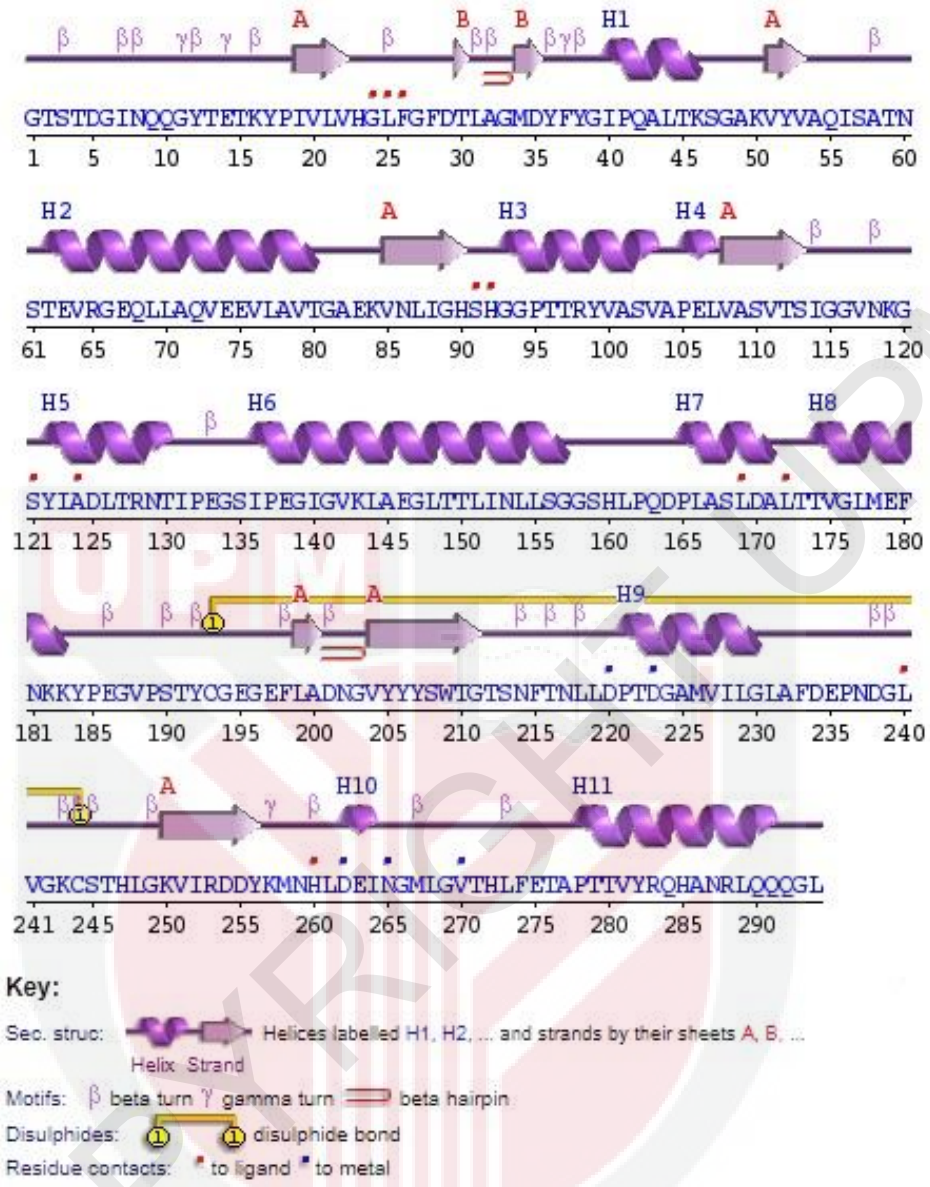

Figure 4.3: Secondary structure of LipJ15. The secondary structure of Lip15 comprises of nine β-strands, two β-hairpins, 11 helices, 31 β-turns, and four γ-turns.

There are two β-hairpins found in LipJ15 structure, connecting two β-strands of β-A and two of the β-strands of β-B of Class 2 and Class 3, respectively. A -hairpin is a polypeptide chain that folds back on itself and has at least two hydrogen bonds between two adjacent strands of an antiparallel β -sheet. Overall, there are two types of β-hairpins in proteins, which are distinguished by the length of the loop and the pattern of hydrogen bonds (Milner-White

and Poet 1986; DuPai et al. 2021). Helices are the most common form of secondary structure with α-helix as the most abundant out of all type of helices. Besides α-helix, another two possible but rare types of helices are 310 helix and α-helix. There are a total of 11 helices found in LipJ15 structure with the average of 3.6 residues per turn. Out of the 11 helices, nine of them are α-helices and two of them are 310 helices. The shortest helices are found to be the 310 helices, the short helices contain three residues (Pro10-Leu107 and Asp262-Ile264) while the longest α-helix involved 22 residues (Ile136-Gly157).

4.2 Evaluation of LipJ15 structure

The accuracy of the molecular structure improves with greater resolution. Validation was performed in this study using the Ramachandran plot (PROCHECK), ERRAT, and Verify3D. Laskowski et al. (1993) developed PROCHECK, a stereochemical validation programme. This programme is highly recommended for crystallographers for structure validation purposes because it provides an overall assessment of the stereochemistry of the structure as well as highlighting the regions that require further investigation. Planarity, chirality, phi/psi preferences, chi angles, non-bonded contact lengths, and unsatisfied donors and acceptors are all measurements that can be applied to evaluate the quality of a structure.

The PROCHECK programme was used to generate the Ramachandran plot shown in Figure 4.4. The Ramachandran plot shows the phi-psi torsion

angles for all residues in the protein structure (except for the chain termini). A good quality model, according to Laskowski et al. (1993), should have more than 90% of its residues in the most favoured region. According to the statistics, 89.8% of the residues are in the most favoured region, 9.4% are in the additional allowed region that excludes glycine and proline residues, and the last is 0.0% in the generously allowed region. There are two residues in the disallowed region (Leu161 and Ser91). Residues in the disallowed region could indicate local errors or poor protein structural accuracy. The distribution of the (ϕ, ψ) torsion angles in a dataset of protein structures is used to calculate the values of the favoured and disallowed regions (Sobolev et al. 2020).

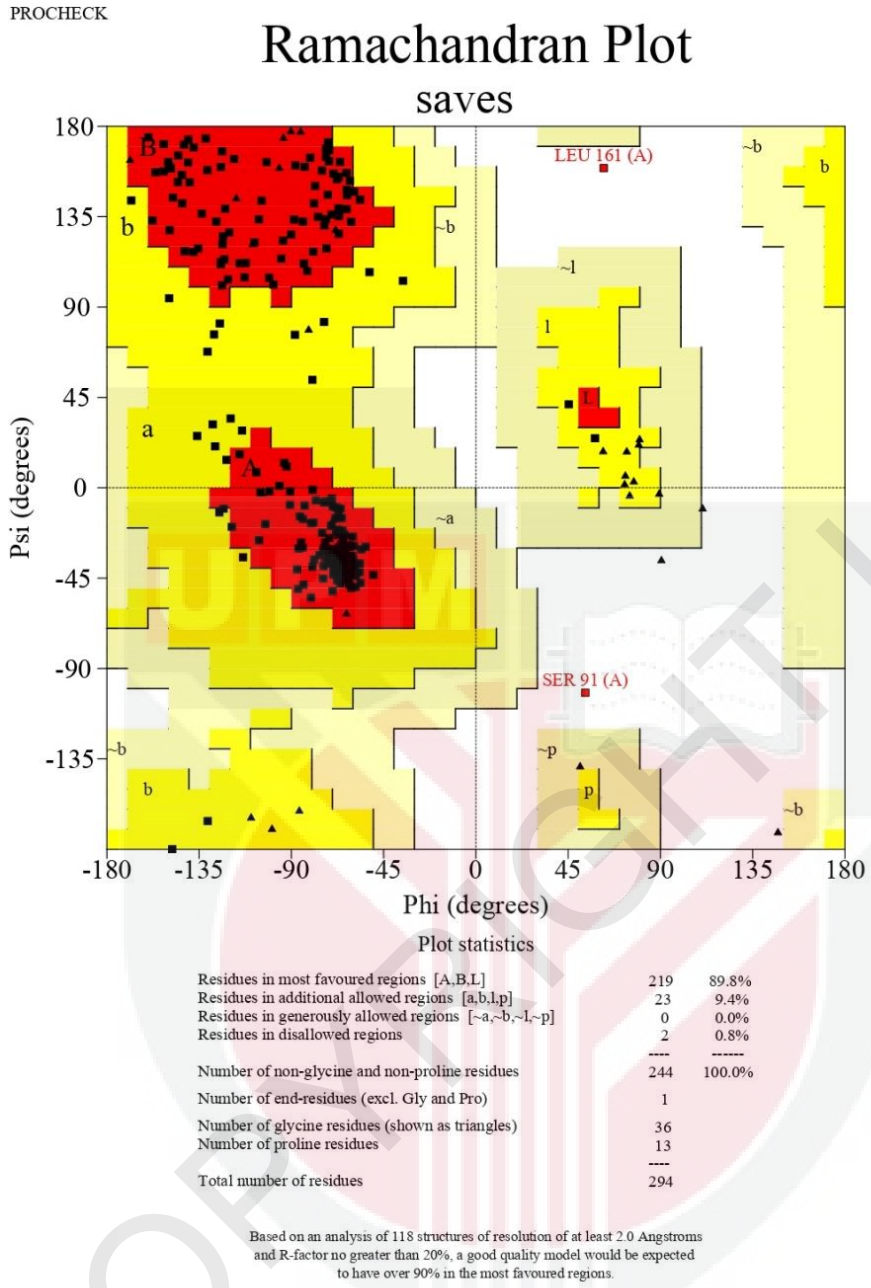

Figure 4.4: Ramachandran plot of LipJ15 model. The quality of the crystal structure is evaluated based on the most favoured region (red), additional allowed region (yellow), generously allowed region (light yellow) and disallowed region (white).

Next verification was performed through Verify3D. Verify3D is a programme that evaluates protein structures by comparing the atomic model (3D) with the amino acid sequence (1D). Based on its location and environment, each

residue in the analysed protein structure is assigned a structural class (Luthy et al. 1997). The propensity of each amino acid to exist in each such structural environment class is determined using statistics gathered from PDB structures, and the final score assigned to the protein structure is the sum of the individual residues' propensities (Kalman and Ben-Tal 2010).

From the analysis, it shows that 69.73% of the residues have averaged 3D-1D score >= 0.1, with the passing score should be at least 80% as shown in Figure 4.5. In the 3D plot, the lowest and the highest averaged scores are -0.17 and 0.45, respectively. Out of 294 residues, 93 residues lie under 0.1 of the 3D-1D score. The low scores of these residues are due to their environments in the structure are not compatible with the residues in the corresponding positions of the sequence.

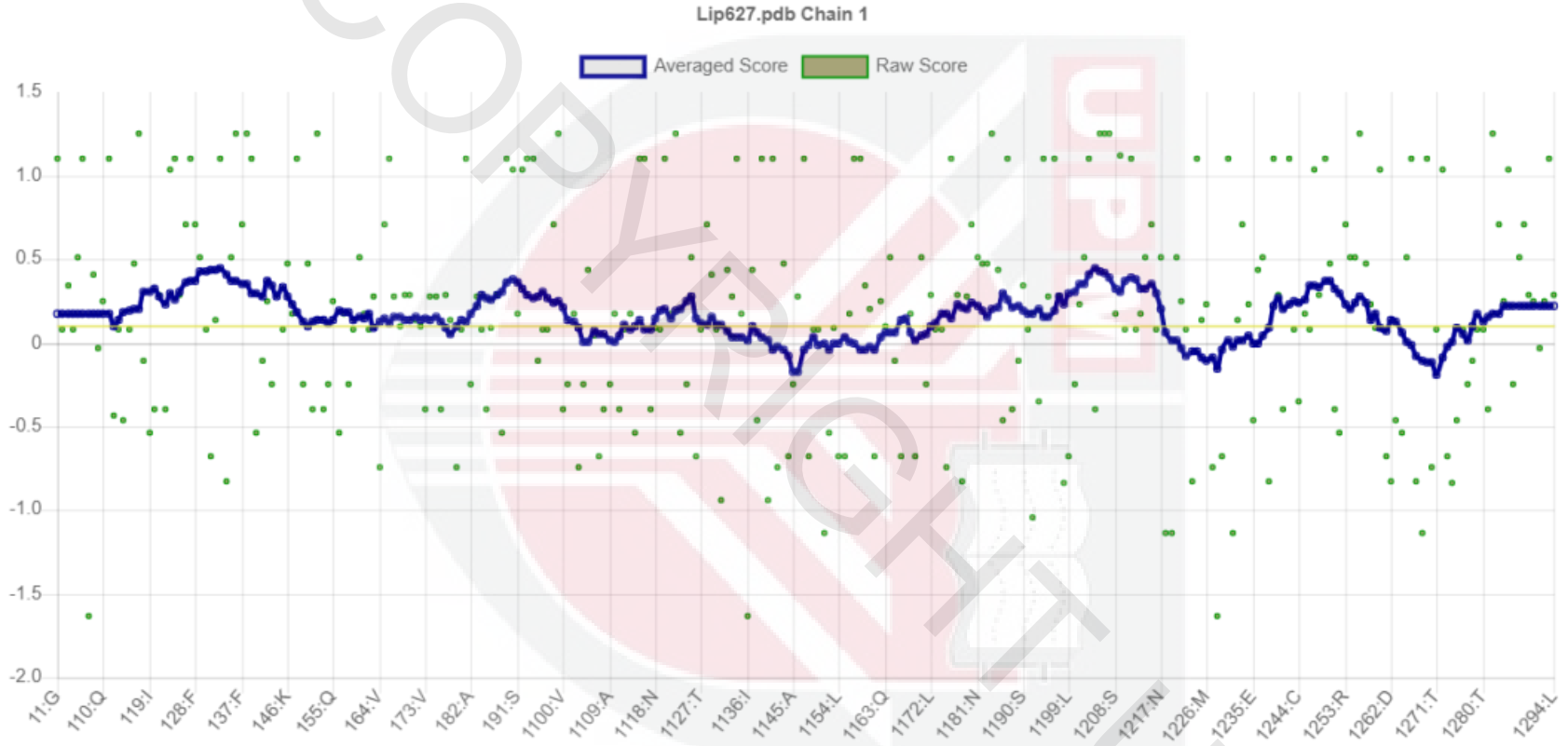

Figure 4.5: Verify3D result with 69.73% of the residues have averaged 3D-1D score >= 0.1

ERRAT was the third verification tool that has been used. ERRAT is a structure validation algorithm that protein crystallographers use to evaluate the progress of crystallographic model construction and refining. The statistics of non-bonded interactions between distinct atom types are analysed by this programme (Coloves and Yeales, 1993). ERRAT shows the error numbers as a function of the sliding 9-residue window position. The error functions are based on the statistics of non-bonded atom-atom interactions in high-resolution structures that have been reported with certainty. With confidence values of 95% and 99%, the programme is useful in validating and locating any regions of the structure that need to be rejected.

Figure 4.6 shows the generated ERRAT plot. Based on the graph, it shows that there are few residues with error confidence percentages of more than 95% which are Thr113, Ser114,Ile115, Gly116, Gly117, Val1188,Ile124, Ser209, Trp210, Thr211, Gly212, Thr213, Ser214, Phe216, Thr217, Asn266, Leu269 and Gly270. Based on ERRAT validation program, LipJ15 crystal structure exhibited an overall quality factor of 93.007% which shows that this structure can be considered as a good model.

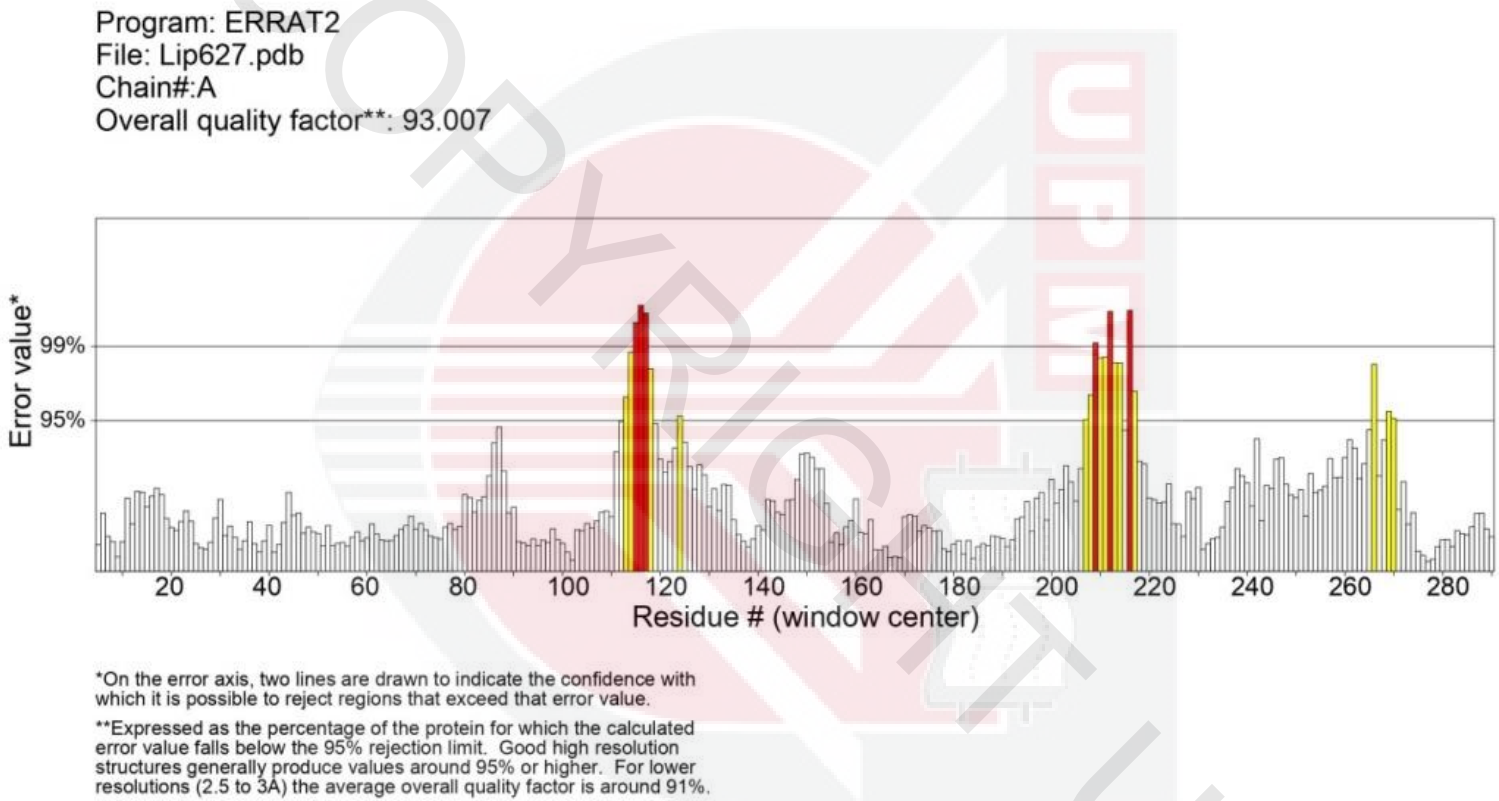

Figure 4.6: ERRAT plot of LipJ15 model. The overall quality factor of LipJ15 is 93.007 %.

4.3 Overall Structure Analysis

The α/β hydrolase fold family comprises a variety of enzymes including esterases, lipases, epoxides, hydrolases, dehalogenases, proteases and peroxidas that have been well studied and characterised. The structure of LipJ15 comprises of a molecule in asymmetric unit exhibiting a typical α/β hydrolase fold consisting of 38.1% helices, 13.9% strands, 11.9% turns, 0.3% of disulphide bond and 35.7% of others. Based on the multiple sequence alignment of LipJ15 with other structurally known family I motif enzymes, in which the N-terminal domain contained the GXSXG motif which included Ser92, Asp239 and His261 as the catalytic triad. There is one disulphide bridge and Ca^{2+} binding site are found in the structure (Figure 4.7).

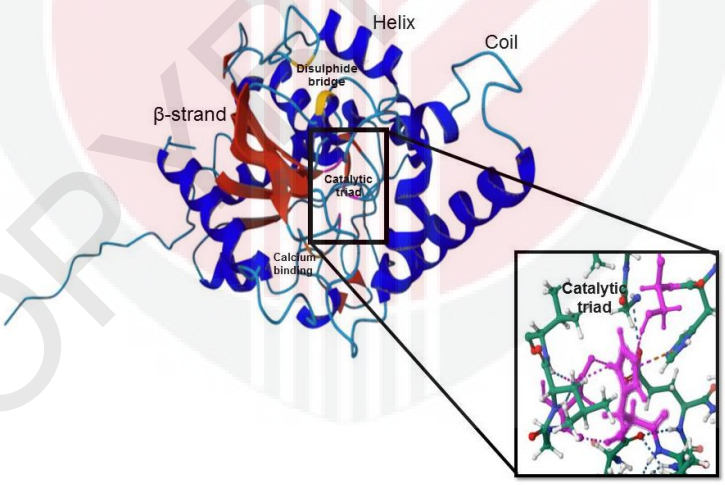

Figure 4.7: Structure of LipJ15 generated through AlphaFold2. Red: β-strand, Blue: Helix, Cyan: Coil, Yellow: Disulphide bridge, Orange: Calcium binding site. The catalytic triad shown in the black box composed of Ser92, Asp239 and His261.

4.3.1 B-factor

B-factor, also known as atomic displacement parameter (ADP) and temperature factor is a measure of how much an atom vibrates from its equilibrium position reflecting its mobility in space. B-factors are normally expressed in Å2 and the values are in the range of 2-200 Å2 (Carugo,2019).

In this study, the B-factor was performed to determine the active region, create structural bioinformatics, and examine the LipJ15 proteins' thermal stability.The primary justification for performing a B-factor analysis is to understand the dynamics of a protein or its active site in a physiological environment. By analysing B-factors, it can distinguish between more stable, rigid area like the active site and more flexible areas of the protein, like loops or unstructured regions (Dziadek et al., 2024; García‐Morales et al., 2024; Hjörleifsson et al., 2021).

This information aids in an understanding of substrate binding, enzyme catalysis, and protein function.Rigidity is crucial in the context of enzyme active sites for precise molecular recognition and catalysis. For an enzyme to effectively bind substrates and catalyse reactions, its active site must maintain a particular shape. The active site may not be able to effectively carry out the reaction or bind the substrate

if it were not flexible (low B-factors).

A stable environment for the enzyme to perform its catalytic function is thus provided by strong B-factors in the active site areas, which indicate that these

regions are rather rigid. Met1, the first residue has the lowest B-factor value of 42.1 Å2. Supposedly, a high B-factor value indicates that the N-terminal region of protein structure is highly flexible. According to Liu et al. (2014), B-factor measures and quantifies the vibrational motion of an atom. A low B-factor indicates that the atom has less mobile and in a well-ordered part of the structure, while a high B-factor usually suggests a highly flexible atom. In addition, study on 69 high resolution structures of apoenzymes by Yuan et al. (2003) found that the active site residues have an average to high B-factors as compared to the non-active site residues. This suggests that active site residues are generally flexible than the non-active site residues.

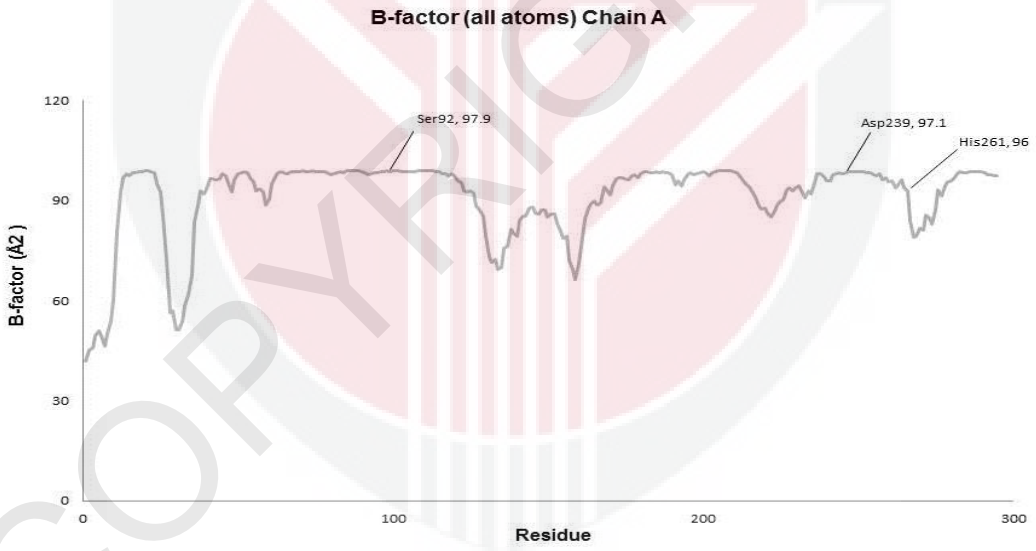

Figure 4.8: Plot of the total B-factor of LipJ15 structure. The B-factors of the active site residues are labelled as Ser92, Asp239 and His261 of 97.9 Å2, 97.1 Å2 and 96.0 Å2, respectively.

An enzyme's catalytic activity depends on the catalytic residues in its active site. These residues frequently participate directly in the actual chemical changes that occur during the reaction, substrate binding, and reaction intermediate

stabilisation. Their rigidity is crucial because it ensures precise interactions with the substrate and enhances the efficiency and specificity of the enzyme (Richard, 2019).Low B-factors for the catalytic residues would suggest that they are less precise and more flexible in their interactions with the substrate. This can make it more difficult for the enzyme to effectively catalyse the process. On the other hand, catalytic residues with high B-factors are stable and maintained in a fixed, ideal shape for catalysis. High catalytic efficiency and specificity depend on the enzyme's active site remaining well-defined, which is ensured by its rigidity (Diao et al., 2023).

In this study, the active site residues of LipJ15, Ser92, Asp239 and His261 have B-factor of 97.9 Å2, 97.1 Å2 and 96.0 Å2, respectively indicating a high rigidity.Besides, the residues lining up the active site region also have low B-factors of less than 90 Å2. The total B-factor for all atoms is shown in Figure 4.8. According to Yuan et al. (2003), kinetic stability of a protein highly depends on the rigidity of its active site. Hence, a protein with highly rigid active site tends to withstand harsh conditions better. This is because, an enzyme with highly rigid active site is hard to denature as the bonding and interactions at the region are strong. Therefore, the three catalytic residues are considered rigid because they typically show high B-factor values, indicating their structural stability and functional importance in catalysis. This rigidity ensures that these residues maintain the necessary interactions for efficient substrate binding and reaction mechanism execution.

4.3.2 Chemical interactions

The stability of a protein structure depends greatly on the chemical interactions such as hydrophobic interactions, hydrogen bonds, ionic interactions. A study on 22 proteins revealed that hydrophobic interactions contribute approximately 60% and hydrogen bonds (40%), making them as the two major contributors to the stability of proteins (Newberry & Raines, 2019). Highly specialised proteins called enzymes efficiently and selectively catalyse biological reactions. A comprehensive analysis of intramolecular and intermolecular interactions sheds light on how enzymes work, remain stable, and catalyse reactions. The structure, stability, and catalytic capabilities of the enzyme are greatly influenced by these interactions.

In this study, the intramolecular and intermolecular interactions of LipJ15 structure were analysed by using YASARA. The analysis by YASARA shows that LipJ15 structure is stabilised by intramolecular hydrophobic interactions, hydrogen bonds, ionic interactions, and π-π interactions. The number of intramolecular and intermolecular interactions are summarised in Table 4.2.

Table 4.2 : Intramolecular and intermolecular interaction of LipJ15

Interactions	Number of interactions
Intramolecular	
Hydrophobic interactions	2043

Table 4.2: Continued

Hydrogen bonds*	221
Ionic interactions	6
π-π interactions	55
Disulphide bond	1
Intermolecular	
Hydrogen bonds*	14 with Ca^{2+}
	110 with H2O

Intramolecular interactions are forces that occur within a single molecule, stabilising its three-dimensional structure and ensuring the integrity of its functional areas, including the active site (Jena et al., 2022). The four main forms of intramolecular interactions that occur in enzymes are hydrophobic, ionic, covalent, and hydrogen bonds.Together, these intramolecular pressures guarantee that the enzyme keeps its useful three-dimensional shape. The active site's spatial organisation is determined by the exact folding fuelled by these interactions, which guarantees appropriate substrate binding and efficient catalysis (Gu et al., 2023).

The interactions between molecules are referred to as intermolecular interactions, and they are essential for both the binding of enzymes to their substrates and the general function of enzymes. These interactions can be

classified as enzyme-substrate interactions, enzyme-cofactor interactions, enzyme-inhibitor interactions and protein-protein interactions.

From the analysis, there are 221 and 110 hydrogen bonds stabilizing the LipJ15 structure intramolecularlly and intermolecularly, respectively. A total of 124 intermolecular hydrogen bonds contributed by water molecules while 14 hydrogen bonds were formed with calcium ion.

Hydrophobic interactions are the major contributor to the stability of a protein structure. Out of 20 amino acids, there are nine hydrophobic residues which include alanine, valine, leucine, isoleucine, proline, phenylalanine, tryptophane, tyrosine and methionine. These residues prefer to contact with each other, and avoid contact with water molecules and mainly found in the core of the protein structure where it is inaccessible by water.

From the analysis, there are a total of 2043 hydrophobic interactions, contributing to the stability of LipJ15 structure. Ionic or ion pair interaction is another major interaction in a protein structure. Ion pair is an electrostatic interaction forms between acidic and basic amino acids which include aspartic acid, glutamic acid, histidine, arginine and lysine.

There are three different types of ion pair in protein which include salt bridge (< 4.0 Å), N-O bridge (centroid > 4.0 Å) and longer-range ion pair (> 5.0 Å) which were described extensively by Kumar and Nussinov (2002). LipJ15 structure has a total of six ionic interactions that occurred intramolecularly involving the side chain of the charged residues that are facing the exterior side of the protein. The

ion pair interactions are listed in Table 4.3.

Table 4.3 : Ion pair interactions of LipJ15

Basic residue	Acidic residue	Bond distance (Å)*
Lys184	Glu64	1.517
Arg129	Asp171	1.008
Lys183	Glu180	1.51
Lys244	Asp255	1.011
Arg254	Asp256	1.318
Arg254	Glu276	1.517

* Shortest bond distance.

The catalytic efficiency of the enzyme is determined by the interaction of intramolecular (such as hydrophobic interactions and hydrogen bonds) and intermolecular (such as enzyme-substrate binding) factors. Effective catalysis is made possible by intermolecular interactions with the substrate, whereas intramolecular factors dictate the stability and shape of the active site (Jin et al., 2020). The enzyme's capacity to reduce the activation energy and speed the reaction is strongly impacted by the strength and specificity of these contacts.

Both intermolecular and intramolecular interactions are fundamental to the structure and function of enzymes. Intermolecular interactions are necessary for substrate binding and catalysis, whereas intramolecular interactions preserve the enzyme's stable structure. Enzymes are particular and effective in their catalytic functions because of the careful balancing and optimisation of these interactions

(Menger et al., 2019). Enhancing medication development, enzyme engineering, and biochemical research requires a molecular understanding of these interactions.

4.3.3 Docking analysis

Protein–ligand docking was performed to predict the structure of the intra-molecular complex of LipJ15 and its substrates. The docking was performed using autodock via YASARA software. The ρ-nitrophenyl substrates (C8 and C18) were docked into LipJ15 to investigate the reason why longer chain substrates were not able to catalyse by LipJ15. This is because previous experimental (data not shown), the LipJ15 does not catalyse the long chain of olive oil. However, the experimental change the olive oil to pnp-butyrate as substrate. Surprisingly, the LipJ15 catalyse the pnp-butyrate.The ρNP-octanoate formed hydrogen bonds with the catalytic residues Asp239 and His261, and the oxyanion hole residue Tyr37 (refer Appendix F). The hydrogen bond distance between Asp239 and His261 in ρNP-octanoate (ρNPO) is 2.83 Å and 2.93 Å, respectively showing that the enzyme has higher affinity for ρNPO.

However, from the docking analysis, it is found that palmitate (C18) was not interacting with the catalytic residues, answering why there are no activity for these substrates (refer Appendix G). Ser92, Asp23 and His261 is an important catalytic residue of LipJ15 to interact with substrates. Although palmitate have high binding energy with Lip15, they are not able to be catalysed as there is no interaction with the nucleophile of the enzyme.

The narrow active site may be the reason for the specificity of LipJ15 on short chain length substrates, up to C8 only. According to Kingsley and Lill (2015), substrate tunnel acts as filters and was found to influence both substrate specificity and catalytic mechanism. Ligand binding occurs in two distinct processes, i) migration of ligand through the tunnel and subsequently, ii) the ligand binding to the active site (Koudelakova et al. 2013). Hence, substrate specificity not only determined by the complementary with the active site, but also the complementary with the binding tunnel. The failure of Lip15 in catalysing substrate longer than C10 may be due to the clashing with the tunnels geometry or substrate distortion caused during the entrance into the active site. From the docking analysis, the oxyanion residues are proven to be important in the catalysis. The identity of the residues made up the oxyanion holes (Tyr37, Asp239 and His261) shown in Figure 4.9.

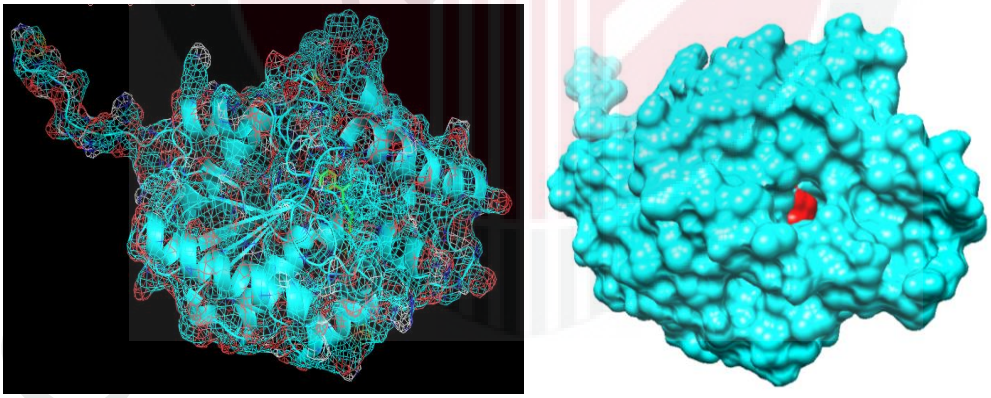

Figure 4.9: The oxyanion hole of LipJ15. Residues Tyr37, Asp239 and His261 made up the oxyanion hole were presented in the red colour. The oxyanion hole residues (Try37 and His261) were observed to hold the substrate (ρNPO) in place during the catalysis.

The docking analysis shows at least two of the oxyanion hole residues formed hydrogen bonds with the substrates showing that these residues are important in

the catalysis. According to Simone et al. (2004),the oxyanion hole residues act as the proton donors where their main chain nitrogen atoms act as hydrogen donors to the cleaved substrate, stabilizing the negative charge on the tetrahedral intermediates after the nucleophilic attack by the catalytic serine. Besides, a single residue may participate in both binding and catalysis (Gagneux and Diego 2016). In the docking analysis, His261 is clearly carried out both roles: binding and catalysis at which it holds the substrate in place by forming hydrogen between its main chain nitrogen atom and the substrate; and also involves as the nucleophile in the catalysis.

4.4 Structural comparison of LipJ15 with its close homologs

A DALI search (Holm 2020) was performed using the structure of LipJ15, and the result confirmed that LipJ15 shared low sequence identity but high structural similarity to the other members of this family as shown in Table 4.4, presented by Z score, root mean square deviation (RMSD), identity and number of aligned residues.

Table 4.4: Enzymes identified as structurally homologous to LipJ15 through DALI.

	PDB ID	Z score	Rmsd (Å)	Identity (%)	NRES[a]	Source of lipase
Lactonizing lipase	1EX9	45.3	1.2	57	285	*Pseudomonas aeruginosa*
Triacyl-glycerol-hydrolase	4LIP	39.7	1.9	44	319	*Burkholderia cepacia*
Alpha/beta	7COF	39.6	1.8	45	320	*Burkholderia*

Table 4.4: Continued

hydrolase						*stabilis*
Lipase	1YS1	39.5	1.9	44	320	*Burkholderia cepacia*
Putative lipase	4GXN	33.1	2.4	49	284	*Proteus mirabilis*

*NRES[a] No. of aligned residues

Lip15 has highest identity of 57% with the passenger domain of a lactonizing lipase (Chain A) from *Pseudomonas aeruginosa* (PDB ID 1EX9).

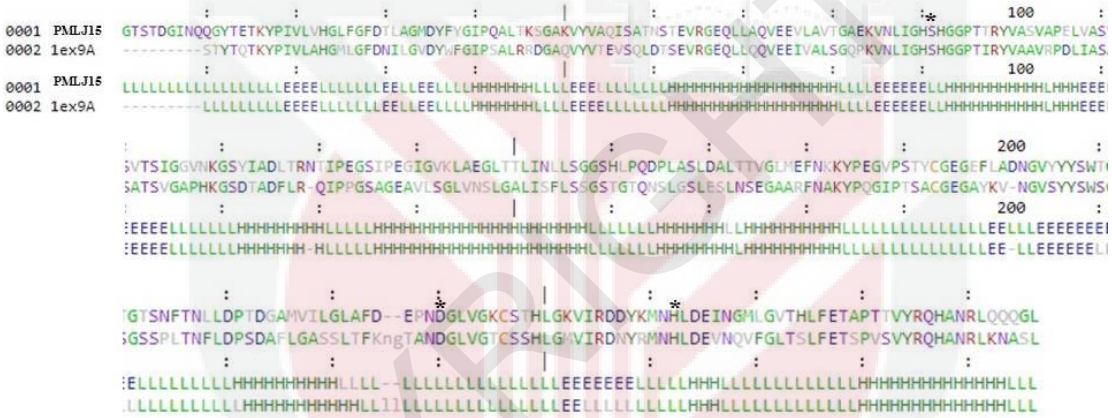

Figure 4.10: DALI Structural sequence alignment between LipJ15 and lactonizing lipase from *Pseudomonas aeruginosa*. Uppercase means structurally equivalent positions with LipJ15. Lowercase means insertions relative to LipJ15. The first part shows the amino acid sequences of the selected neighbours. The second part shows the secondary structure assignments by DSSP (H/h: helix, E/e: strand, L/l: coil). The most frequent amino acid type is coloured green in each column. The catalytic triad, Ser, Asp and His are marked with '*'.

4.5 Gene synthesis, cloning and expression

4.5.1 Plasmid construction and lipase gene cloning

The gene encoding for LipJ15 and its chaperone were subjected to codon

analysis in order to identify the presence of rare codon according to the codon usage of *E. coli* Origami B (DE3). The number of rare codon is about 9 codons. The codon-optimized synthetic *Photobacterium marinum* J15 lipase gene was designed as LipJ15 (888 bp) at the upstream region and its chaperone gene designated as LifJ15 (854 bp) at downstream region.This also included the 6X-His and thrombin cleavage site sequences making up 1,882 bp in-length. The cloning strategy for PMLJ15 was shown in Figure 4.11.

The *Msc*I site was located at the upstream region (5' end) followed by gene coding sequence for 6x-His, thrombin cleavage site, PMLJ15 and lastly *Blp*I site located at the downstream region (3' end). The restriction endonuclease sites are useful for subcloning of targeted gene into the expression vector. The 6x-His also known as 6xHis-tag originally developed for efficient protein purification (Hochuli et al. 1988). This six or more consecutive histidine residues is the most widely used purification tag. The thrombin cleavage site (TCS) typically incorporated between the linker region of fusion or affinity tagged and recombinant proteins. These two are very important during protein purification.

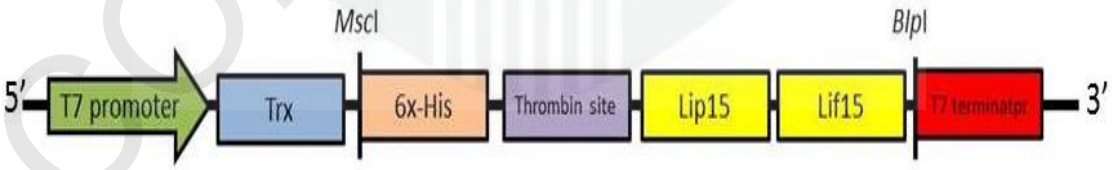

Figure 4.11: schematic presentation of cloning strategy for PMLJ15. The synthetic PMLJ15 had been included with the restriction endonuclease sites, His-tag and thrombin cleavage site at the upstream of the PMLJ15. The PMLJ15 have two genes which are Lip15 and Lif15 (lipase and lipase chaperone, respectively).

The PMLJ15 was digested by restriction enzymes which are *Msc*I and *Bpu*1102I

(*Blp*I) and cloned into pET-32b(+) vector as described in the materials and methods section. The construction of recombinant plasmid was illustrated in Figure 4.12. Both pET-32b(+) and PMLJ15 , the vector and the insert have compatible ends that share the same restriction sites, enabling them to join and form a circular DNA molecule.

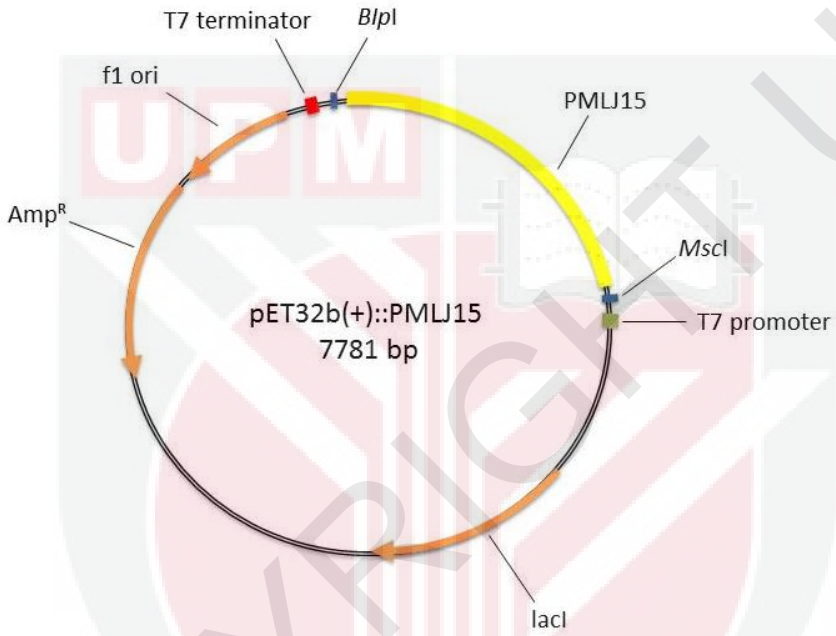

Figure 4.12: Schematic presentation of construction of the recombinant plasmid pET-32b(+)::PMLJ15. Relative positions of restriction sites are shown. Amp^R, β-lactamase gene conferring resistance to ampicillin; f1 ori, f1 bacteriophage origin of replication, which the arrow indicates the direction of (+) strand synthesis and, a *lac*I repressor that will bind to the *lac* operator to inhibit the transcription in *E. coli*.

The empty pET-32b(+) and pUCIDT::PMLJ15 was digested through double digestion. The double digestion means the gene was digested by using two different enzymes at the same time. In this study, both vectors used *Msc*I and *Blp*I that were cut at both end of the gene. After incubation at 37°C for 1 hour, the digested pET-32b(+) and PMLJ15 were analyzed on 1% agarose gel. As shown in Figure 4.13, the desired band of pET-32b(+) and PMLJ15 (~5,899 bp and

1,882 bp, respectively) were excised from the gel and purified using DNA gel purification kit. The purified PMLJ15 was then ligated into complementary end of digested pET-32b(+) vector using T4 DNA ligase at 4°C for 18 hours. The ligation mixture was then transformed into *E. coli* TOP10 competent cell with a volume ratio of 1:10 (ligation mixture:competent cell) through heat shock method. Heat shock transformation is a method of transformation that uses a calcium-rich environment generated by calcium chloride to overcome the electrostatic attraction between the plasmid DNA and the bacterial cellular membrane (Asif et al. 2017).

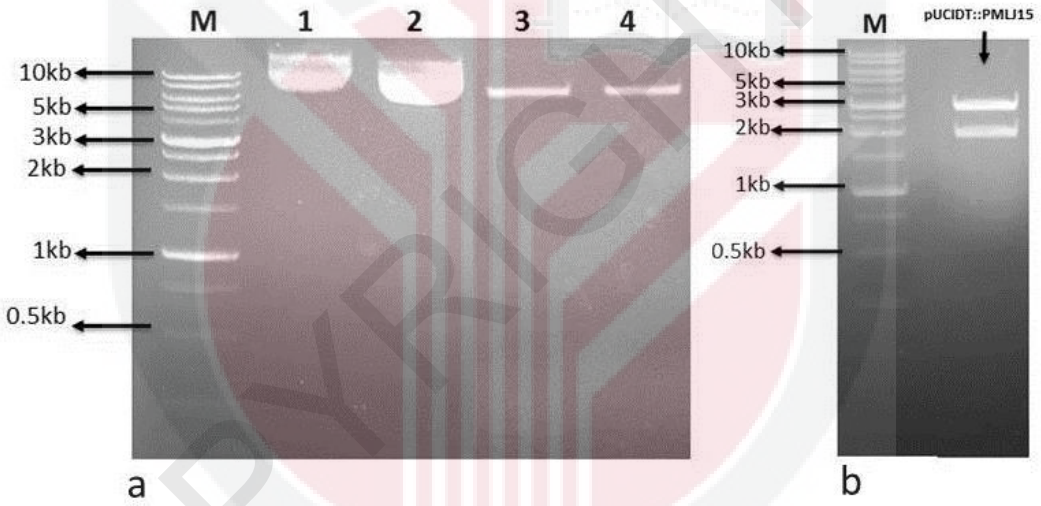

Figure 4.13: RE digestion for pET-32b(+) (a) and pUCIDT::PMLJ15 (b) with expected size 5,899 bp and 1,882 bp, respectively. Figure 4.13a Lane 1-2, Undigested pET-32b(+); lane 3-4, double digested pET-32b(+) and M, 1kb DNA ladder.

After a successful cloning, there are few methods of screening for the presence of an insert. Conventionally, the verification of insert has been done with restriction enzyme profiling; nonetheless colony PCR can perform which is also affordable and save time. Colony PCR is a technique for rapidly confirming if the desired gene construct is present in colonies of yeast or bacteria that have grown

up on selective media after a transformation step, or to amplify a specific portion of the construct (Bergkessel and Guthrie 2013). From the transformed plate, five colonies were picked to screen for the presence of PMLJ15 through this method. The colony PCR was used to amplify the insert DNA with primers that had *Msc*I and *Bpu*1102I restriction sites at their 5' ends, respectively, as described in the materials and methods section. As shown in Figure 4.14, it was verified and confirmed that the PMLJ15 was successfully inserted into the pET-32b(+). The expected size was about 1,882 bp, however further verification of insert need to be done in order to detect is there any mutation introduced during PCR.

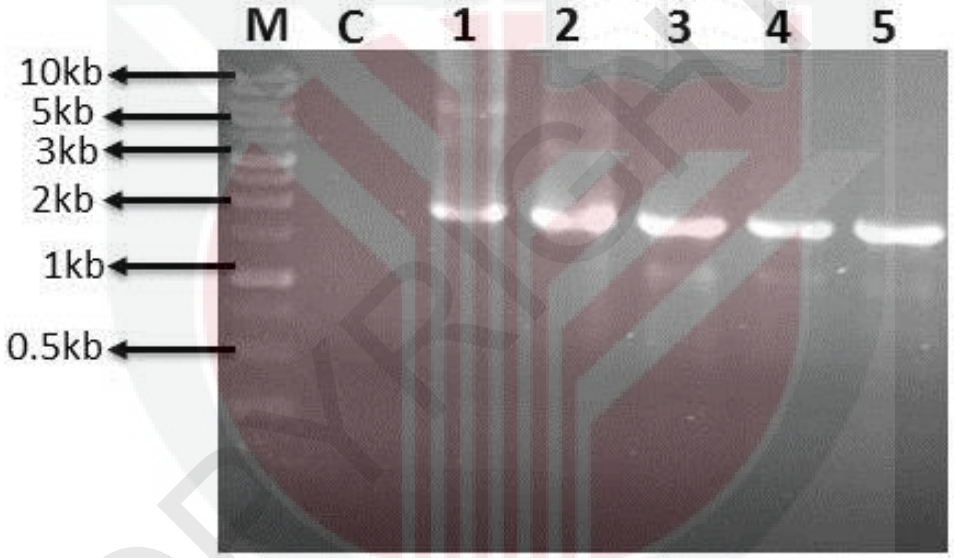

Figure 4.14: Colony PCR for pET-32b(+)::PMLJ15 with expected size 1,882 bp. Lane 1-5: successful transformed colonies; C: the negative control without the DNA template, and M:1kb DNA ladder.

Following the identification of a few positive clones, the recombinant plasmid pET-32b(+)::PMLJ15 were extracted and sent for Sanger sequencing. Sanger sequencing is a targeted sequencing method that seeks for specific DNA regions using oligonucleotide primers (Cheng et al., 2023). Sequencing helps to verify the sequence of the insert, the orientation of the insert, and the sequences of

junctions between the vectors and inserted genes. The insert was sequenced using universal primers which are T7 promoter and T7 terminator. The sequencing results of the positive clone pET-32b(+)::PMLJ15 were then undergo the multiple sequence alignment through Clustal Omega (https://www.ebi.ac.uk/Tools/msa/clustalo/). The data shows that the sequence does not have any mutation and was in the correct orientation (refer appendix F). To conclude, the cloning of PMLJ15 into pET-32b(+) was verified and successfull.

4.5.2 Expression of PMLJ15 in *E. coli* Origami B (DE3)

After the PMLJ15 sequence has been verified, the pET-32b(+)::PMLJ15 was transformed into the expression host *E. coli* Origami B (DE3) as described in the materials and methods section. However, there was no activity of lipase by using Kwon and Rhee method which is the olive oil (data not shown). The reaction should change its colour from blue to green. It was presumed that might the LifJ15 gene does not functional to help the Lip15 have a proper folding of its structure. Another alternative for this study was by co-expressing the pET-32b(+)::PMLJ15 with pBB550 as described in the materials and methods section. The pBB550 is a vector contains the insert molecular chaperone such as dnaK, dnaJ, GroESL. The GroESL chaperone is a well-characterized chaperone system in *E. coli* that forms a molecular "folding cage" for proteins. While the DnaK/DnaJ is a heat shock protein system in *E. coli* is involved in protein folding and is often used for co-expression to assist with lipase solubility. The co-expressing with these chaperones can reduce protein aggregation and enhance the production of soluble lipase.

Tributyrin agar plates are often used to test esterases and lipases because they contain tributyrin, a triglyceride. A visible zone of clearing or degradation surrounds the bacterial growth when lipases or esterases hydrolyse tributyrin, breaking the ester link and producing butyric acid. Lipase production by *E. coli* Origami B (DE3)/ pET-32b(+)::PMLJ15 and *E. coli* Origami B (DE3)/ pET-32b(+)::PMLJ15+pBB550 was verified by tributyrin agar plate assay using tributyrin as a substrate (Figure 4.15). Tributyrin agar plate is a differential media that tests an organism's ability to produce an enzyme that is able to hydrolyzed tributyrin. The presence of lipolytic enzyme hydrolyzes tributyrin surrounding colony, thus forming clearing zone (Carrazco-Palafox et al. 2018).

The empty vector pET-32b(+) in all host did not produce any halo zone showing that there is no lipase activity. The breakdown of tributyrin by plate Origami B (DE3) / pET-32b(+)::PMLJ15+pBB550 produced halo zone indicative of lipase production, whereas the Origami B (DE3) / pET-32b(+)::PMLJ15 did not produce any sign of halo zone (Figure 4.15b and 4.15a, respectively). This was possibly due to the formation of lipase inclusion bodies in the heterologous host (Shao et al. 2019). High-level expression of recombinant proteins in bacterial hosts such as *E. coli* often leads to the formation of insoluble inclusion bodies, which are composed of densely packed denatured protein molecules in the form of particles (Kaur et al. 2018).

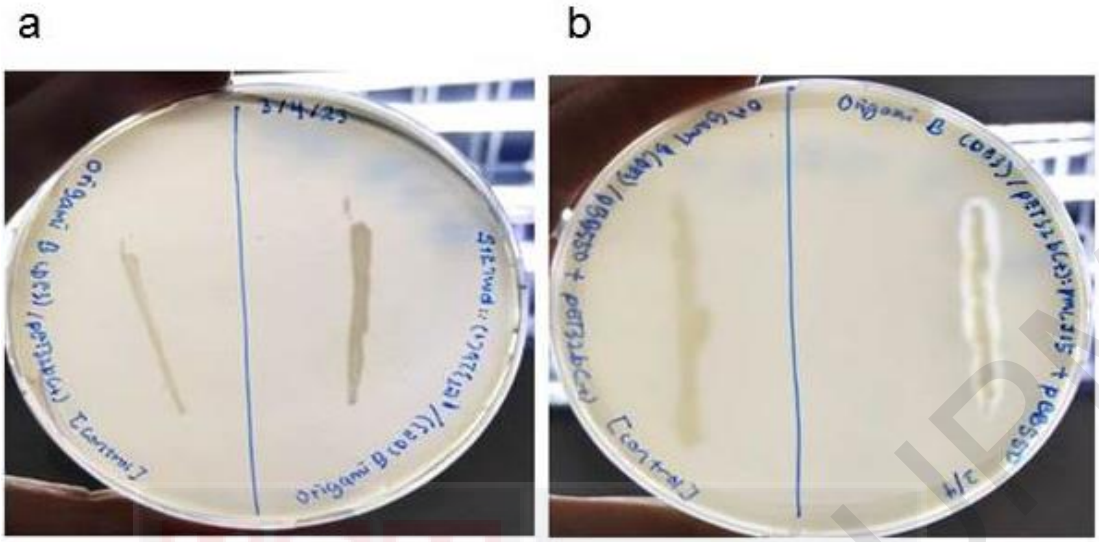

Figure 4.15: Lipase expression on tributyrin agar plates at 37 °C. (a) Origami B (DE3) / pET-32b(+)::PMLJ15. (b) Origami B (DE3) / pET-32b(+)::PMLJ15+pBB550. Plate Origami B (DE3) / pET-32b(+)::PMLJ15+pBB produced the lipase enzyme, which hydrolyzed the substrate tributyrin resulting in the formation of transparent halos around colonies, indicative of functional lipase. There was no halo zone surround the colonies of the Origami B (DE3) / pET-32b(+)::PMLJ15.

However, tributyrin alone is not sufficient to specifically verify lipase activity. This is due to the fact that tributyrin functions as a substrate for lipases and esterases. Tributyrin will be broken down by esterases, which also catalyse the hydrolysis of ester bonds, resulting in a clearing zone on the agar plate that is comparable to this. Because esterases also act on this substrate, tributyrin does not only confirm lipase action, even though it can show esterolytic activity.

Moreover, lipases typically act on larger triglyceride molecules and require a more specific test that distinguishes lipases from other esterases. Substrates such as olive oil, tributyrin in emulsions, or other triglycerides that more closely resemble natural lipids and give a more distinct signal of lipase activity than simple esterases might be used in a more conclusive experiment. However,

previously stated that the test using olive oil has been done but there is no sign of lipase activity (data not shown). The gene sequencing was confirmed it was a LipJ15 but the questioning is remained unanswered why it cannot hydrolase the longer chain of triglyceride, for example in this study by using olive oil. Still, through this study it was confirm it is a lipase because the PMLJ15 (Lip15 + unfunctional LifJ15) does not hydrolase the tributryrin but Lip15+pBB550 does hydrolase the tributryin. This shows that chaperones are required for the expression of lipases because they play a crucial role in ensuring the proper folding, stability, and functionality of the enzyme. Lipases are hydrolases that catalyze the breakdown of fats (lipids), and their proper folding is essential for maintaining the correct active site configuration for catalytic activity.

In order to improve the production of soluble active PMLJ15, the expression conditions of PMLJ15 in Origami B (DE3) were optimized (Figure 4.16 and 4.17). The expression was evaluated at seven different inducer concentrations (0.0mM, 0.1mM, 0.2mM, 0.3mM, 0.4mM, 0.5mM and 0.6mM). The *E. coli* strain was incubated at a temperature of 20°C, shaken at 180 rpm to achieve a maximum growth. The 20°C is a post induction temperature and this temperature since LipJ15 is a cold adaptive bacteria. Figure 4.16 shows the SDS-PAGE analysis of optimization of expression of Origami B (DE3) / pET-32b(+)::PMLJ15 both in supernatant and cells (Figure 4.16a and 4.16b, respectively), after induction with seven different concentration of IPTG.

Comparisons of the soluble and insoluble form show that PMLJ15 mostly present in the insoluble form obtained in each culture. A band with the expected size for

the lipase both in soluble and insoluble form was shown in Figure 4.16a and 4.16b, respectively. The overexpression of just one protein near to 45 KDa, presume that it corresponds to LipJ15. The fusions LipJ15 with the size of approximately 44.2 kDa (11.8kDa TrxA, 0.8kDa His-tag, 0.6kDa thrombin site, 31kDa LipJ15) while the LifJ15 with the size of approximately 33kDa. The size does not include LifJ15+LifJ15 because the gene was design as ATG in DNA for both LipJ15 and LifJ15. Thus, it is a start codon that codes for methionine. Translation begins by recognizing the start codon and incorporating methionine as the first amino acid.

When the cells were induced with IPTG, it showed that the insoluble fractions of the protein were higher than those in soluble fractions. The production of soluble lipase was similar for almost all IPTG concentration (0.1mM, 0.2mM, 0.3mM, 0.4mM, 0.5mM and 0.6mM). In contrast, the lipase expression in insoluble form exhibited different intensity of band, with maximum intensity was at 0.3mM of IPTG concentration (Figure 4.16b). Presume that the optimum IPTG concentration for LipJ15 was at 0.3mM. The result may be attributed to a decrease in the expression of genes controlled by T7*lac*, which may lead to a lower in the production of recombinant proteins, preventing protein overcrowding in the cytoplasm and promoting proper folding (Pulido et al. 2020; Ravitchandirane et al. 2022).

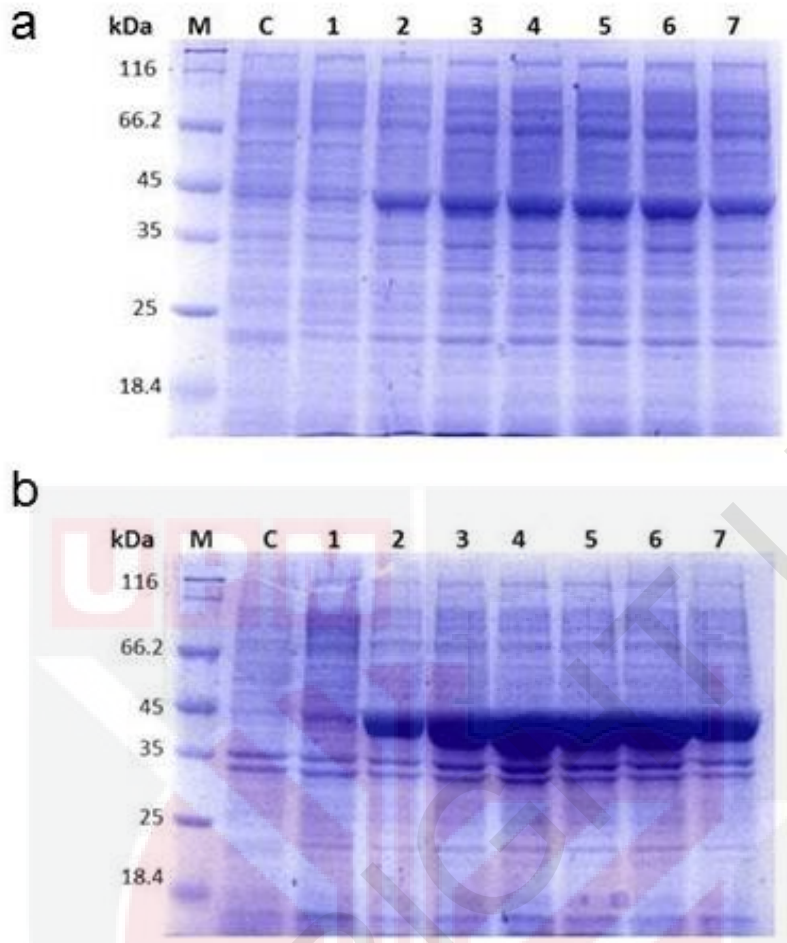

Figure 4.16: SDS-PAGE analysis of LipJ15 expression. A) Origami B (DE3)/ pET-32b(+)::PMLJ15 in soluble form; B) Origami B (DE3) / pET-32b(+)::PMLJ15 in insoluble form with induction at different concentration of IPTG at 20 °C for 18 hours. M: Ustained protein ladder. C: pET-32b(+) without insert gene. Lanes 1-7: IPTG concentration (0.0mM, 0.1mM,0.2mM,0.3mM,0.4mM,0.5mM and 0.6mM, respectively).

The cloning the PMLJ15 gene with fragment of its chaperone gene in the same plasmid is an acceptable strategy for soluble and active heterologous LipJ15 production. However, *E. coli* Origami B (DE3) / pET-32b(+)::PMLJ15 does not show any lipase activity as described in Figure 4.16 even though the LifJ15 was included. This is probably due to the LifJ15 either not functioning or low chaperone production. Other research conducted with foldases from *P. cepacia* or *Ralstonia* sp. have revealed similar results, including non-observable or low

chaperone production despite a strong promoter upstream of the gene (Quyen et al. 2012; Pulido et al. 2020).

Another strategy is to utilize foreign chaperone such pBB550 which contain dnaK, dnaJ and GroESL (Ravitchandirane et al. 2022). Surprisingly, it shows that there is lipase activity as compared to Origami B (DE3)/ pET-32b(+)::PMLJ15 as described in Figure 4.15 previously. However the expression for Origami B (DE3) / pET-32b(+)::PMLJ15 + pBB550 was unable to differentiate its appearance band. Maybe this is due to foreign chaperones, thus producing too many band. Strongly confirm that, it is proved that a chaperone is needed for LipJ15 expression as mentioned from the previous justification.

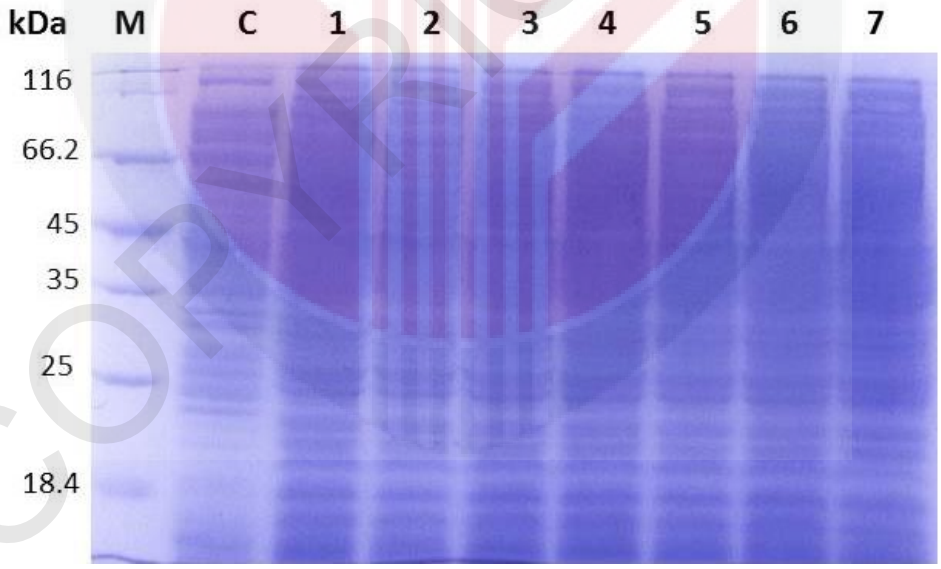

Figure 4.17: SDS-PAGE analysis of Lip15 expression in *E. coli* Origami B (DE3)/ pET-32b(+)::PMLJ15 + pBB550 in soluble form with induction at different concentration of IPTG at 20 °C for 18 hours M: Unstained protein ladder. C: pET-32b(+) without insert gene. Lanes 1-7: IPTG concentration (0.0mM, 0.1mM,0.2mM,0.3mM,0.4mM,0.5mM and 0.6mM, respectively).

4.5.3 Quantitative determination of lipase activity, lipase zymogram and ELISA analysis

Lipase from Origami B/pET-32b(+)::PMLJ15 + pBB550 was run for lipase assay. Lipase assay is typically carried out to show the lipase activity. One unit (U) of lipase activity is defined as the amount of enzyme that generates 1 µmol of fatty acids per minute under the specified assay conditions (Nema et al., 2019). The quantitative assays with IPTG concentration range of 0.0mM-0.6mM and at optimum temperature 20 ℃ were carried out to determine IPTG concentration profile. Based on Figure 4.18, it shows that the lipase activity was highest at 0.6mM. The activity profile does not correspond well to the SDS PAGE result.

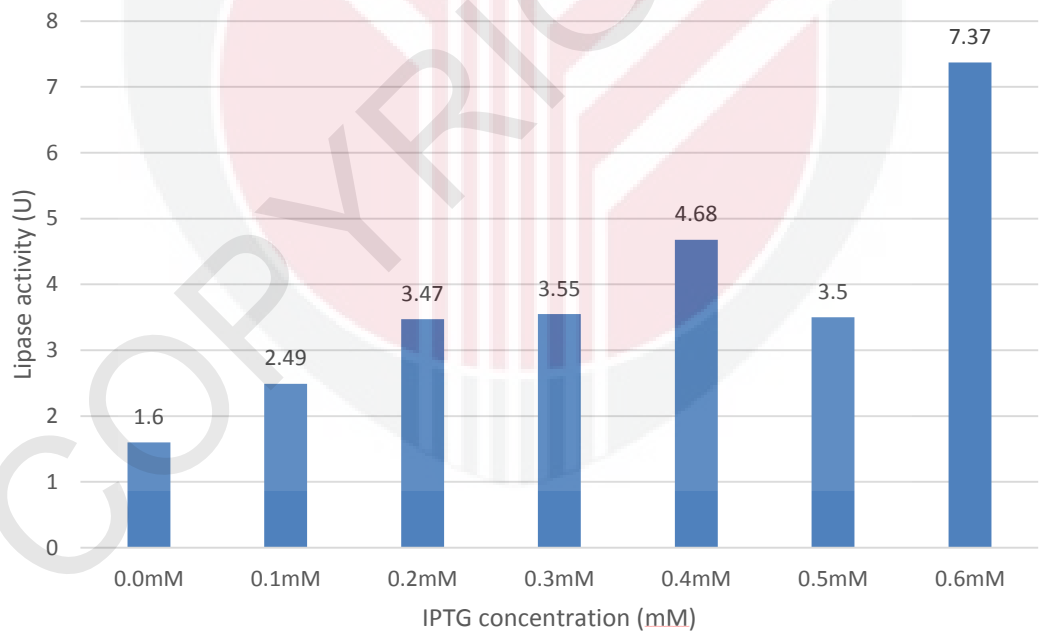

Figure 4.18: The quantitative assay to determine the optimum lipase activity at different IPTG concentration. The pNP-butyrate was used as a substrate for lipase assay. Lipase activity Origami B/pET-32b(+)::PMLJ15 + pBB550 by using pNP butyrate as substrate at different IPTG concentration. Incubate at 20C for 10min, 250rpm.

From the previous SDS PAGE analysis, it was concluded that 0.3 mM of IPTG was the optimal for LipJ15 activity. The difference in lipase production observed in SDS-PAGE analysis and lipase activity assays can be attributed to several factors related to protein expression, folding, maturation, and the assay conditions. At 0.3mM IPTG concentrations, SDS-PAGE may show high levels of lipase protein because more protein is being synthesised. Lower enzymatic activity can result from a significant amount of this protein being inactive or misfolded if the conditions are not ideal for protein folding. At 0.6mM IPTG concentrations, lipase production may be lower in terms of total protein (as seen in SDS-PAGE), but the protein may fold more efficiently and be more active, resulting in increased lipase activity.This implies that while moderate levels of IPTG may result in a more functionally active enzyme, overexpression at very high IPTG concentrations may cause misfolding, aggregation, or the production of inactive protein. Thus, in this study, a pNP-butyrate was used as lipase assay for LipJ15 to investigate whether this lipase it a functional enzyme or not.

Zymogram, or substrate gel electrophoresis, is a non-quantitative method for evaluation of enzymatic profiles (Leonard et al. 2018). The zymogram test is a validated observation test of enzyme activity that is carried out under non-denaturation situations. The LipJ15 inside the gel after running the NATIVE-PAGE will show the lipase activity through interaction with tributyrin through counterstaining method. The expression of LipJ15 demonstrated the positive zymogram test which reveal that the lipase activity in gel of heterologous expression (Figure 22).

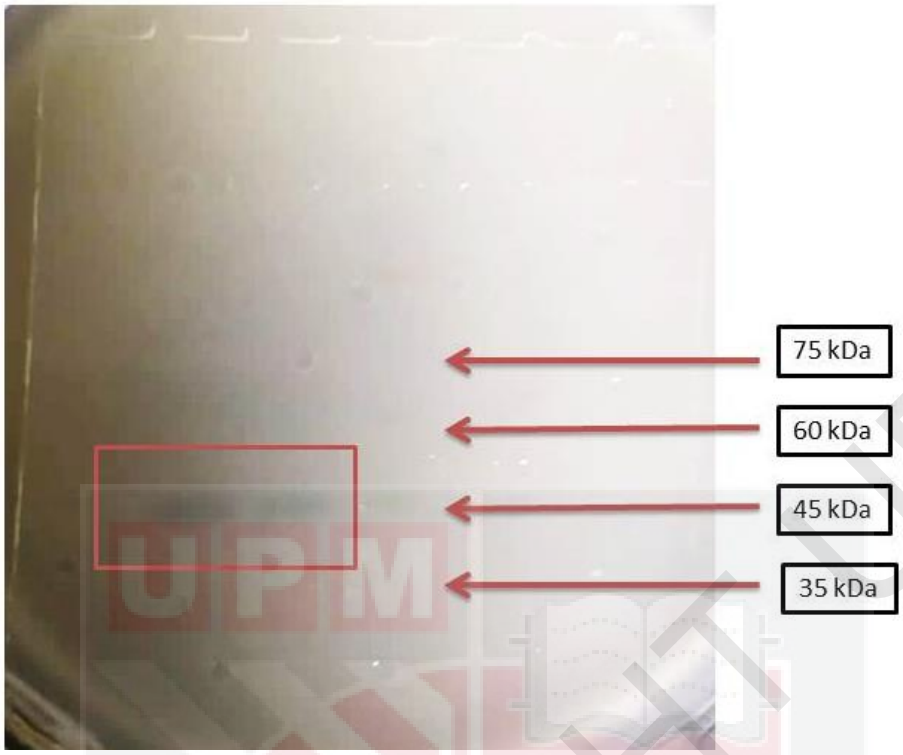

Figure 4.19: Zymogram demonstrating lipase activity towards tributyrin. The gel was overlaid on tributyrin agar plate and incubated at 37°C for 18h. A clear zone of hydrolysis could be seen, demonstrating lipase activity towards tributyrin along with pre-stained protein marker.

The quantitative analysis of his-tagged LipJ15 was carried out to determine the concentration (ng/ml) of his-tagged protein in the sample through ELISA assay. His- tagged ELISA assay demonstrated the concentrations of his-tag protein as shown in Table 4.5.

Table 4.5 : The concentration of his-tag protein in each respective sample

Sample	His-tag protein (ng/ml)
pET32b(+)::PMLJ15 (non-induced)	68.32
pET32b(+)::PMLJ15 (with IPTG)	256.13

The validation tests using His-tagged ELISA assay were carried out to confirm the His-tagged protein concentration based on antibody of His-tag and substrate interaction. The higher His-tag proteins showed the lighter blue or colorless, while the lower His-tag protein concentrations showed the darker yellow color (Figure 4.20).

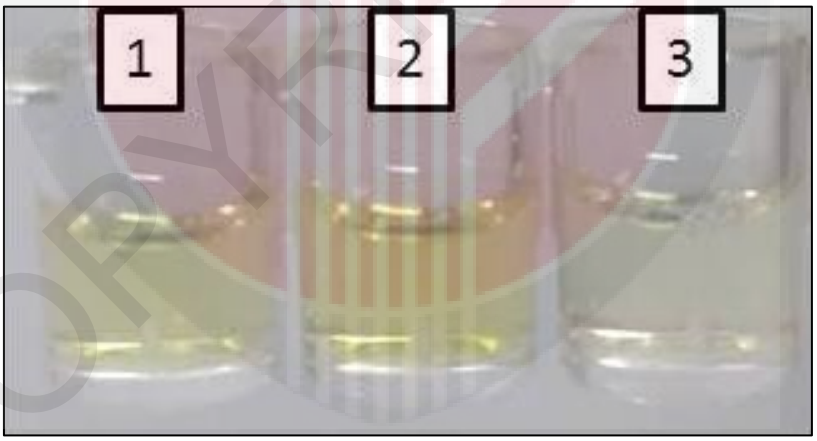

Figure 4.20: His-tag ELISA assay. Lane 1 to 3 shows the 98.62, 68.32, and 256.13 ng/mL for empty pET-32b(+), pET-32b(+)::PMLJ15, and pET-32b(+)::PMLJ15 induced with 0.3mM IPTG. The darker yellow color represents the less concentration of protein His-tag and the more colorless represents the higher His-tag protein concentration.

CHAPTER 5

CONCLUSION AND RECOMMENDATIONS FOR FUTURE RESEARCH

5.1 Conclusion

The study of macromolecular structure has been a great interest for decades. Many applications such as biodiesel may benefit through the understanding of the structures. The low structural identity of 57% of LipJ15 to a structurally available crystal model make this study as a great interest. The information provided by the structure can help to better understand the function and mechanism of the protein.

The final model of LipJ15 was validated by using Ramachandran plot, Verify3D and ERRAT programs. Through the structural comparison of LipJ15 structure with its closest homologs, it was found that LipJ15shared low sequence identity but high structural similarity to the other lipase, especially to its closest homolog, the lactonizing lipase of *Pseudomonas aeruginosa*. Besides, protein-ligand docking analysis of LipJ15 unlocked the riddle on its high substrate specificity toward short chain length substrates. From the analysis, LipJ15 has high binding energies toward all the substrates, but substrates longer than C10 were not interacting with the nucleophile Ser92, unabling them from being catalysed. The introduction of foreign chaperone does improve the folding of LipJ15 to become functional protein. However, further study need to be done in order to increase the activity of the LipJ15. While chaperones can significantly improve the soluble expression of lipases

by assisting with proper folding and preventing aggregation, several challenges remain. The potential for overburdening the host system, the risk of chaperone-induced misfolding, and the need for optimized expression conditions all require careful consideration.

5.2 Recommendation for future research

In this study, the cloning of LipJ15 and its structure was successfully modelled and various structural analysis ware conducted. All these works and informations explore several areas of studies in the future. These studies are listed below:

i. Further optimization need to be done regarding to increase the level of expression LipJ15 and quantitative determination of LipJ15. This also includes the purification so that crystallisation can be done.

ii. Crystallisation and structural elucidation of LipJ15 complexed with substrate or substrate analog. This study might provide more comprehensive explanation on the high substrate specificity of LipJ15 towards short chain length substrate..

iii. Molecular dynamics simulation in order to understand the physical basis of the structure and function. The study can be conducted using various physical parameters such as pH, temperature and solvent.

REFERENCES

Abed SM, Elbandy M, Abdel-Samie MA, et al (2020) Screening of lipases for production of novel structured lipids from single cell oils. Process Biochem 91:181–188. https://doi.org/10.1016/j.procbio.2019.12.010

Ahmed EH, Raghavendra T, Madamwar D (2010) An alkaline lipase from organic solvent tolerant *Acinetobacter* sp. EH28: Application for ethyl caprylate synthesis. Bioresour Technol 101:3628–3634. https://doi.org/10.1016/j.biortech.2009.12.107

Al-Ghanayem, A. A., & Joseph, B. (2020). Current prospective in using cold-active enzymes as eco-friendly detergent additive. Applied microbiology and biotechnology, 104(7), 2871-2882.

Alabdalall AH, Al-Anazi NA, Aldakheel LA, et al (2021) Application and characterization of crude fungal lipases used to degrade fat and oil wastes. Sci Rep 11:1–10. https://doi.org/10.1038/s41598-021-98927-4

Albayati SH, Masomian M, Ishak SNH, et al (2020) Main Structural Targets for Engineering Lipase. Catalysts 10:1–34

Alias FL, Nezhad NG, Normi YM, et al (2023) Recent Advances in Overexpression of Functional Recombinant Lipases. Mol Biotechnol 65:1737–1749. https://doi.org/10.1007/s12033-023-00725-y

Alnoch RC, Stefanello AA, Paula Martini V, et al (2018) Co-expression, purification and characterization of the lipase and foldase of *Burkholderia* contaminans LTEB11. Int J Biol Macromol 116:1222–1231. https://doi.org/10.1016/j.ijbiomac.2018.05.086

Andualema B, Gessesse A (2012) Microbial lipases and their industrial applications: Review. Biotechnology 11:100–118

Angkawidjaja C, You D ju, Matsumura H, et al (2007) Crystal structure of a family I.3 lipase from *Pseudomonas* sp. MIS38 in a closed conformation. FEBS Lett 581:5060–5064. https://doi.org/10.1016/j.febslet.2007.09.048

Anobom CD, Pinheiro AS, De-Andrade RA, et al (2014) From structure to catalysis: Recent developments in the biotechnological applications of lipases. Biomed Res Int 2014:. https://doi.org/10.1155/2014/684506

Arpigny JL, Jaeger KE (1999) Bacterial lipolytic enzymes: Classification and properties. Biochem J 343:177–183. https://doi.org/10.1042/0264-6021:3430177

Arumugam A, Ponnusami V (2017) Production of biodiesel by enzymatic transesterification of waste sardine oil and evaluation of its engine

performance. Heliyon 3:e00486. https://doi.org/10.1016/j.heliyon.2017.e00486

Asif A, Mohsin H, Tanvir R, Rehman Y (2017) Revisiting the mechanisms involved in calcium chloride induced bacterial transformation. Front Microbiol 8:6–10. https://doi.org/10.3389/fmicb.2017.02169

Azanaw A, Birlie B, Teshome B, Jemberie M (2022) Case Studies in Chemical and Environmental Engineering Textile effluent treatment methods and eco-friendly resolution of textile wastewater. Case Stud Chem Environ Eng 6:100230. https://doi.org/10.1016/j.cscee.2022.100230

Basheer SM, Chellappan S, Beena PS, et al (2011) Lipase from marine *Aspergillus awamori* BTMFW032: Production, partial purification and application in oil effluent treatment. N Biotechnol 28:627–638. https://doi.org/10.1016/j.nbt.2011.04.007

Bassegoda A, Pastor FIJ, Diaz P (2012) *Rhodococcus* sp. strain CR-53 lipr, the first member of a new bacterial lipase family (Family X) displaying an unusual Y-type oxyanion hole, similar to the *Candida antarctica* lipase clan. Appl Environ Microbiol 78:1724–1732. https://doi.org/10.1128/AEM.06332-11

Basso A, Serban S (2019) Industrial applications of immobilized enzymes—A review. Mol Catal 479:110607. https://doi.org/10.1016/j.mcat.2019.110607

Bender J, Rydzewski K, Broich M, et al (2009) Phospholipase PlaB of *Legionella pneumophila* represents a novel lipase family. Protein residues essential for lipolytic activity, substrate specificity and hemolysis. J Biol Chem 284:27185–27194. https://doi.org/10.1074/jbc.M109.026021

Bergkessel M, Guthrie C (2013) Colony PCR. Methods Enzymol 529:299–309. https://doi.org/10.1016/B978-0-12-418687-3.00025-2

Bhatwa A, Wang W, Hassan YI, et al (2021) Challenges Associated With the Formation of Recombinant Protein Inclusion Bodies in *Escherichia coli* and Strategies to Address Them for Industrial Applications. Front Bioeng Biotechnol 9:. https://doi.org/10.3389/fbioe.2021.630551

Biškauskaitė R, Valeikienė V, Valeika V (2021) Enzymes for leather processing: Effect on pickling and chroming. Materials (Basel) 14:1–11. https://doi.org/10.3390/ma14061480

Bornscheuer UT (2018) The fourth wave of biocatalysis is approaching. Philos Trans R Soc A Math Phys Eng Sci 376:1–7. https://doi.org/10.1098/rsta.2017.0063

Bornscheuer UT, Huisman GW, Kazlauskas RJ, et al (2012) Engineering the third wave of biocatalysis. Nature 485:185–194. https://doi.org/10.1038/nature11117

Borrelli GM, Trono D (2015) Recombinant lipases and phospholipases and their use as biocatalysts for industrial applications. Int J Mol Sci 16:20774–20840. https://doi.org/10.3390/ijms160920774

Borza P, Peter F, Paul C (2015) Improved enantioselectivity of *Candida antarctica* A lipase through sol-gel entrapment. Univ (Timisoara) 60:49–54

Cai Y, Wang L, Liao X, et al (2009) Purification and partial characterization of two new cold-adapted lipases from mesophilic *Geotrichum* sp. SYBC WU-3. Process Biochem 44:786–790. https://doi.org/10.1016/j.procbio.2009.03.011

Carrazco-Palafox J, Rivera-Chavira BE, Ramírez-Baca N, et al (2018) Improved method for qualitative screening of lipolytic bacterial strains. MethodsX 5:68–74. https://doi.org/10.1016/j.mex.2018.01.004

Carugo, O. (2019). Maximal B-factors in protein crystal structures. Zeitschrift für Kristallographie-Crystalline Materials, 234(1), 73-77.

Castilla A, Panizza P, Rodríguez D, et al (2017) A novel thermophilic and halophilic esterase from *Janibacter* sp. R02, the first member of a new lipase family (Family XVII). Enzyme Microb Technol 98:86–95. https://doi.org/10.1016/j.enzmictec.2016.12.010

Cavalcante FTT, Neto FS, Rafael de Aguiar Falcão I, et al (2021) Opportunities for improving biodiesel production via lipase catalysis. Fuel 288:. https://doi.org/10.1016/j.fuel.2020.119577

Cesário LM, Pires GP, Pereira RFS, et al (2021) Optimization of lipase production using fungal isolates from oily residues. BMC Biotechnol 21:1–13. https://doi.org/10.1186/s12896-021-00724-4

Chandra P, Enespa, Singh R, Arora PK (2020a) Microbial lipases and their industrial applications: A comprehensive review. BioMed Central

Chandra P, Enespa, Singh R, Arora PK (2020b) Microbial lipases and their industrial applications: A comprehensive review. BioMed Central

Charbonneau DM, Beauregard M (2013) Role of Key Salt Bridges in Thermostability of *G. thermodenitrificans* EstGtA2: Distinctive Patterns within the New Bacterial Lipolytic Enzyme Family XV. PLoS One 8:1–18. https://doi.org/10.1371/journal.pone.0076675

Chauhan M, Chauhan RS, Garlapati VK (2013) Evaluation of a new lipase from *Staphylococcus* sp. for detergent additive capability. Biomed Res

Int 2013:. https://doi.org/10.1155/2013/374967

Cheng, C., Fei, Z., & Xiao, P. (2023). Methods to improve the accuracy of next-generation sequencing. Frontiers in bioengineering and biotechnology, 11, 982111.

Choi JM, Han SS, Kim HS (2015) Industrial applications of enzyme biocatalysis: Current status and future aspects. Biotechnol Adv 33:1443–1454. https://doi.org/10.1016/j.biotechadv.2015.02.014

Choudhury P, Bhunia B (2015) Review Article Industrial Application of Lipase : a Review. Biopharm J 1:41–47

Cipolatti EP, Valério A, Henriques RO, et al (2020) Production of new nanobiocatalysts via immobilization of lipase B from *C. antarctica* on polyurethane nanosupports for application on food and pharmaceutical industries. Int J Biol Macromol 165:2957–2963. https://doi.org/10.1016/j.ijbiomac.2020.10.179

Colovos C, Yeates TO (1993) Verification of protein structures: Patterns of nonbonded atomic interactions. Protein Sci 2:1511–1519. https://doi.org/10.1002/pro.5560020916

Contesini FJ, Davanço MG, Borin GP, et al (2020) Advances in recombinant lipases: Production, engineering, immobilization and application in the pharmaceutical industry. Catalysts 10:1–33. https://doi.org/10.3390/catal10091032

Costa MJ, Silva MRL, Ferreira EEA, et al (2020) Enzymatic biodiesel production by hydroesterification using waste cooking oil as feedstock. Chem Eng Process - Process Intensif 157:108131. https://doi.org/10.1016/j.cep.2020.108131

Cowan D.A. , Fernandez-Lafuente R (2011) Enhancing the functional properties of thermophilic enzymes by chemical modification and immobilization. Enzyme Microb Technol 49:326–346. https://doi.org/10.1016/j.enzmictec.2011.06.023

Cowan, D. A., & Tombs, M. P. (2020). Industrial enzymes. In *Biotechnology-The science and the business* (pp. 319-350). CRC Press.

da Silva JL, Sales MB, de Castro Bizerra V, et al (2023) Lipase from *Yarrowia lipolytica*: Prospects as an Industrial Biocatalyst for Biotechnological Applications. Fermentation 9:. https://doi.org/10.3390/fermentation9070581

De Marco A, Ferrer-Miralles N, Garcia-Fruitós E, et al (2019) Bacterial inclusion bodies are industrially exploitable amyloids. FEMS Microbiol Rev 43:53–72. https://doi.org/10.1093/femsre/fuy038

Degórska O, Szada D, Zdarta A, et al (2022) Immobilized Lipase in Resolution of Ketoprofen Enantiomers: Examination of Biocatalysts Properties and Process Characterization. Pharmaceutics 14:. https://doi.org/10.3390/pharmaceutics14071443

Diao, D., Simaan, A. J., Martinez, A., & Colomban, C. (2023). Bioinspired complexes confined in well-defined capsules: getting closer to metalloenzyme functionalities. *Chemical Communications*, *59*(29), 4288-4299.

Dulęba J, Czirson K, Siódmiak T, Marszałł MP (2019) Lipase B from *Candida antarctica* — the wide applicable biocatalyst in obtaining pharmaceutical compounds. Med Res J 4:174–177. https://doi.org/10.5603/mrj.a2019.0030

DuPai CD, Davies BW, Wilke CO (2021) A systematic analysis of the beta hairpin motif in the Protein Data Bank. Protein Sci 30:613–623. https://doi.org/10.1002/pro.4020

Dziadek, Ł. J., Sieradzan, A. K., Czaplewski, C., Zalewski, M., Banaś, F., Toczek, M., ... & Giełdoń, A. (2024). Assessment of Four Theoretical Approaches to Predict Protein Flexibility in the Crystal Phase and Solution. Journal of Chemical Theory and Computation, 20(17), 7667-7681.

Eddehech A, Rahier R, Smichi N, et al (2021) Heterologous expression, kinetic characterization and molecular modeling of a new sn-1,3-regioselective triacylglycerol lipase from *Serratia* sp. W3. Process Biochem 103:87–97. https://doi.org/10.1016/j.procbio.2021.02.009

Ehlert J, Konemann J, Zumbrägel N, Preller M (2019) Lipase-Catalyzed Chemoselective Ester Hydrolysis of Unsymmetric Biphenyl Esters. Molecules 24:4272

Elemosho R, Suwanto A, Thenawidjaja M (2021) Extracellular expression in *Bacillus subtilis* of a thermostable *Geobacillus stearothermophilus* lipase. Electron J Biotechnol 53:71–79. https://doi.org/10.1016/j.ejbt.2021.07.003

Ewis HE, Abdelal AT, Lu CD (2004) Molecular cloning and characterization of two thermostable carboxyl esterases from *Geobacillus stearothermophilus*. Gene 329:187–195. https://doi.org/10.1016/j.gene.2003.12.029

Ferrero GO, Sánchez Faba EM, Rickert AA, Eimer GA (2020) Alternatives to rethink tomorrow: Biodiesel production from residual and non-edible oils using biocatalyst technology. Renew Energy 150:128–135. https://doi.org/10.1016/j.renene.2019.12.114

Fu, J., Gao, J., Liang, Z., & Yang, D. (2020). PDI-regulated disulfide bond

formation in protein folding and biomolecular assembly. Molecules, 26(1), 171.

Gagneux P, Diego S (2016) Protein Structure and Function. https://doi.org/10.1093/jhered/esh040

García‐Morales, A., Pulido, N. O., & Balleza, D. (2024). Relation between flexibility and intrinsically disorder regions in thermosensitive TRP channels reveal allosteric effects. European Biophysics Journal, 53(1), 77-90.

Goodell V, McNeel D, Disis ML (2008) His-tag ELISA for the detection of humoral tumor-specific immunity. BMC Immunol 9:1–8. https://doi.org/10.1186/1471-2172-9-23

Gu, J., Xu, Y., & Nie, Y. (2023). Role of distal sites in enzyme engineering. *Biotechnology Advances*, *63*, 108094.

Gürkök S (2019) Microbial Enzymes in Detergents: A Review. Int J Sci Eng Res 10:75–81

Hadži S, Purič S, Zavrtanik U, Vranken W (2022) What Stabilizes Pre-Folded Structures in the Intrinsically Disordered A-Helical Binding Motifs? SSRN Electron J 1–20. https://doi.org/10.2139/ssrn.4017561

Hartl FU, Bracher A, Hayer-Hartl M (2011) Molecular chaperones in protein folding and proteostasis. Nature 475:324–332. https://doi.org/10.1038/nature10317

Hasan F, Shah AA, Hameed A (2006) Industrial applications of microbial lipases. Enzyme Microb Technol 39:235–251. https://doi.org/10.1016/j.enzmictec.2005.10.016

Hasan J, Haque P, Mizanur M (2022) Protease enzyme based cleaner leather processing : A review. J Clean Prod 365:132826. https://doi.org/10.1016/j.jclepro.2022.132826

He L, Zeng C, Wei L, et al (2023) Fabrication of immobilized lipases for efficient preparation of 1,3-dioleoyl-2-palmitoylglycerol. Food Chem 408:. https://doi.org/10.1016/j.foodchem.2022.135236

Hitch TCA, Clavel T (2019) A proposed update for the classification and description of bacterial lipolytic enzymes. PeerJ 2019:. https://doi.org/10.7717/peerj.7249

Hjörleifsson, J. G., Helland, R., Magnúsdóttir, M., & Ásgeirsson, B. (2021). The high catalytic rate of the cold-active *Vibrio* alkaline phosphatase requires a hydrogen bonding network involving a large interface loop. FEBS Open bio, 11(1), 173-184.

Hochuli E, Bannwarth W, Dobeli H, et al (1988) Genetic approach to facilitate purification of recombinant proteins with a novel metal chelate adsorbent. Bio/Technology 6:1321–1325. https://doi.org/10.1038/nbt1188-1321

Holm L (2020) Using Dali for Protein Structure Comparison. In: Structural Bioinformatics: Methods and Protocols, Methods in Molecular Biology. pp 29–42

Holm L, Rosenström P (2010) Dali server: Conservation mapping in 3D. Nucleic Acids Res 38:545–549. https://doi.org/10.1093/nar/gkq366

Hu C, Yang J, Qi Z, et al (2022) Heat shock proteins: Biological functions, pathological roles, and therapeutic opportunities. MedComm 3:1–39. https://doi.org/10.1002/mco2.161

Hwang HT, Qi F, Yuan C, et al (2014) Lipase-catalyzed process for biodiesel production: Protein engineering and lipase production. Biotechnol Bioeng 111:639–653. https://doi.org/10.1002/bit.25162

Jaeger KE, Dijkstra BW, Reetz MT (1999) Bacterial biocatalysts: Molecular biology, three-dimensional structures, and biotechnological applications of lipases. Annu Rev Microbiol 53:315–351. https://doi.org/10.1146/annurev.micro.53.1.315

Jaeger KE, Eggert T (2002) Lipases for biotechnology. Curr Opin Biotechnol 13:390–397. https://doi.org/10.1016/S0958-1669(02)00341-5

Jallouli R, Parsiegla G, Carrière F, et al (2017) Efficient heterologous expression of *Fusarium solani* lipase, FSL2, in *Pichia pastoris*, functional characterization of the recombinant enzyme and molecular modeling. Int J Biol Macromol 94:61–71. https://doi.org/10.1016/j.ijbiomac.2016.09.030

Jena, S., Dutta, J., Tulsiyan, K. D., Sahu, A. K., Choudhury, S. S., & Biswal, H. S. (2022). Noncovalent interactions in proteins and nucleic acids: Beyond hydrogen bonding and π-stacking. *Chemical Society Reviews*, *51*(11), 4261-4286.

Jin, R., Li, G., Sharma, S., Li, Y., & Du, X. (2020). Toward active-site tailoring in heterogeneous catalysis by atomically precise metal nanoclusters with crystallographic structures. Chemical Reviews, 121(2), 567-648.

Johnson M, Zaretskaya I, Raytselis Y, et al (2008) NCBI BLAST: a better web interface. Nucleic Acids Res 36:5–9. https://doi.org/10.1093/nar/gkn201

Juan B, Quevedo JM, Zamora A, et al (2015) Lipolysis of cheeses made from goat milk treated by ultra-high pressure homogenization. Lwt 60:1034–1038. https://doi.org/10.1016/j.lwt.2014.10.003

Kalantzi I, Shimmield TM, Pergantis SA, et al (2013) Heavy metals, trace elements and sediment geochemistry at four Mediterranean fish farms. Sci Total Environ 444:128–137. https://doi.org/10.1016/j.scitotenv.2012.11.082

Kalita P, Basumatary B, Saikia P, et al (2022) Biodiesel as renewable biofuel produced via enzyme-based catalyzed transesterification. Energy Nexus 6:100087. https://doi.org/10.1016/j.nexus.2022.100087

Kalman M, Ben-Tal N (2010) Quality assessment of protein model-structures using evolutionary conservation. Bioinformatics 26:1299–1307. https://doi.org/10.1093/bioinformatics/btq114

Kanagaraj J, Panda RC, Prasanna R, Tamilselvi A (2023) An efficient dehairing system supported by oxidative-enzymatic auxiliary towards sustainability. Environ Sci Pollut Res 30:43817–43832. https://doi.org/10.1007/s11356-023-25380-3

Karadzic I, Masui A, Zivkovic LI, Fujiwara N (2006) Purification and characterization of an alkaline lipase from *Pseudomonas aeruginosa* isolated from putrid mineral cutting oil as component of metalworking fluid. J Biosci Bioeng 102:82–89. https://doi.org/10.1263/jbb.102.82

Karakaş F, Arslanoğlu A (2020) Gene cloning, heterologous expression, and partial characterization of a novel cold-adapted subfamily I.3 lipase from *Pseudomonas* fluorescence KE38. Sci Rep 10:1–13. https://doi.org/10.1038/s41598-020-79199-w

Karbalaei M, Rezaee SA, Farsiani H (2020) *Pichia pastoris*: A highly successful expression system for optimal synthesis of heterologous proteins. J Cell Physiol 235:5867–5881. https://doi.org/10.1002/jcp.29583

Kaur G, Singh A, Sharma R, et al (2016) Cloning, expression, purification and characterization of lipase from *Bacillus licheniformis*, isolated from hot spring of Himachal Pradesh, India. 3 Biotech 6:1–10. https://doi.org/10.1007/s13205-016-0369-y

Kaur J, Kumar A, Kaur J (2018) Strategies for optimization of heterologous protein expression in *E. coli*: Roadblocks and reinforcements. Int J Biol Macromol 106:803–822. https://doi.org/10.1016/j.ijbiomac.2017.08.080

Khan FI, Lan D, Durrani R, et al (2017) The lid domain in lipases: Structural and functional determinant of enzymatic properties. Front Bioeng Biotechnol 5:1–13. https://doi.org/10.3389/fbioe.2017.00016

Khan HA, Mutus B (2014) Protein disulfide isomerase a multifunctional protein with multiple physiological roles. Front Chem 2:1–9.

https://doi.org/10.3389/fchem.2014.00070

Koyanagi, T., Hara, A., Kobayashi, K., Habara, Y., Nakagawa, A., Minami, H., ... & Misawa, N. (2021). *Thermococcus* sp. KS-1 PPIase as a fusion partner improving soluble production of aromatic amino acid decarboxylase. AMB Express, 11, 1-7.

Korman TP, Bowie JU (2012) Crystal Structure of *Proteus mirabilis* Lipase, a Novel Lipase from the *Proteus/Psychrophilic* Subfamily of Lipase Family I.1. PLoS One 7:1–8. https://doi.org/10.1371/journal.pone.0052890

Korman TP, Sahachartsiri B, Charbonneau DM, et al (2013) Dieselzymes: Development of a stable and methanol tolerant lipase for biodiesel production by directed evolution. Biotechnol Biofuels 6:1–13. https://doi.org/10.1186/1754-6834-6-70

Koudelakova T, Chaloupkova R, Brezovsky J, et al (2013) Engineering enzyme stability and resistance to an organic cosolvent by modification of residues in the access tunnel. Angew Chemie - Int Ed 52:1959–1963. https://doi.org/10.1002/anie.201206708

Kovacic, F., Babic, N., Krauss, U., & Jaeger, K. E. (2019). Classification of lipolytic enzymes from bacteria. *Aerobic Utilization of Hydrocarbons, Oils, and Lipids*, *24*, 255-289

Kumar A (2020) *Aspergillus nidulans*: A Potential Resource of the Production of the Native and Heterologous Enzymes for Industrial Applications. Int J Microbiol 2020:. https://doi.org/10.1155/2020/8894215

Kumar A, Verma V, Dubey VK, et al (2023) Industrial applications of fungal lipases: a review. Front Microbiol 14:. https://doi.org/10.3389/fmicb.2023.1142536

Kumar D, Das T, Giri BS, et al (2019) Biodiesel production from hybrid non-edible oil using bio-support beads immobilized with lipase from *Pseudomonas cepacia*. Fuel 255:115801. https://doi.org/10.1016/j.fuel.2019.115801

Kumar S, Nussinov R (2002) Relationship between ion pair geometries and electrostatic strengths in proteins. Biophys J 83:1595–1612. https://doi.org/10.1016/S0006-3495(02)73929-5

Kurjan J, Herskowitz I (1982) Structure of a yeast pheromone gene (MFα): A putative α-factor precursor contains four tandem copies of mature α-factor. Cell 30:933–943. https://doi.org/10.1016/0092-8674(82)90298-7

Kwon DY, Rhee JS (1986) A simple and rapid colorimetric method for determination of free fatty acids for lipase assay. J Am Oil Chem Soc

63:89–92. https://doi.org/10.1007/BF02676129

Laemmli UK (1970) Cleavage of Structural Proteins during the Assembly of the Head of Bacteriophage T4. Nature 227:680–685. https://doi.org/https://doi.org/10.1038/227680a0

Lan D, Qu M, Yang B, Wang Y (2016) Enhancing production of lipase MAS1 frommarine *Streptomyces* sp. strain in *Pichia pastoris* by chaperones co-expression. Electron J Biotechnol 22:62–67. https://doi.org/10.1016/j.ejbt.2016.06.003

Laskowski RA (2001) PDBsum: Summaries and analyses of PDB structures. Nucleic Acids Res 29:221–222. https://doi.org/10.1093/nar/29.1.221

Laskowski RA, MacArthur MW, Moss DS, Thornton JM (1993) PROCHECK: a program to check the stereochemical quality of protein structures. J Appl Crystallogr 26:283–291. https://doi.org/10.1107/s0021889892009944

Leonard AK, Loughran EA, Klymenko Y, et al (2018) Methods for the visualization and analysis of extracellular matrix protein structure and degradation, 1st edn. Elsevier Inc.

Li S, Yang X, Yang S, et al (2012) Technology prospecting on enzymes: Application, marketing and engineering. Comput Struct Biotechnol J 2:e201209017. https://doi.org/10.5936/csbj.201209017

Li Y, Du W, Liu D (2015) Efficient biodiesel production from phospholipids-containing oil: Synchronous catalysis with phospholipase and lipase. Biochem Eng J 94:45–49. https://doi.org/10.1016/j.bej.2014.11.001

Li Y, Li G, Sun H, Chen Y (2021) Characterization of a novel sn1,3 lipase from *Ricinus communis* L. suitable for production of oleic acid-palmitic acid-glycerol oleate. Sci Rep 11:1–12. https://doi.org/10.1038/s41598-021-86305-z

Lill LJK and MA (2015) Substrate tunnels in enzymes: structure–function relationships and computational methodology. Proteins Struct Funct Bioinforma 83:599–611. https://doi.org/10.1159/000444169.Carotid

Lin-Cereghino GP, Stark CM, Kim D, et al (2013) The effect of α-mating factor secretion signal mutations on recombinant protein expression in *Pichia pastoris*. Gene 519:311–317. https://doi.org/10.1016/j.gene.2013.01.062

Lončarić A, Šarkanj B, Gotal AM, et al (2021) *Penicillium expansum* impact and patulin accumulation on conventional and traditional apple cultivars. Toxins (Basel) 13:. https://doi.org/10.3390/toxins13100703

Luthy R, Bowei J, Einsenberg D (1997) Verify3D: Assessment of protein

models with three-dimensional profiles. Methods Enzymol 277:396–404

Lv Y, Sun S, Liu J (2019) Biodiesel Production Catalyzed by a Methanol-Tolerant Lipase A from *Candida antarctic*a in the Presence of Excess Water. ACS Omega 4:20064–20071. https://doi.org/10.1021/acsomega.9b03249

Ma J, Hou X, Gao D, et al (2014) Greener approach to efficient leather soaking process : role of enzymes and their synergistic effect. J Clean Prod 78:226–232. https://doi.org/10.1016/j.jclepro.2014.04.058

Ma J, Ma Y, Wei W, Wei D zhi (2015) In vivo functional expression of an extracellular Ca^{2+}-independent *Bacillus pumilus* lipase in *Bacillus subtilis* WB800N. Ann Microbiol 65:1973–1983. https://doi.org/10.1007/s13213-015-1035-z

Maina P, Ollengo MA, Nthiga EW (2019) Trends in leather processing : A Review. https://doi.org/10.29322/IJSRP.9.12.2019.p9626

Mao Y, Lee YY, Xie X, et al (2023) Preparation, acyl migration and applications of the acylglycerols and their isomers: A review. J Funct Foods 106:105616. https://doi.org/10.1016/j.jff.2023.105616

Mathangasinghe, Y., Fauvet, B., Jane, S. M., Goloubinoff, P., & Nillegoda, N. B. (2021). The Hsp70 chaperone system: distinct roles in erythrocyte formation and maintenance. Haematologica, 106(6), 1519

Menger, F. M., & Nome, F. (2019). Interaction vs preorganization in enzyme catalysis. A dispute that calls for resolution. ACS Chemical Biology, 14(7), 1386-1392.

Milner-White EJ, Poet R (1986) Four classes of beta-hairpins in proteins. Biochem J 240:289–292. https://doi.org/10.1042/bj2400289

Mir Khan U, Selamoglu Z (2020) Use of enzymes in dairy industry: A review of current progress. Arch Razi Inst 75:131–136. https://doi.org/10.22092/ARI.2019.126286.1341

Monika, Banga S, Pathak V V. (2023) Biodiesel production from waste cooking oil: A comprehensive review on the application of heterogenous catalysts. Energy Nexus 10:100209. https://doi.org/10.1016/j.nexus.2023.100209

Moraleda-Muñoz A, Shimkets LJ (2007) Lipolytic enzymes in *Myxococcus xanthus*. J Bacteriol 189:3072–3080. https://doi.org/10.1128/JB.01772-06

Moujehed E, Zarai Z, Khemir H, et al (2022) Cleaner degreasing of sheepskins by the *Yarrowia lipolytica* LIP2 lipase as a chemical-free

alternative in the leather industry. Colloids Surfaces B Biointerfaces 211:. https://doi.org/10.1016/j.colsurfb.2021.112292

MsangoSoko K, Gandotra S, Bhattacharya R, et al (2022) Screening and characterization of lipase producing bacteria isolated from the gut of a lepidopteran larvae, *Samia ricini.* J Asia Pac Entomol 25:101856. https://doi.org/10.1016/j.aspen.2021.101856

Nakamura AM, Kadowaki MAS, Godoy A, et al (2018) Low-resolution envelope, biophysical analysis and biochemical characterization of a short-chain specific and halotolerant carboxylesterase from *Bacillus licheniformis.* Int J Biol Macromol 120:1893–1905. https://doi.org/10.1016/j.ijbiomac.2018.10.003

Nema, A., Patnala, S. H., Mandari, V., Kota, S., & Devarai, S. K. (2019). Production and optimization of lipase using *Aspergillus nige*r MTCC 872 by solid-state fermentation. Bulletin of the National Research Centre, 43(1), 1-8.

Newberry, R. W., & Raines, R. T. (2019). Secondary forces in protein folding. ACS chemical biology, 14(8), 1677-1686.

Parakh S, Atkin JD (2015) Novel roles for protein disulphide isomerase in disease states: a double edged sword? Front Cell Dev Biol 3:1–11. https://doi.org/10.3389/fcell.2015.00030

Patel R, Trivedi U, Patel K (2022) Lipases: an Efficient Biocatalyst for Biotechnological Applications. J Microbiol Biotechnol Food Sci 11:. https://doi.org/10.55251/jmbfs.2498

Phuah ET, Tang TK, Lee YY, et al (2015) Review on the Current State of Diacylglycerol Production Using Enzymatic Approach. Food Bioprocess Technol 8:1169–1186. https://doi.org/10.1007/s11947-015-1505-0

Prabhu, A. A., Bharali, B., Singh, A. K., Allaka, M., Sukumar, P., & Veeranki, V. D. (2018). Engineering folding mechanism through Hsp70 and Hsp40 chaperones for enhancing the production of recombinant human interferon gamma (rhIFN-γ) in *Pichia pastoris* cell factory. Chemical Engineering Science, 181, 58-67.

Pulido IY, Prieto E, Pieffet GP, et al (2020) Functional heterologous expression of mature lipase lipA from *Pseudomonas aeruginosa* PSA01 in *Escherichia coli* shuffle and BL21 (DE3): Effect of the expression host on thermal stability and solvent tolerance of the enzyme produced. Int J Mol Sci 21:1–19. https://doi.org/10.3390/ijms21113925

Putra L, Natadiputri GH, Meryandini A, Suwanto A (2019) Isolation, cloning and co-expression of lipase and foldase genes of *Burkholderia territorii*

GP3 from mount papandayan soil. J Microbiol Biotechnol 29:944–951. https://doi.org/10.4014/jmb.1812.12013

Qu, C., Dai, K., Fu, H., & Wang, J. (2021). Enhanced ethanol production from lignocellulosic hydrolysates by *Thermoanaerobacterium aotearoense* SCUT27/ΔargR1864 with improved lignocellulose-derived inhibitors tolerance. Renewable Energy, 173, 652-661.

Quayson E, Amoah J, Rachmadona N, et al (2020) Biodiesel-mediated biodiesel production: A recombinant *Fusarium heterosporum* lipase-catalyzed transesterification of crude plant oils. Fuel Process Technol 199:106278. https://doi.org/10.1016/j.fuproc.2019.106278

Quyen TD, Vu CH, Thu Le GT (2012) Enhancing functional production of a chaperone-dependent lipase in *Escherichia coli* using the dual expression cassette plasmid. Microb Cell Fact 11:. https://doi.org/10.1186/1475-2859-11-29

Rabbani, G., Ahmad, E., Ahmad, A., & Khan, R. H. (2023). Structural features, temperature adaptation and industrial applications of microbial lipases from psychrophilic, mesophilic and thermophilic origins. International Journal of Biological Macromolecules, 225, 822-839.

Rajendran A, Palanisamy A, Thangavelu V (2009) Brazilian Archives Of Biology And Technology Lipase Catalyzed Ester Synthesis for Food Processing Industries. Arch Biol Technol v 52:207–219

Raschmanová H, Weninger A, Knejzlík Z, et al (2021) Engineering of the unfolded protein response pathway in *Pichia pastoris*: enhancing production of secreted recombinant proteins. Appl Microbiol Biotechnol 105:4397–4414. https://doi.org/10.1007/s00253-021-11336-5

Ravitchandirane G, Bandhu S, Chaudhuri TK (2022) Multimodal approaches for the improvement of the cellular folding of a recombinant iron regulatory protein in *E. coli*. Microb Cell Fact 21:1–19. https://doi.org/10.1186/s12934-022-01749-w

Richard, J. P. (2019). Protein flexibility and stiffness enable efficient enzymatic catalysis. *Journal of the American Chemical Society*, *141*(8), 3320-3331.

Rios NS, Morais EG, dos Santos Galvão W, et al (2019) Further stabilization of lipase from *Pseudomonas fluorescens* immobilized on octyl coated nanoparticles via chemical modification with bifunctional agents. Int J Biol Macromol 141:313–324. https://doi.org/10.1016/j.ijbiomac.2019.09.003

Rios NS, Pinheiro BB, Pinheiro MP, et al (2018) Biotechnological potential of

lipases from *Pseudomonas*: Sources, properties and applications. Process Biochem 75:99–120. https://doi.org/10.1016/j.procbio.2018.09.003

Rosano GL, Ceccarelli EA (2014) Recombinant protein expression in *Escherichia coli*: Advances and challenges. Front Microbiol 5:1–17. https://doi.org/10.3389/fmicb.2014.00172

Roslan NN, Sabri S, Oslan N, et al (2016) Complete Genome Sequence of *Photobacterium* sp . Strain J15 , Isolated. Genome Announc 4:15–16. https://doi.org/10.1128/genomeA.00739-16.Copyright

Rozi MFAM, Rahman RNZRA, Leow ATC, Ali MSM (2022) Ancestral sequence reconstruction of ancient lipase from family I.3 bacterial lipolytic enzymes. Mol Phylogenet Evol 168:107381. https://doi.org/10.1016/j.ympev.2021.107381

Sahoo RK, Kumari KS, Sahoo S, et al (2021) Bio-statistical optimization of lipase production by thermophilic *Pseudomonas formosensis* and its application on oral biofilm degradation. Biocatal Agric Biotechnol 33:. https://doi.org/10.1016/j.bcab.2021.101969

Saibil H (2013) Chaperone machines for protein folding, unfolding and disaggregation. Nat Rev Mol Cell Biol 14:630–642. https://doi.org/10.1038/nrm3658

Santana CC, Barbosa LA, Basílio Júnior ID, et al (2017) Lipase activity in the larval midgut of *Rhynchophorus palmarum*: Biochemical characterization and the effects of reducing agents. Insects 8:. https://doi.org/10.3390/insects8030100

Sarmah N, Revathi D, Sheelu G, et al (2018) Recent advances on sources and industrial applications of lipases. Biotechnol Prog 34:5–28. https://doi.org/10.1002/btpr.2581

Scholz DAYM (2019) Textile dye wastewater characteristics and constituents of synthetic effluents : a critical review. Springer Berlin Heidelberg

Sena RO, Carneiro C, Moura MVH, et al (2021) Application of *Rhizomucor miehei* lipase-displaying *Pichia pastoris* whole cell for biodiesel production using agro-industrial residuals as substrate. Int J Biol Macromol 189:734–743. https://doi.org/10.1016/j.ijbiomac.2021.08.173

Shao H, Hu X, Sun L, Zhou W (2019) Gene cloning, expression in *E. coli*, and *in vitro* refolding of a lipase from *Proteus* sp. NH 2-2 and its application for biodiesel production. Biotechnol Lett 41:159–169. https://doi.org/10.1007/s10529-018-2625-1

Shen J (2019) Enzymatic treatment of wool and silk fibers. Adv Text Biotechnol 77–105. https://doi.org/10.1016/B978-0-08-102632-

8.00005-0

Shu, P., Liang, H., Zhang, J., Lin, Y., Chen, W., & Zhang, D. (2023). Reactive oxygen species formation and its effect on CD4+ T cell-mediated inflammation. Frontiers in Immunology, 14, 1199233.

Silano V, Barat Baviera JM, Bolognesi C, et al (2019) Safety evaluation of the food enzyme triacylglycerol lipase from *Trichoderma reesei* (strain RF10625). EFSA J 17:1–16. https://doi.org/10.2903/j.efsa.2019.5837

Silva Dias G, Bandeira PT, Jaerger S, et al (2019) Immobilization of *Pseudomonas cepacia* lipase on layered double hydroxide of Zn/Al-Cl for kinetic resolution of rac-1-phenylethanol. Enzyme Microb Technol 130:109365. https://doi.org/10.1016/j.enzmictec.2019.109365

Simone G De, Mandrich L, Menchise V, et al (2004) A Substrate-induced Switch in the Reaction Mechanism of a. 279:6815–6823. https://doi.org/10.1074/jbc.M307738200

Singh AK, Mukhopadhyay M (2012) Overview of fungal lipase: A review. Appl Biochem Biotechnol 166:486–520. https://doi.org/10.1007/s12010-011-9444-3

Singh R, Kumar M, Mittal A, Mehta PK (2016) Microbial enzymes: industrial progress in 21st century. 3 Biotech 6:1–15. https://doi.org/10.1007/s13205-016-0485-8

Sobolev O V., Afonine P V., Moriarty NW, et al (2020) A Global Ramachandran Score Identifies Protein Structures with Unlikely Stereochemistry. Structure 28:1249-1258.e2. https://doi.org/10.1016/j.str.2020.08.005

Su E, Xu J, You P (2014) Functional expression of *Serratia marcescens* H30 lipase in *Escherichia coli* for efficient kinetic resolution of racemic alcohols in organic solvents. J Mol Catal B Enzym 106:11–16. https://doi.org/10.1016/j.molcatb.2014.04.012

Su, H. G., Zhang, X. H., Wang, T. T., Wei, W. L., Wang, Y. X., Chen, J., ... & Min, D. H. (2020). Genome-wide identification, evolution, and expression of GDSL-type esterase/lipase gene family in soybean. Frontiers in Plant Science, 11, 726.

Subroto E (2020) Monoacylglycerols and diacylglycerols for fat-based food products: A review. Food Res 4:932–943. https://doi.org/10.26656/fr.2017.4(4).398

Sun C, Wu S, Wu Y, et al (2023) Lipase AK from *Pseudomonas fluorescens* immobilized on metal organic frameworks for efficient biosynthesis of enantiopure (S)− 1-(4-bromophenyl) ethanol. Process Biochem 124:132–139. https://doi.org/10.1016/j.procbio.2022.11.022

Taleb MA, Gomaa SK, Wahba MI, et al (2022) Bioscouring of wool fibres using immobilized thermophilic lipase. Int J Biol Macromol 194:800–810. https://doi.org/10.1016/j.ijbiomac.2021.11.128

Tamura K, Stecher G, Kumar S (2021) MEGA11: Molecular Evolutionary Genetics Analysis Version 11. Mol Biol Evol 38:3022–3027. https://doi.org/10.1093/molbev/msab120

Teja M, Kumar DM, Pavani S, et al (2022) Screening and optimization of candidate alkaline protease for dehairing potential from marine Bacillus paramycoides M2. Res J Biotechnol 17:78–89. https://doi.org/10.25303/1702rjbt7889

Thangaraj B, Solomon PR, Muniyandi B, et al (2019) Catalysis in biodiesel production - A review. Clean Energy 3:2–23. https://doi.org/10.1093/ce/zky020

Toldrá-Reig F, Mora L, Toldrá F (2020) Developments in the use of lipase transesterification for biodiesel production from animal fat waste. Appl Sci 10:. https://doi.org/10.3390/app10155085

Tshisevhe V, Mitton B, Skosana L (2021) Invasive *Geotrichum klebahnii* fungal infection: A case report. Access Microbiol 3:1–4. https://doi.org/10.1099/acmi.0.000287

Uddin F (2019) Introductory Chapter: Textile Manufacturing Processes. Intech. https://doi.org/http://dx.doi.org/10.5772/intechopen.87968

Valério RBR, Cavalcante ALG, Mota GF, et al (2022) Understanding the biocatalytic potential of lipase from *Rhizopus chinensis.* Biointerface Res Appl Chem 12:4230–4260. https://doi.org/10.33263/BRIAC123.42304260

Vallejo LF, Rinas U (2004) Strategies for the recovery of active proteins through refolding of bacterial inclusion body proteins. Microb Cell Fact 3:1–12. https://doi.org/10.1186/1475-2859-3-11

Verma N, Dollinger P, Kovacic F, et al (2020) The Membrane-Integrated Steric Chaperone Lif Facilitates Active Site Opening of *Pseudomonas aeruginosa* Lipase A. J Comput Chem 41:500–512. https://doi.org/10.1002/jcc.26085

Verma S, Meghwanshi GK, Kumar R (2021) Current perspectives for microbial lipases from extremophiles and metagenomics. Biochimie 182:23–36. https://doi.org/10.1016/j.biochi.2020.12.027

Viegas A, Dollinger P, Verma N, et al (2020) Structural and dynamic insights revealing how lipase binding domain MD1 of *Pseudomonas aeruginosa* foldase affects lipase activation. Sci Rep 10:1–15.

https://doi.org/10.1038/s41598-020-60093-4

Wang J, Wang X, Shi L, et al (2017) Methanol-Independent Protein Expression by AOX1 Promoter with trans-Acting Elements Engineering and Glucose-Glycerol-Shift Induction in *Pichia pastoris*. Sci Rep 7:1–12. https://doi.org/10.1038/srep41850

Webster JM, Darling AL, Uversky VN, Blair LJ (2019) Small heat shock proteins, big impact on protein aggregation in neurodegenerative disease. Front Pharmacol 10:1–18. https://doi.org/10.3389/fphar.2019.01047

White A, Koelper A, Russell A, et al (2018) Fluorogenic structure activity library pinpoints molecular variations in substrate specificity of structurally homologous esterases. J Biol Chem 293:13851–13862. https://doi.org/10.1074/jbc.RA118.003972

Wohlgemuth R (2010) Biocatalysis-key to sustainable industrial chemistry. Curr Opin Biotechnol 21:713–724. https://doi.org/10.1016/j.copbio.2010.09.016

Wongwatanapaiboon J, Klinbunga S, Ruangchainikom C, et al (2016) Cloning, expression, and characterization of *Aureobasidium melanogenum* lipase in *Pichia pastoris*. Biosci Biotechnol Biochem 80:2231–2240. https://doi.org/10.1080/09168451.2016.1206809

Wu X, You P, Su E, et al (2012) *In vivo* functional expression of a screened *P. aeruginosa* chaperone-dependent lipase in *E. coli*. BMC Biotechnol 12:. https://doi.org/10.1186/1472-6750-12-58

Wyganowski KT, Kaltenbach M, Tokuriki N (2013) GroEL/ES buffering and compensatory mutations promote protein evolution by stabilizing folding intermediates. J Mol Biol 425:3403–3414. https://doi.org/10.1016/j.jmb.2013.06.028

Xiong J, Wang Q, Xu H, Sun W (2023). Immobilization of *Pseudomonas Fluorescens* lipase on hollow poly (o-phenylenediamine) microspheres and its application in the preparation of citronellyl acetate. Processes, 11(6), 1842

Xu, X., Chiu, J., Chen, S., & Fang, C. (2021). Pathophysiological roles of cell surface and extracellular protein disulfide isomerase and their molecular mechanisms. British journal of pharmacology, 178(15), 2911-2930.

Yan, P., Zou, Z., Zhang, S., Wang, R., Niu, T., Zhang, X., ... & He, J. (2021). Defining the mechanism of PDI interaction with disulfide-free amyloidogenic proteins: Implications for exogenous protein expression and neurodegenerative disease. International Journal of Biological Macromolecules, 174, 175-184.

Yao C, Yuan A, Zhang H, et al (2019) Journal of Colloid and Interface Science Facile surface modification of textiles with photocatalytic carbon nitride nanosheets and the excellent performance for self-cleaning and degradation of gaseous formaldehyde. J Colloid Interface Sci 533:144–153. https://doi.org/10.1016/j.jcis.2018.08.058

Yao W, Liu K, Liu H, et al (2021) A Valuable Product of Microbial Cell Factories: Microbial Lipase. Front Microbiol 12:1–16. https://doi.org/10.3389/fmicb.2021.743377

Yuan X, Liu Y, Cao F, et al (2020) Immobilization of lipase onto metal–organic frameworks for enantioselective hydrolysis and transesterification. AIChE J 66:. https://doi.org/10.1002/aic.16292

Yuan Z, Zhao J, Wang ZX (2003) Flexibility analysis of enzyme active sites by crystallographic temperature factors. Protein Eng 16:109–114. https://doi.org/10.1093/proeng/gzg014

Zhang HH, Yang BJ, Wu Y, et al (2023) Characterization of neutral lipases revealed the tissue-specific triacylglycerol hydrolytic activity in *Nilaparvata lugens*. Insect Sci 30:693–704. https://doi.org/10.1111/1744-7917.13118

Zhang XM, Ai NS, Wang J, et al (2016) Lipase-catalyzed modification of the flavor profiles in recombined skim milk products by enriching the volatile components. J Dairy Sci 99:8665–8679. https://doi.org/10.3168/jds.2015-10773

Zhang Z, Ryoo D, Balusek C, et al (2021) Inward-facing glycine residues create sharp turns in β-barrel membrane proteins. Biochim Biophys Acta - Biomembr 1863:1–24. https://doi.org/10.1016/j.bbamem.2021.183662

Zhao J, Ma M, Yan X, et al (2022) Expression and characterization of a novel lipase from *Bacillus licheniformis* NCU CS-5 for application in enhancing fatty acids flavor release for low-fat cheeses. Food Chem 368:130868. https://doi.org/10.1016/j.foodchem.2021.130868

Zhou W, Chen F, Zhao S, et al (2019) DA-6 promotes germination and seedling establishment from aged soybean seeds by mediating fatty acid metabolism and glycometabolism. J Exp Bot 70:101–114. https://doi.org/10.1093/jxb/ery247

APPENDICES

Appendix A

Chemicals	Manufacturers
Acetic acid	Merck, Germany
Coomassie blue	Merck, Germany
Di-Potassium hydrogen phosphate	Merck, Germany
Di-sodium Hydrogen phosphate	Merck, Germany
2X Taq Polymerase Mastermix	Abm, USA
Glycerol	Merck, Germany
Glycine	Merck, Germany
Hydrogen chloride (HCl)	Merck, Germany
Imidazole	Merck, Germany
Isoropyl ß-D Thiogalactoside (IPTG)	Amresco, USA
Luria-Bertani Agar	DifcoTM
Luria-Bertani Broth	DifcoTM
Tris–maleate	Sigma, USA
Magnesium chloride	Merck, Germany
Methanol	Merck, Germany
Sodium chloride	Merck, Germany
Sodium dihydrogen phosphate	Merck, Germany
Sodium dodecyl sulphate (SDS)	Merck, Germany
Trichloroacetic acid	Merck, Germany
Ampicillin	Sigma, USA

Appendix A : Continued

Spectinomycin	Sigma, USA
EasyPure Plasmid Extraction kit	Nanogensolutions, China
Wizard SV Gel and PCR clean-UP	Promega, USA
EasyPure® Quick Gel Extraction Kit	Transgen, (Beijing, China)

Appendix B

Software	Manufacturer/Developer/Server
DALI Server	Institute of Biotechnology
Errat	NIH MBI Laboratory
PDBsum	European Bioinformatics Institute (EMBL-EBI)
PROCHECK	EMBL-EBI
Pymol	Schrödinger, Inc.
Verify3D	NIH MBI Laboratory
YASARA	YASARA Biosciences GmbH

Appendix C

Standard curve p-nitrophenol (pNP)

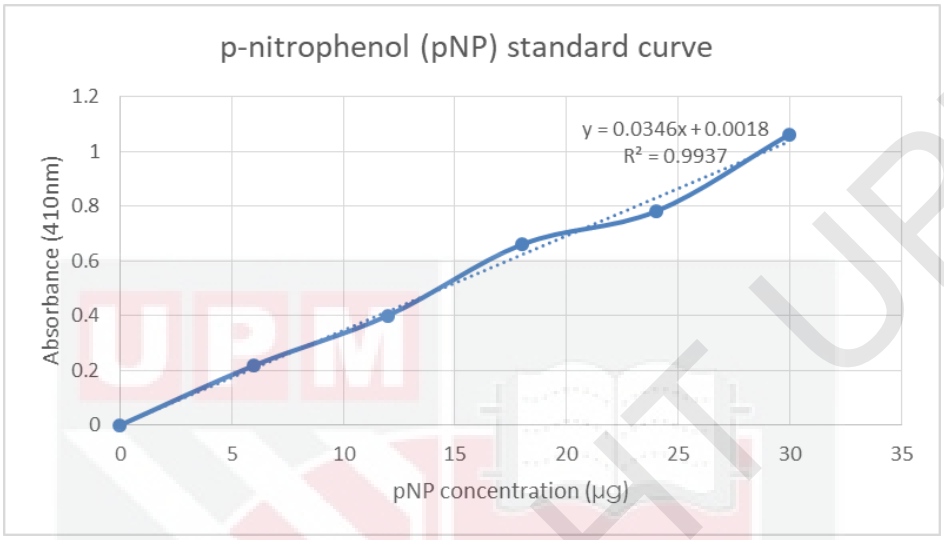

Appendix D

Standard curve of ELISA

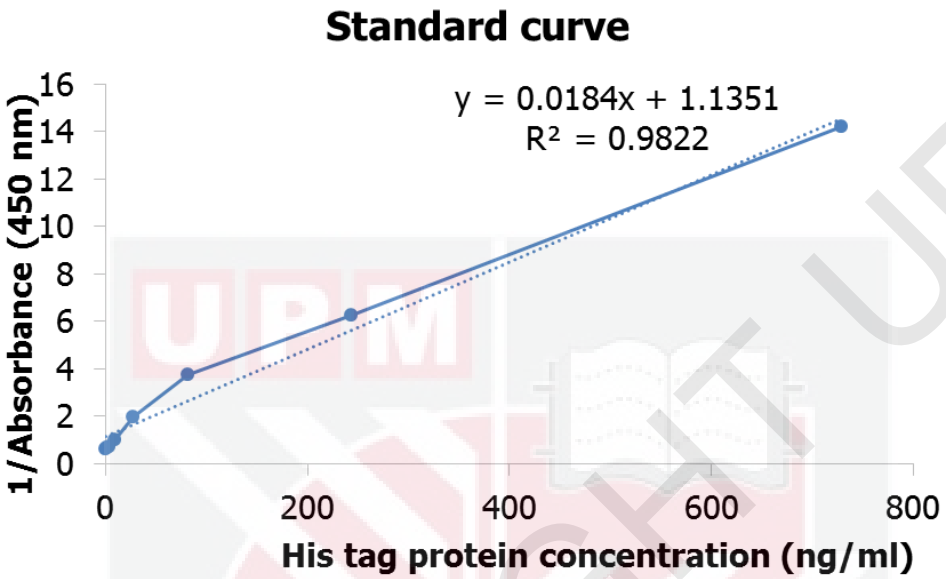

Appendix E

Para nitro phenol (PNP) working standard solution (30 µg/ml): Weigh accurately 0.03 g of PNP and carefully transfer it into a clean 100 ml standard volumetric flask, dissolve it in some amount of distilled water. Then, make up the volume upto 100 ml using distilled water. This solution contains 300 µg/ml PNP (stock solution - 10X). From this stock solution, pipette out 10 ml into a clean 100 ml standard volumetric flask and make upto the mark using distilled water. This solution contains 30 µg/ml PNP (working standard solution). Prepare PNP calibration curve of concentration range 0 - 30 µg and volume range 0 - 1 ml.

Determination of PNP Calibration Curve

	Volume of PNP (ml)	Volume of distilled water (ml)	Concentration of PNP (µg)	Volume of 0.1 N NaOH (ml)	O.D at 405 nm
1	0.0	1.0	0	2	
2	0.2	0.8	6	2	
3	0.4	0.6	12	2	
4	0.6	0.4	18	2	
5	0.8	0.2	24	2	
6	1.0	0.0	30	2	

Appendix F

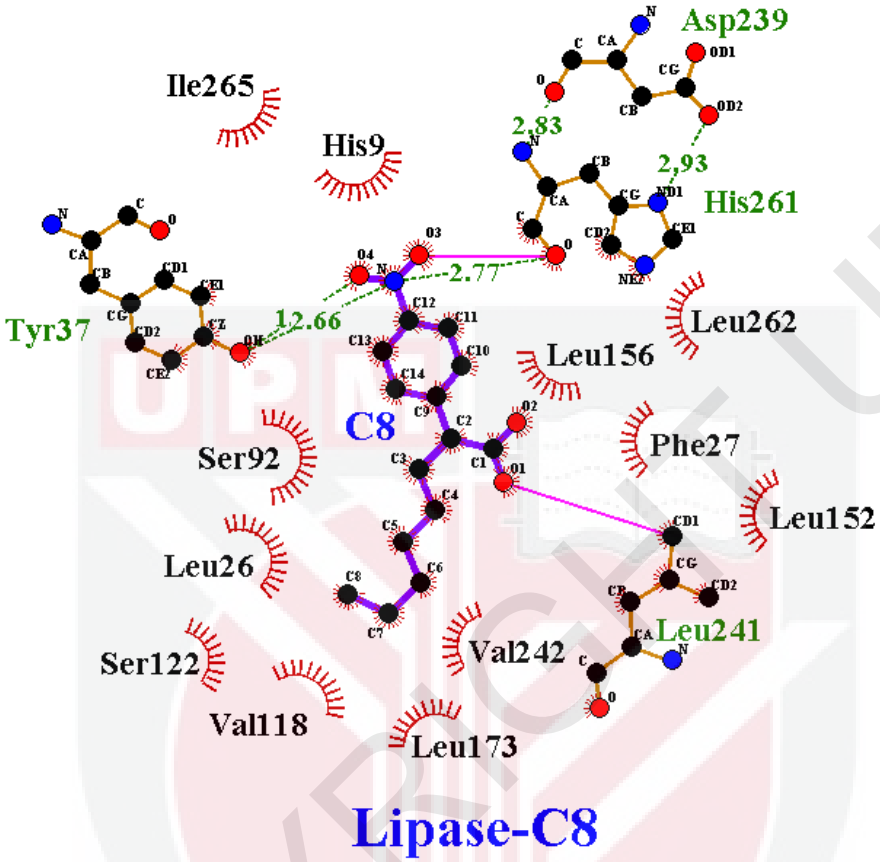

Docking analysis of LipJ15 with pNP-octanoate

Appendix G

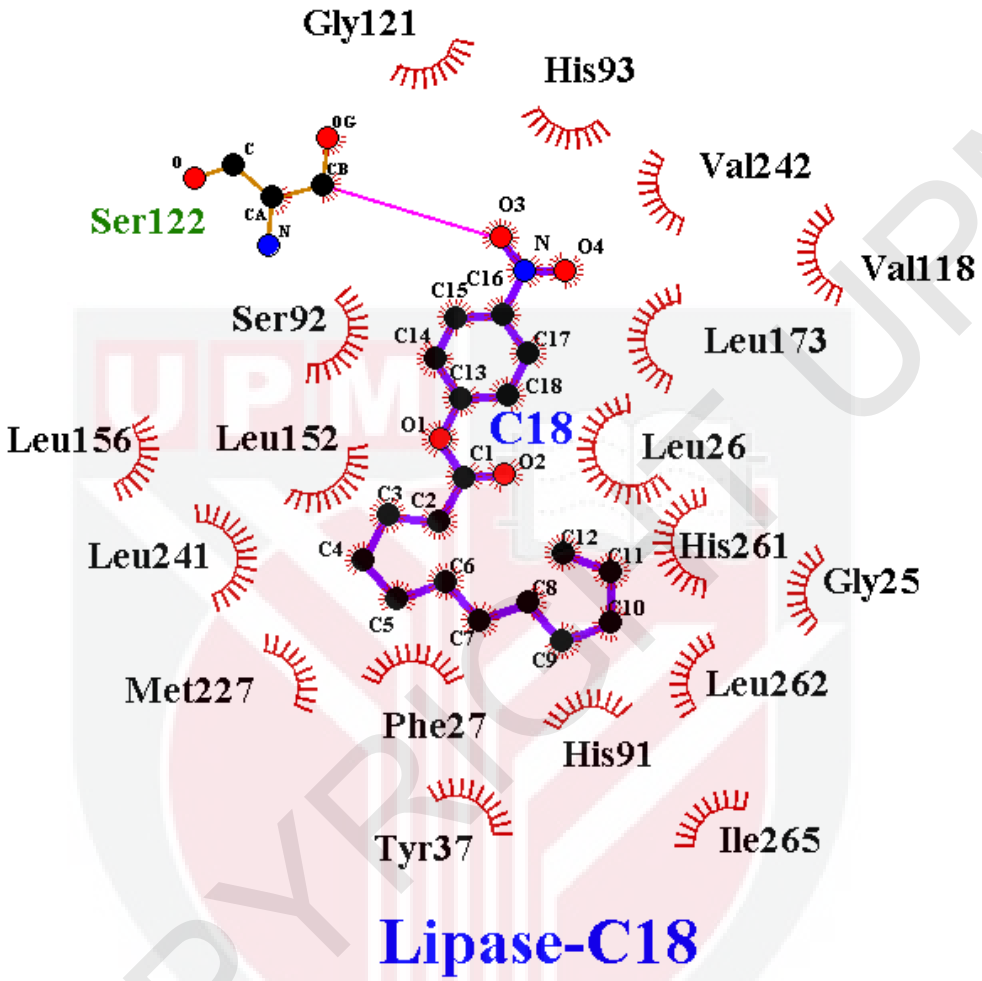

Docking analysis of LipJ15 with ρNP-palmitate

Appendix H

Sequencing result for LipJ15

```
PMLJ15_Lip15          CTGCGGGAGCTTGCGCTGAAAAAATTAGAGCTTAAAAAACTGGCTACCGACGAGGAAGAT
PMLJ15_T7_Terminator  CTGCGGGAGCTTGCGCTGAAAAAATTAGAGCTTAAAAAACTGGCTACCGACGAGGAAGAT
                      ************************************************************

PMLJ15_Lip15          TTCCAAAACCAGTGGCAGCAAGAAATTAATCAGCTCCCACCAGATTTACAGTCTAGTTAT
PMLJ15_T7_Terminator  TTCCAAAACCAGTGGCAGCAAGAAATTAATCAGCTCCCACCAGATTTACAGTCTAGTTAT
                      ************************************************************

PMLJ15_Lip15          CGGAACGCCCAGTTGTTGCCGCAGTTGCAAACTACTAATAACCTGGATCCGCAGGAGCGC
PMLJ15_T7_Terminator  CGGAACGCCCAGTTGTTGCCGCAGTTGCAAACTACTAATAACCTGGATCCGCAGGAGCGC
                      ************************************************************

PMLJ15_Lip15          TTTTTGGCGAATCAGGAACTCGTAGGGAGTGAAGCGGCGGCACGGCTGGAAAAACTGGCT
PMLJ15_T7_Terminator  TTTTTGGCGAATCAGGAACTCGTAGGGAGTGAAGCGGCGGCACGGCTGGAAAAACTGGCT
                      ************************************************************

PMLJ15_Lip15          GGCGAACGGGAGGCATTCCAGAATAAGGTGTCGCAATACTTGGAGGAACGTGAAGCTATC
PMLJ15_T7_Terminator  GGCGAACGGGAGGCATTCCAGAATAAGGTGTCGCAATACTTGGAGGAACGTGAAGCTATC
                      ************************************************************

PMLJ15_Lip15          CAGAATGACGATAGTTTAAATTACGAAGAGCAAGAGAAAGCAATTGAAGATTTGCGTAAC
PMLJ15_T7_Terminator  CAGAATGACGATAGTTTAAATTACGAAGAGCAAGAGAAAGCAATTGAAGATTTGCGTAAC
                      ************************************************************

PMLJ15_Lip15          TCAACGTTTTCCGAAAAACATAAGCGGCGCATTCAGGCACTGGAATCCATCCACGATGAA
PMLJ15_T7_Terminator  TCAACGTTTTCCGAAAAACATAAGCGGCGCATTCAGGCACTGGAATCCATCCACGATGAA
                      ************************************************************

PMLJ15_Lip15          CAGGCAGGCAACAATAGTCACCACCACCACCACCACTAG
PMLJ15_T7_Terminator  CAGGCAGGCAACAATAGTCACCACCACCACCACCACTAG
                      ****************************************
```

BIODATA OF STUDENT

Fatin Liyana binti Alias was born in Tanjong Malim, Perak on April 18, 1995. She received her secondary education (PMR) at Sekolah Menengah Kebangsaan Khir Johari, Tanjong Malim before proceeding to Sekolah Menengah Slim River, Perak to complete her Sijil Pelajaran Malaysia (SPM). Upon completion of her secondary study, she was offered to do matriculation study at Kolej Matrikulasi Melaka, Melaka before continued her tertiary education in Bachelor of Cell and Molecular Biology (Honours) at Universiti Putra Malaysia, Serdang and graduated with second class upper. Due to her passion in scientific findings, she has decided to pursue her education at Universiti Putra Malaysia under the supervision of Associate Professor Dr. Adam Leow Thean Chor to obtain her MSc in Enzyme Biotechnology.

LIST OF PUBLICATIONS

.

Alias, F. L., Nezhad, N. G., Normi, Y. M., Ali, M. S. M., Budiman, C., & Leow. T.C. (2023). Recent advances in overexpression of functional recombinant lipases. Molecular Biotechnology, 65(11), 1737-1749.